



Virginia Commonwealth University
VCU Scholars Compass

Theses and Dissertations


Graduate School

2015

XLF-Dependent Nonhomologous End Joining of Complex DNA Double-Strand Breaks with Proximal Thymine Glycol and Screening for XRCC4-XLF Interaction Inhibitors

MOHAMMED AL MOHAINI
Virginia Commonwealth University

Follow this and additional works at: <https://scholarscompass.vcu.edu/etd>

 Part of the [Amino Acids, Peptides, and Proteins Commons](#), [Molecular Biology Commons](#), and the [Pharmacology Commons](#)

© The Author

Downloaded from

<https://scholarscompass.vcu.edu/etd/3988>

This Dissertation is brought to you for free and open access by the Graduate School at VCU Scholars Compass. It has been accepted for inclusion in Theses and Dissertations by an authorized administrator of VCU Scholars Compass. For more information, please contact libcompass@vcu.edu.

©Mohammed Al Mohaini 2015

All Rights Reserved

XLF-Dependent Nonhomologous End Joining of Complex DNA Double-Strand Breaks with Proximal
Thymine Glycol and Screening for XRCC4-XLF Interaction Inhibitors

A dissertation submitted in partial fulfillment of the requirements for the degree of Doctor of Philosophy
at Virginia Commonwealth University

By

Mohammed Al Mohaini

M.S. in Pharmacology and Toxicology, Virginia Commonwealth University, 2012

B.Sc. in Pharmaceutical Sciences, King Saud University, 2006

Director: Lawrence F. Povirk, Professor, Department of Pharmacology and Toxicology

Virginia Commonwealth University
Richmond, Virginia
May, 2015

ACKNOWLEDGEMENT

I would like to thank my parents, Ahmad Almohaini and Hejjiah Almutlaq, for their prayer, care, love and support throughout my life. High regards also go to my brothers and sisters, especially Abbas and Yousef, for their sincere encouragement and inspiration throughout my research work. I must thank my wife Zainab Alramadhan for her love, understanding and taking care of me, my son Hasan and daughter Fatimah during my study.

I would like to express my deepest gratitude to my advisor, Dr. Lawrence Povirk for his excellent guidance, caring, patience, and advice that are necessary for me to proceed through the PhD program and complete my dissertation. I warmly thank Dr. Matthew Hartman for his valuable advice, enthusiasm and encouragement and for pushing me farther than I thought I could go. His extensive knowledge and experience in mRNA display technique have a great impact on this project. Also, I would like to thank my committee members Dr. Richard Moran, Dr. Nicholas P Farrell, Dr. Laura J Sim-Selley and Dr. Ashton Cropp for their insightful comments and suggestions throughout my project.

I would like to thank the current and former members of Dr. Povirk's lab. Special thanks goes to Dr. Konstantin Akopiants for the training I received when I came to the lab in Fall 2010. His advice and help in cloning are highly appreciable. Also, I would like to thank the current and former members of Dr. Hartman's lab for their help and advice in the selection process.

Finally, I would like to thank Virginia Commonwealth University for giving me the opportunity to be a student in the Department of Pharmacology and Toxicology. I would like to thank King Saud bin Abdulaziz University for Health Sciences (KSAU-HS) for awarding me a scholarship to study abroad. I am so thankful to have KSAU-HS supporting me financially in order to achieve my goal of getting a PhD degree. I would like also to thank all of my friends for their love and support.

TABLE OF CONTENT

List of Figures	vi
List of Abbreviations.....	viii
Abstract.....	xi
I. Introduction.....	1
1.1 DNA Damage.....	1
1.2 Ionizing Radiation.....	1
1.3 Thymine Glycol.....	4
1.4 Base Excision Repair.....	5
1.5 Major DSB Repair Mechanisms.....	5
1.5.1 Homologous Recombination (HRR).....	5
1.5.2 Clasical Non-Homologous End Joining (NHEJ).....	6
1.5.3 The Choice of DSBs Repair Method.....	8
1.6 NHEJ Core Proteins.....	8
1.7 Other Proteins Involved in NHEJ.....	10
1.8 Upregulation of NHEJ in Breast Cancer.....	13
1.8.1 Breast Cancer.....	13
1.8.2 The Choice of DSBs Repair Mechanism in Breast Cancer.....	14
1.8.3 XRCC4-XLF Interaction as a Target for Radiosensitization.....	14
1.9 XRCC4-XLF Interaction as a Good Druggable Target.....	19
1.10 mRNA Display.....	19
1.11 Advantages of mRNA Display Technique.....	21
1.11.1 Removal of Non-Specific Binders.....	21
1.11.2 Development of Large Libraries.....	21
1.12 Applications of mRNA Display.....	22
1.13 Specific Aims.....	23

II. Methods.....	24
2.1 Production of Wild-Type XLF and XLF mutants (L115A and L115D) Proteins.....	24
2.1.1 Construction of XLF Mutants.....	24
2.1.2 Production of Wild-Type XLF, XLF ^{L115A} and XLF ^{L115D} Proteins.....	27
2.1.3 Ni-NTA Purification.....	27
2.2 Substrate.....	30
2.3 End Joining Reactions.....	31
2.4 Polyacrylamide Gel Electrophoresis.....	31
2.5 Statistics.....	32
2.5 mRNA Display and <i>In Vitro</i> Selection.....	32
2.5.1 DNA library Synthesis.....	32
2.5.2 PCR Amplification of Library DNA.....	33
2.5.3 StrataClone Cloning and Sequencing.....	35
2.5.4 Transcription and Purification of mRNA.....	36
2.5.5 Psoralen Photo-Crosslinking.....	37
2.5.6 <i>In Vitro</i> Translation.....	37
2.5.7 Oligo(dT) Purification and Cyclization.....	38
2.5.8 Reverse Transcription.....	39
2.5.9 Ni-NTA Purification.....	39
2.5.10 <i>In Vitro</i> Selection.....	40
2.5.11 PCR Amplification of Selected Fusions.....	41
2.6 Peptide Synthesis.....	46
2.6.1 Solid Phase Peptide Synthesis.....	46
2.6.2 Labeling with 5(6)-Carboxyfluorescein.....	46
2.6.3 Cleavage of the Peptide from the Resin.....	46
2.6.4 Purification by HPLC.....	46
2.6.5 Cyclization with α - α' -dibromo- <i>m</i> -xylene in Solution.....	47
2.6.6 Cysteine Protecting Group Removal to Prepare for Cyclization on the Solid Phase...47	
2.6.7 Cyclization of the Peptide with α - α' -dibromo- <i>m</i> -xylene on the Resin.....	48
2.7 MALDI-TOF Analysis.....	48
2.8 K _D Determination Using Bead Capture of <i>In Vitro</i> Translated Peptides.....	48

III. Results	50
3.1 NHEJ is Tolerant of a Substrate Containing Tg Near a DSB End	50
3.2 Tg as the Terminal or Penultimate Base at the 3' End of a DSB is a Barrier to NHEJ	52
3.3 Ligation of Tg-Containing Substrates does not Require Prior Tg Removal	54
3.4 An Initial Delay in Ligation is Dependent on Tg Position	56
3.5 Mutations in XLF at its Interface with XRCC4 Reduce or Eliminate Ligation	58
3.6 Development of a Diverse Peptide Libraries Composed of Cyclic Peptides to Inhibit XRCC4-XLF Interaction	60
3.6.1 <i>In Vitro</i> Selection	60
3.7 Sequencing	65
3.8 Synthesis of the Selected Peptides	69
3.8.1 Challenges	71
3.9 Determination the Binding Affinity of the Selected Peptides to XRCC4 Protein	76
3.9.1 Fluorescence Polarization	76
3.9.2 Scintillation-based K _d Determination	76
3.10 Inhibition of NHEJ in Cell Extracts	80
IV. Discussion and Future Direction	82
4.1 Therapeutic potential of Suppressing DSB Repair by Targeting XRCC4-XLF Interaction	84
References	88
Vita	102

LIST OF FIGURES

Figure 1-1	Major damaged termini of free radical-mediated DNA Strand Breaks.....	3
Figure 1-2	Oxidation of thymine to thymine glycol.....	4
Figure 1.3	Nonhomologous end joining.....	7
Figure 1-4	Crystal structures of XRCC4 and XLF.....	16
Figure 1-5	Filaments of alternating XRCC4-XLF dimers.....	17
Figure 1-6	Interface of the XRCC4 ¹⁻¹⁵⁷ -XLF ¹⁻²²⁴ complex formed by the distal part of their N-terminal head domains.....	18
Figure 1-7	XRCC4-XLF interaction interface.....	20
Figure 2-1	The full length XLF ^{L115D} cut from pQE80L Vector.....	25
Figure 2-2	XLF ^{L115D} sequence.....	26
Figure 2-3	Protein Composition of A) WT XLF and B) XLF ^{L115D} after Ni-NTA purification as determined by SDS-PAGE.....	28
Figure 2-4	Protein Composition after FPLC purification as determined by SDS-PAGE.....	29
Figure 2-5	Tg-containing DSB substrates.....	30
Figure 2-6	DNA library on 2% agarose gel.....	34
Figure 2-7	DNA libraries sequence.....	35
Figure 2-8	<i>In vitro</i> transcription, photo crosslinking and <i>in vitro</i> translation.....	43
Figure 2-9	mRNA-Peptide Fusions Purification Steps.....	44
Figure 2-10	Pre-clearing (negative selection) with GST protein only immobilized on magnetic beads.....	45
Figure 3.1	Tg-containing DSB substrates.....	51
Figure 3.2	Effect of Tg on joining of blunt-ended substrates by NHEJ.....	53
Figure 3.3	Presence of Tg in end joining products.....	55
Figure 3.4	Time course for Tg3 and Tg1 end joining and effect of dideoxynucleotides.....	57
Figure 3.5	Effect of L115 mutations in XLF on end joining.....	59
Figure 3.6	DNA libraries structure.....	61
Figure 3.7	<i>In vitro</i> selection process search for XRCC4-XLF inhibitors.....	62

Figure 3.8	<i>In vitro</i> selection Results.....	64
Figure 3.9	Sequencing result.....	66
Figure 3.10	Second generation sequencing result.....	67
Figure 3.10	Top 30 sequences of round 3, 4, 5, and 6 after second generation sequencing.....	68
Figure 3.12	Peptide synthesis approaches.....	69
Figure 3.13	HPLC spectrum of Pep 7.4.....	70
Figure 3.14	MALDI-TOF analysis of Pep 7.4 and Pep 3.2.....	70
Figure 3.15	MALDI-TOF analysis of Pep 7.1 (MCSWMWRIETCGMIL).....	73
Figure 3.16	The synthesis of 1,3-bis(bromomethyl)benzyl 2-[2-(2-methoxyethoxy)ethoxy]acetate...	74
Figure 3.17	Fluorescence polarization data of Pep 7.1 and Pep 7.2.....	77
Figure 3.18	Preparation for scintillation-based K_d determination.....	78
Figure 3.19	<i>In vitro</i> translation of Pep 7.1.....	79
Figure 3.20	EJ inhibition assay.....	81

LIST OF TABLES

Table 3.1	Summary of peptide synthesis.....	71
Table 3.2	Percentage of the hydrophobicity of each peptide.....	72
Table 3.3	Modification of the peptides to increase their solubility.....	74

LIST OF ABBREVIATIONS

53BP1	p53 binding protein 1
Å	Angstrom
APS	Ammonium persulfate
ATM	Ataxia Telangiectasia Mutated
ATP	Adenosine triphosphate
BER	Base Excision Repair
BRCA	Breast cancer susceptibility protein
BRCT	BRCA1 C-terminal
BSA	Bovine serum albumin
°C	Celsius
Ca ₂	Calcium
CD	Circular dichroism
CDK	Cyclin-dependent kinase
cDNA	ComplementaryDNA
CHCA	α-Cyano-4-hydroxycinnamic acid
CtIP	CtBP-interacting protein
DCC	N,N'-Dicyclohexylcarbodiimide
DCM	Dichloromethane
ddCTP	2',3'-Dideoxycytidine-5'-Triphosphate
ddTTP	2',3'-Dideoxythymidine-5'-Triphosphate
DMF	Dimethylformamide
DNA	Deoxyribonucleic acid
DNA-PK	DNA-dependent protein kinase
DNA-PKcs	DNA-dependent protein kinase catalytic subunit
DODT	3,6-dioxa-1,8-octanedithiol
DSBs	Double-strand breaks
DTT	Dithiothreitol

EDTA	Ethylenediaminetetraacetic acid
EtBr	Ethidium bromide
FEN1	Flap endonuclease 1
FPLC	Fast protein liquid chromatography
HOBt	Hydroxybenzotriazole
HRR	Homologous recombination repair
HPLC	High performance liquid chromatography
IPTG	Isopropyl β -D-1-thiogalactopyranoside
IR	Ionizing radiation
Kb	Kilobase
kD	Kilodalton
K_d	Dissociation constant
μ l	Microliter
Min	Minute
Mre11	Meiotic recombination 11 homolog
MRN	Mre11/Rad50/Nbs1
NHEJ	Nonhomologous end joining
PAGE	Polyacrylamide gel electrophoresis
PBS	Phosphate buffered saline
PCNA	Proliferating cell nuclear antigen
PCR	Polymerase chain reaction
PNKP	Polynucleotide phosphatase/kinase
RAD50	Family of RADiation sensitive genes(50 homolog)
RNA	Ribonucleic acid
Rpm	Rotations per minute
RT	Room temperature
SCID	Severe combined immune-deficiency
Sec	Seconds
SDS	Sodium dodecyl sulfate
ssDNA	Single-strand DNA
TBE	Tris/borate/EDTA

TCEP	Tris-carboxyethylphosphine
TEG	Triethylene glycol
TEMED	N, N, N', N'-tetramethylenediamine
TFA	Trifluoroacetic acid
TIS	Triisopropylsilane
UV	Ultraviolet
V	Volts
V(D)J	Variable, diversity, joining
WT	Wild type
XLF	XRCC4-like factor
XRCC	X-ray cross complement protein

ABSTRACT

XLF-DEPENDENT NONHOMOLOGOUS END JOINING OF COMPLEX DNA DOUBLE-STRAND BREAKS WITH PROXIMAL THYMINE GLYCOL AND SCREENING FOR XRCC4-XLF INTERACTION INHIBITORS

By Mohammed Al Mohaini, M.S. Pharmacology and Toxicology

A dissertation submitted in partial fulfillment of the requirements for the degree of Doctor of Philosophy at Virginia Commonwealth University

Virginia Commonwealth University, 2015

Advisor: Lawrence F. Povirk, Professor, Department of Pharmacology and Toxicology

DNA double-strand breaks induced by ionizing radiation are often accompanied by ancillary oxidative base damage that may prevent or delay their repair. In order to better define the features that make some DSBs repair-resistant, XLF-dependent nonhomologous end joining of blunt-ended DSB substrates having the oxidatively modified nonplanar base thymine glycol (Tg) at the first (Tg1), second (Tg2), third (Tg3) or fifth (Tg5) positions from one 3' terminus was examined in human whole-cell extracts. Tg at the third position had little effect on end-joining even when present on both ends of the break. However, Tg as the terminal or penultimate base was a major barrier to end joining (>10-fold reduction in ligated products) and an absolute barrier when present at both ends. Dideoxy trapping of base excision repair intermediates indicated that Tg was excised from Tg1, Tg2 and Tg3 largely if not exclusively after DSB ligation. However, Tg was rapidly excised from the Tg5 substrate, resulting in a reduced level of DSB

ligation, as well as slow concomitant resection of the opposite strand. XLF^{L115D} mutant completely eliminates ligation of all five substrates and previous X-ray crystallography shows that XLF binds to XRCC4 via a “leucine lock” motif wherein L115 of XLF slips into a hydrophobic pocket in XRCC4. This makes the XRCC4-XLF interaction a good target to develop peptide inhibitors in order to radiosensitize breast tumor cells that are dependent on NHEJ to repair their DSBs after ionizing radiation exposure. Using mRNA display, we created a diverse library of 870 billion unique peptide sequences. After seven rounds of *in vitro* selection, the eluted fusions were cloned and sequenced. The results showed homology of sequences of five main families. We have selected representative peptides from those families (Pep 7.1-7.5), and several were chemically synthesized. However, none of these significantly inhibited XLF-dependent end joining in whole-cell extracts. Overall, the results suggest that promoting ligation of DSBs with proximal base damage may be an important function of XLF, but that Tg can still be a major impediment to repair, being relatively resistant to both trimming and ligation. The effectiveness of XLF-XRCC4 inhibitors in blocking nonhomologous end joining remains to be determined.

1. INTRODUCTION

1.1 DNA Damage

DNA damage can arise from endogenous and exogenous sources. There are different forms of DNA damage such as intrastrand crosslinks, interstrand crosslinks, base lesions, DNA single-strand breaks (SSBs), and DNA double-strand breaks (DSBs) (Lindahl, 1993). DSBs are the most deleterious lesions among all forms of DNA damage and they are characterized by a breakage in the sugar phosphate backbone of both DNA strands. The sources of DNA DSBs include ionizing radiation (IR), radiomimetic drugs (e.g. bleomycin and neocarzinostatin), oxidative stress, topoisomerase poisons, and cellular processes such as V(D)J recombination, class-switch recombination and stalled replication forks (Povirk, 2012; Kasten and Bartek, 2004). Unrepaired DNA DSBs can lead to cell death whereas mis-repaired DNA DSBs can result in mutation, chromosomal translocation, genomic instability and cancer (Alberto & Stephan, 2010).

1.2 Ionizing Radiation

Ionizing radiation (IR) is an essential part in the treatment of many types of cancer. Electromagnetic radiation such as X- and γ -rays and particulate radiation such as electrons, protons, alpha-particles, heavy charged ions and neutrons can cause DNA damage through direct and indirect actions (Han and Yu, 2009). The direct pathway is through a direct interaction with DNA to cause ionization that results in biological changes. The indirect pathway is through the ionization of atoms or molecules, mainly water, in cells to form free radicals, which interact with and damage DNA. Free radicals are highly reactive,

and they are formed when water inside a cell absorbs the deposited energy and rapidly produces oxidizing and reducing reactive hydroxyl radicals ($\cdot\text{OH}$) that interact with DNA and induce damage.

In general, IR causes base damages, SSBs and DSBs. Damage to nucleotide bases can be repaired by the base excision repair pathway, which also repairs SSBs (von Sonntag, 1987). However, the dominant and most serious DNA damage after an exposure to ionizing radiation is DSB which can be repaired by homologous recombination (HR) and non-homologous end joining (NHEJ). Nevertheless, IR can cause “clustered” damages that include SSBs or DSBs in addition to base damages, or multiple DSBs at different closely adjacent positions (Nikjoo et al., 1999; Boudaiffa et al., 2000). It is also very important to differentiate between the DNA damage produced exogenously by IR and that produced endogenously by reactive oxygen species (ROS) such as O_2^- , H_2O_2 and $\cdot\text{OH}$ which resulted from normal cellular metabolism (Wiseman & Hall, 1996; Ward, 1998). While both IR and ROS produce damaged termini such as 3'-phosphate, the dominant DNA damage induced by ROS are base damage and SSBs, with about 0.5% of the generated damage being DSBs. The distribution of DSBs induced by ROS throughout the DNA appears to be “uniform” to some extent. However, IR produces complex lesions with clustered damages as a result of heterogeneous energy deposition by IR (Han and Yu, 2009).

The free radicals produced by IR generate blocked termini such as 3'-phosphoglycolate (3'-PG), 3'-phosphoglycoaldehyde, 3'-formyl phosphate 3'-3'-keto-2'- deoxynucleotide and 5'-aldehyde (Hutchinson, 1985; Dedon, 2008; Ildar et al., 1981) (Figure 1.1). In general, these products are unstable and degrade immediately to produce breaks with 5'- and 3'- phosphate. Interestingly, 3'-PG as well as another oxidative product, thymine glycol (Tg), are chemically stable, which makes experiments involving these modifications more tractable (Evans et al., 2004).

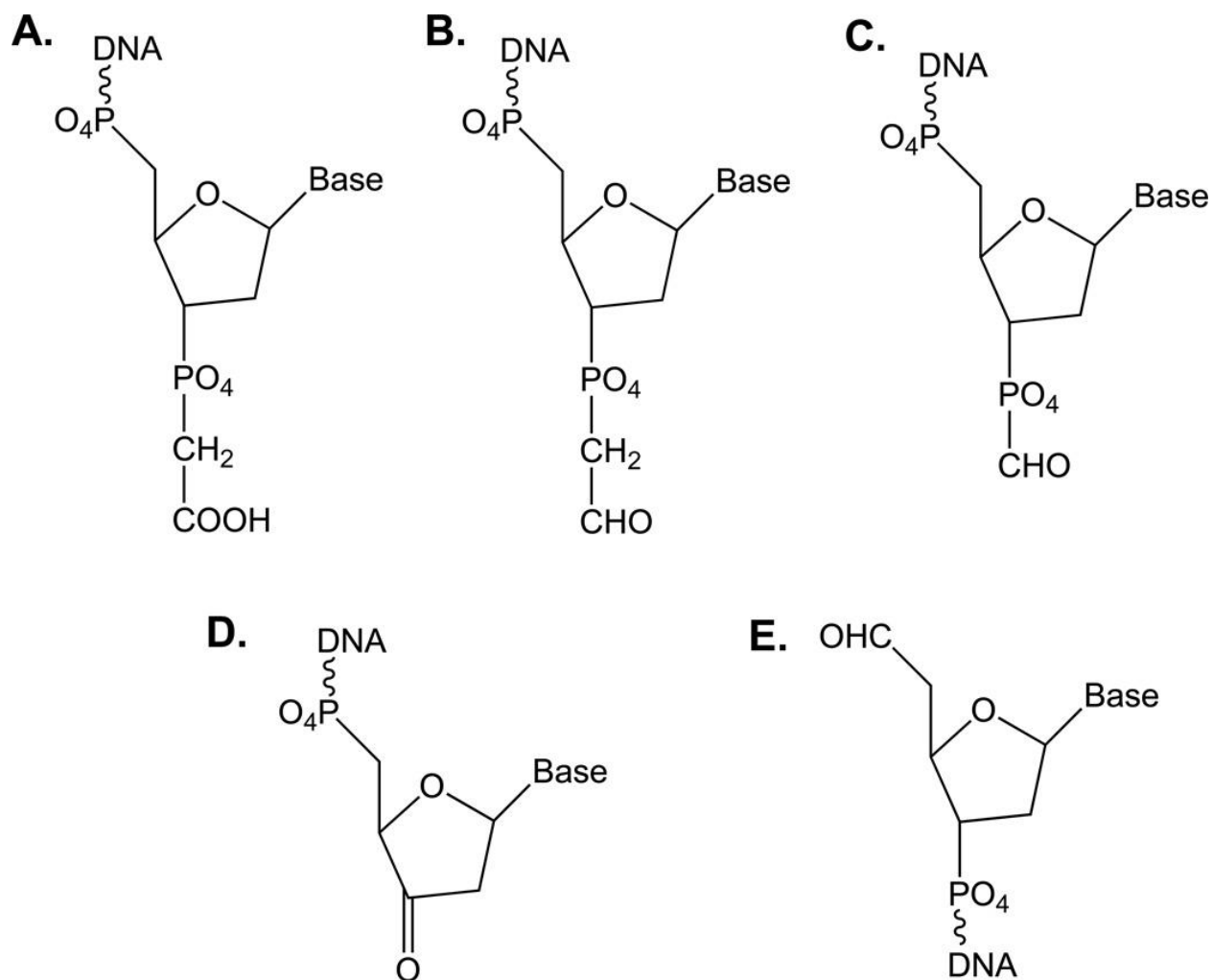


Figure 1.1. Some of the major damaged termini of free radical-mediated DNA strand breaks. A. 3'-phosphoglycolate (PG). B. 3'-phosphoglycoaldehyde. C. 3'-formyl phosphate. D. 3'-keto-2'-deoxynucleotide. E. 5'-aldehyde. (Povirk, 2013)

1.3 Thymine Glycol

Thymine is paired to adenine in the opposite strand in duplex DNA. Oxidative damage to thymine by IR, including that used in cancer therapy, and other chemical oxidizing agents results in 5,6-dihydroxy-5,6-dihydrothymine, known as thymine glycol (Tg) which is the most common thymine oxidation product (Teoule et al., 1974; Frenkel et al., 1981) (Figure 1.2). Tg is also formed endogenously as result of aerobic metabolism. It is predicted that about 400 Tg moieties are generated per cell per day (Cathcart et al., 1984; Saul and Ames, 1986). Also, Tg causes distortion in the regular structure of DNA. The loss of aromatic property, and the presence of hydroxyl groups at the 5 and 6 sites of the ring makes Tg nonplanar (Evans and Dizdaroglu, 2004). Thymine glycol has been shown to be less mutagenic but a lethal lesion *in vivo* (Hayes et al., 1988). Nevertheless, the presence of both Tg and 8-oxoguanine in the bistranded clustered damage site led to an increase in the mutagenic potential of 8-oxoguanine by Tg (Bellon et al., 2009).

While most of the IR-induced DSBs are efficiently being repaired by C-NHEJ, Tg may have a potential to render DSBs resistant to DSB repair and to block or slow their rejoining. Therefore, it is very important to understand how the Tg is being processed in DSB repair pathways and particularly through the NHEJ.

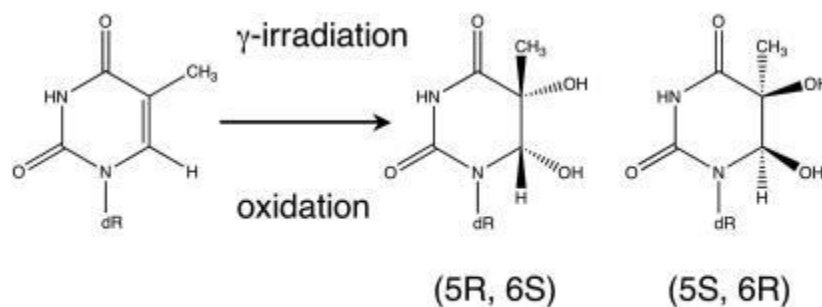


Figure 1.2. Oxidation of thymine to thymine glycol. (Pierre et al., 2007)

1.4 Base Excision Repair

Base excision repair (BER) plays an important role in repairing oxidative DNA damage (McCullough et al, 1999, Rahmaniana et al., 2014). The first step in BER pathway is the recognition of the damaged base by a specific DNA glycosylase (Frosina et al., 1996). The main DNA glycosylase in *E. coli* that is responsible for removing oxidatized pyrimidines such as thymine glycol is endonuclease III (Nth) (Eide et al., 1996) while the endonuclease III homologue in mammalian is NTH1 (Aspinwall et al., 1997). The DNA glycosylase catalyzes the excision of the base by hydrolyzing the N-glycosidic bond leaving an Apurinic/Apyrimidinic (AP) site (Dianov et al., 2003). The developed AP site can be removed by AP endonucleases (APE1) in humans. Some glycosylases such as Nth and NTH1 also hold an intrinsic AP-lyase function and are able to hydrolyze the AP 3'-phosphodiester bond of the AP site generating 3' α,β -unsaturated aldehyde and 5'-phosphate products (Miral, 2005). The phosphodiesterase activity of APE1 removes the sugar leaving a 3'-hydroxyl. The repair proceeds with either short-patch repair or long-patch repair pathways (Slivar et al., 2011). The short-patch repair replaces only one nucleotide which is synthesized by DNA Polymerase β and the nick is ligated with XRCC1 and Ligase III proteins (Hegde et al., 2008). Long-patch repair involves replacement of several nucleotides (2-13 nucleotides). RFC, Polymerase δ/ϵ , and proliferating cell nuclear antigen (PCNA) are enzymes that are responsible for adding the missing nucleotides. This will result in 5' flap structure that can be removed by FEN1 while the nick is sealed by Ligase 1.

1.5 Major DSB Repair Mechanisms

1.5.1 Homologous Recombination (HRR)

HRR requires a sister chromatid to act as a template for repair; therefore, HRR is only active in late S and G2 phases of the cell cycle and it is an error-free repair pathway (Helleday et al., 2007). HRR is highly efficient in repairing DSBs due to replication fork collapse, IR and interstrand cross-links (Sung & Klein, 2006). In HRR, the DSB is first detected by the MRN complex, and the DNA ends subjected to 5'→3' resection by CtIP, DNA2 and exonuclease 1 to generate a 3'-single strand DNA (ssDNA) overhang (Li and

Heyer, 2008). Also, CtIP is known to be regulated by CDK and ATM (Chen et al, 2008; Li et al, 2000). After that, replication protein A (RPA) binds to the 3'-ssDNA overhang to prevent premature strand invasion. Then, different proteins including Rad52, BRCA2 and the Rad51 paralogues (Rad51B, Rad51C, Rad51D, XRCC2 and XRCC3) are recruited to replace RPA with RAD51 (San et al., 2008). This allows Rad51 to form a filament to invade a homologous sequence. After that, DNA polymerase η is recruited to extend the 3'-DNA end which leads to capturing a second DSB end to form Holliday junctions; these junctions are resolved in a process involving different proteins resulting in crossover or non-crossover products (Helleday et al., 2007; Li & Heyer, 2008).

1.5.2 Classical Non-Homologous End Joining (NHEJ)

NHEJ is the primary repair mechanism of DSBs (Figure 1.3), and it is the main repair mechanism in G0 and G1; even though it can function throughout the cell cycle (Rothkamm et al., 2003). Also, NHEJ is essential mechanism in repairing DSBs due to V(D)J recombination (Jankovic et al., 2007). There are three main steps in the NHEJ pathway including the detection of DSBs, removal of the non-ligatable end groups and religation of the processed DNA ends (Williamson et al., 2009). In other words, repairing DSBs by NHEJ pathway involves nuclease, polymerase, and ligase activities (Lieber, 2010). Several studies have shown the importance of some proteins in NHEJ pathway in human cells. These proteins are Ku70/80 heterodimer (Ku), DNA-dependent protein kinase catalytic subunit (DNA-PKcs), DNA ligase IV, XRCC4 and XLF (Cernunnos) (Lieber, 2010). Once DSBs occur, the first step in NHEJ is the detection of the breaks, which is achieved by Ku in which Ku heterodimer is recruited to the end of the DNA damage (Weterings and Chen, 2008). When Ku binds, it acts as a scaffold to facilitate the binding of other NHEJ proteins. Also, Ku recruits DNA-PKcs, a member of the phosphatidylinositol-3 kinase-like family of serine-threonine protein kinases (PIKKs), to form the DNA-PK complex which tethers the DNA ends together (Williamson et al., 2009). Upon synapsis of the two DNA ends, DNA-PKcs phosphorylates itself in trans leading to its dis-

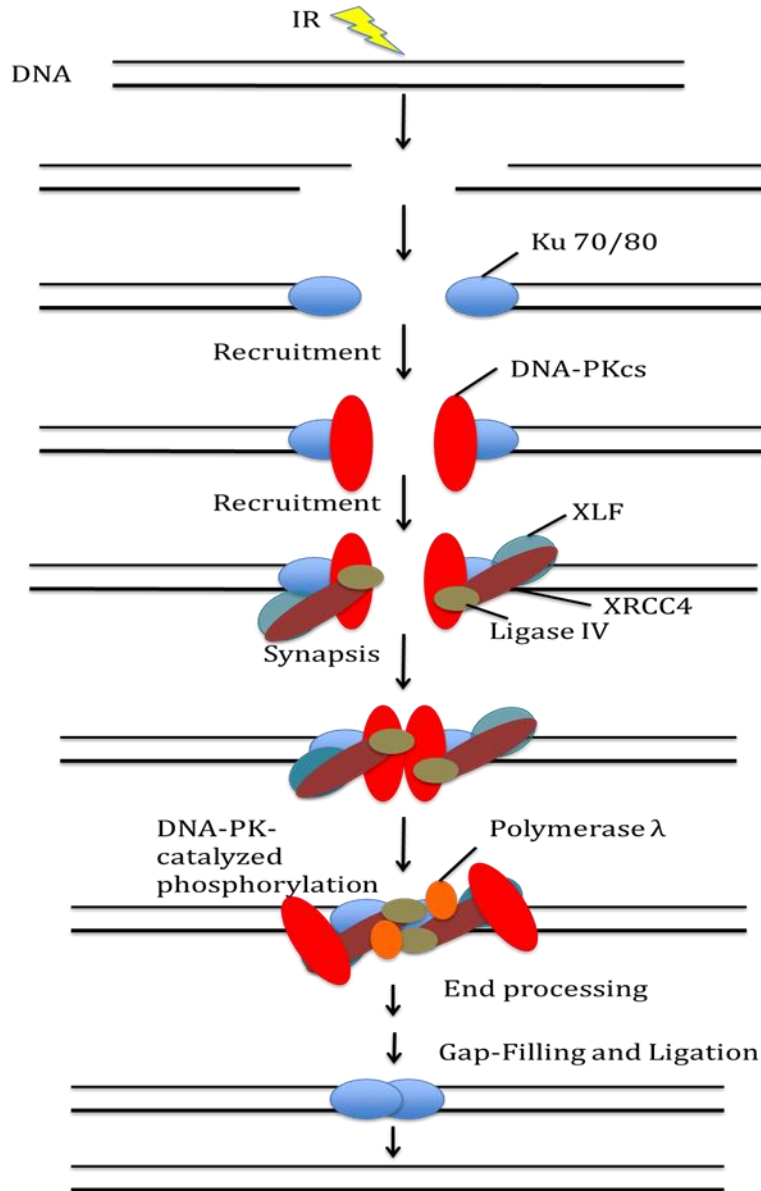


Figure 1.3. Nonhomologous end joining. The Ku 70/80 heterodimer binds to DNA DSB ends and recruits DNA-PKcs. This is followed by the recruitment of XLF:XRCC4:DNA ligase IV to the DNA ends which in turn leads to the synapsis of the two ends. DNA-PK autophosphorylation causes a conformational change followed by its dissociation from the DNA ends. This facilitates the access of downstream endonucleases proteins to process the DNA ends before gap filling by pol μ and λ and ligation that mediated by DNA ligase IV. Adapted from (Povirk and Valerie 2003).

sociation from the DNA ends, which facilitates the access of downstream proteins, to the ends of the DSB (Weterings, 2007). After that, polymerases μ and λ are involved in gap filling (Mahaney et al., 2009), and the ends are ligated by the XRCC4-DNA ligase IV complex (X4L4), which is stimulated by an interaction between XLF and XRCC4. Also, there is a subpathway of NHEJ which may be necessary for a subpopulation of more-difficult-to repair DSBs, such as DSBs with heavily damaged termini, DSBs in heterochromatin, or DSB whose ends have become physically separated (reviewed in Valerie & Povirk, 2003). This subpathway requires additional proteins (see below).

1.5.3 The Choice of DSBs Repair Method

Both DSB structure and chromatin complexities can affect the speed and choice of DSB repair pathway (Shibata et al., 2011). When the DSBs occur in euchromatin DNA (EC-DNA) without DSB complexity, DSBs would be efficiently repaired with faster kinetics by NHEJ pathway independent to the cell cycle phase. However, if DSBs occur in EC-DNA with high complexity, these DSBs would be repaired with slow kinetics in G1 and G2 phases by NHEJ, but NHEJ will stall in G2 phase allowing the DSBs to undergo resection to be repaired by HR. However, in case of chromatin complexity, the DSBs would be repaired by NHEJ with slow kinetics in G1 phase. Again, in G2 phase, NHEJ is inefficient and will stall allowing resection of the DSBs that would be repaired by HR. However, the HR pathway can be switched to NHEJ for DSB repair in heterochromatin if the CtIP-dependent DSB end resection does not occur (Shibata et al., 2011).

1.6 NHEJ Core Proteins

1- The Ku70/80 heterodimer:

The Ku heterodimer is composed of Ku70 (70 kDa) and Ku80 (86 kDa) subunits (Walker 2001), and it is responsible for detecting the DSB and tethering the DNA ends. Ku shows high binding affinity to ends of dsDNA without sequence specificity (Downs and Jackson, 2004). X-ray crystallography

indicates that the end-bound Ku occupies about 16-18 bp (Walker et al., 2001). The DNA binding domain is located at the C-terminus of Ku70 (Lees-Miller, 2003), while Ku80 has a conserved regions at the extreme C-terminus which is required for the interaction with DNA-PKcs. (Falck et al., 2005). *In vitro* studies have shown that Ku also interacts with other NHEJ proteins including XRCC4-DNA ligase IV (X4L4) complex, XLF, DNA pol μ and DNA pol λ (Mahaney et al., 2009). *In vivo* studies have shown that Ku is essential for the recruitment of DNA-PKcs, XRCC4 and XLF to DNA damage sites.

2- DNA-PKcs:

The molecular weight of DNA-PKcs is 469 kDa (4128 amino acids). It is a product of PRKDC gene, and it is a member of the phosphatidylinositol 3-kinase like family of protein kinases (PIKKs) (Williamson et al., 2009). DNA-PKcs deficient cells have shown an increase in radiosensitivity as well as a defect in V(D)J recombination while the deficiency of DNA-PKcs in animals shows phenotype of severe combined immunodeficiency (SCID) (Meek et al., 2004). The DNA binding domain of DNA-PKcs is located within the amino terminal region (Gupta and Meek, 2005). DNA-PKcs interacts with Ku through its C-terminus regions (Jin et al., 1997; Mordes et al., 2008). The binding affinity of DNA-PKcs to DNA increases in the presence of Ku (West et al., 1998). Once DNA-PKcs is recruited to DNA ends, it displaces Ku inward by about 10 bp (Yoo and Dynan, 1999). Then, it starts to phosphorylate other proteins but it initially starts by phosphorylating itself in trans (Meek & Lees-Miller 2008).

3- POL X Polymerases:

The pol X family of DNA polymerases including pol μ , lambda λ and terminal deoxynucleotidyl-transferase (TdT) have been reported to be involved in NHEJ. They are essential in filling of DNA gaps that usually form after processing of IR-induced DNA damage (Povirk, 2006; Bertocci et al., 2006; Lee et al., 2003). These enzymes have a BRCT (BRCA1 C-terminal) domain which is essential

for their interactions with core NHEJ proteins forming a complex at the DNA ends (Ramsden, 2011). BRCT-containing proteins have shown to be directly or indirectly involved in DNA damage response and repair (Bork et al., 1997). DNA pol μ and λ interact with Ku and X4L4 complex through their BRCT domains in order to be loaded at the DSBs. These two polymerases appear to function in most of the NHEJ process while TdT interacts with Ku and appears to be involved in V(D)J recombination only (Nick McElhinny and Ramsden, 2004). The quality of NHEJ repair depends on these polymerases even though cells deficient in pol μ and λ do not show an increase in radiosensitivity (Ramsden, 2011).

4- XRCC4:DNA ligase IV and XLF:XRCC4:DNA ligase IV complex:

The XRCC4 gene was isolated by complementation of radiosensitivity, V(D)J recombination deficiency and DSB repair deficiency of the Chinese Hamster ovary derivative XR-1 (Li et al., 1995). XRCC4 was found to be associated with DNA ligase IV, and in *in vitro*, the X4L4 complex is critical for ligation of broken DNA ends through the NHEJ mechanism (Critchlow et al., 1997). Also, XRCC4 in cells was found to stabilize the DNA Ligase IV (Bryans et al., 1999). The ligation activity of X4L4 is stimulated by an interaction with XLF; the most recently discovered core protein of NHEJ (Ahnesorg et al., 2006; Buck et al., 2006). XLF was identified initially as missing gene in a subset of severe combined immune deficiency (SCID) patients with characteristics of growth retardation, microcephaly, immunodeficiency, increased cellular radiosensitivity and a defective V(D)J recombination (Buck et al., 2006). Both proteins have no known enzymatic function, yet in mammalian cells, XRCC4^{-/-} and XLF^{-/-} genotype show increased sensitivity to ionizing radiation associated with severe defects in DSB repair (Giaccia et al., 1990; Zha et al., 2007).

1.7 Other Proteins Involved in NHEJ

5- Tyrosyl-DNA phosphodiesterases:

TDP1 is a highly conserved eukaryotic DNA repair enzyme that catalyzes the removal of covalent 3'-DNA. The gene initially was isolated from *Saccharomyces cerevisiae* and was shown to repair stalled TOP1-DNA covalent complexes (Yang et al., 1996). Also, yeast TDP1 was shown to regulate the accuracy of NHEJ (Bahmed et al., 2010). Human TDP1 works on both SSBs and DSBs and it is involved in the removal of tyrosyl-linked peptides and simple tyrosyl moieties from 3' ends to produce a 3'-phosphate that can be converted to 3'-hydroxyl by PNKP (Reviewed in Povirk, 2012). However, TDP1 is less efficient in removing other 3' lesions such as 3'-PG and cleaved abasic sites. TDP1 is associated with the autosomal recessive neurodegenerative disease spinocerebellar ataxia with axonal neuropathy (SCAN1) (Takashima et al., 2002). TDP 2 is involved in the NHEJ mechanism through resolving the DSBs induced by TOP 2 (Gómez-Herreros et al., 2013). The mechanism by which TOP 2 induces DSBs is through promoting the relaxation and passage of duplex DNA (Deweese and Osheroff, 2009). TOP 2 is covalently attached to the two DNA ends through a phosphodiesterase bond to form tyrosyl DNA ends. TDP 2 has a strong activity toward the 5'-tyrosyl DNA ends and weak activity toward the 3' ends (Gómez-Herreros et al., 2013)

6- Polynucleotide kinase/phosphatase (PNKP)

PNKP has 3'-DNA phosphatase and 5'-DNA kinase activities which removes 3'-phosphate and phosphorylates 5' ends (Pheiffer and Zimmerman, 1982; Habraken and Verly, 1988) with no known function on other modified ends such as 3'-PG (Inamdar et al., 2002). PNKP has shown a role in NHEJ through an interaction with XRCC4 which promotes its recruitment to the DSB (Koch et al., 2004). PNKP also binds to XRCC1 to work on SSBs (Whitehouse et al., 2001).

7- Artemis:

Artemis possesses an intrinsic 5'→3' exonuclease activity and, in the presence of DNA-PKcs and ATP, it acquires endonuclease activity that opens DNA hairpins during V(D)J recombination process (Ma et al., 2002 and 2004) and removes and shortens long 3' and 5' overhangs at DSBs.

Deficiency of Artemis in humans results in radiation-sensitive severe combined immunodeficiency (RS-SCID) (Moshous et al., 2001). Artemis doesn't appear to be a major enzyme in DSB repair; nevertheless, it may be required for optimal rejoining of a subset of DNA damage events (Poinsignon et al., 2004; Wang et al., 2005). Artemis has been shown to trim 3'-PG-terminated overhangs to provide a 3'-hydroxyl ends (Povirk et al., 2007). Interestingly, the presence of a 5'-phosphate terminus is essential for the 5'→3' exonucleolytic activity of Artemis while it is not required for the endonucleolytic trimming activity (Povirk et al., 2007)

8- p53 binding protein 1 (53BP1)

53BP1 was identified to bind to the central domain of human tumor suppressor protein p53 (Iwabuchi et al., 1994) that is responsible for site-specific DNA binding. Interestingly, the binding of 53BP1 requires the p53 protein to be in its wild type conformation. The interaction between 53BP1 and p53 appears to be through the BRCT domains of these proteins (Joo et al., 2002, Derbyshire et al., 2002). The BRCT motif of 53BP1 has a homology to BRCA1 and scRad9 (Callebaut and Morion, 1997). 53BP1 has been shown to be involved in the DNA damage response pathway (Rappold et al., 2001) and it becomes hyperphosphorylated and immediately relocates to multiple nuclear foci in response to IR. In addition, 53BP1 has been shown to promote c-NHEJ in Ku 70/80 and DNA ligase IV dependent manner (reviewed in Zimmermann and de Lange, 2014) mainly in class switch recombination (CSR), V(D) J recombination, telomere dysfunction, BRCA1-deficient cells, and centromeric heterochromatin.

Other enzymes that may be involved in the end processing include MRE11, Werner's syndrome protein (WRN), Aprataxin, PNK like factor (APLF), Apurinic/apyrimidic lyases (APE1 and APE2), Metnase (Valarie & Povirk, 2003, Mahaney et al., 2009; Povirk, 2012).

1.8 Upregulation of NHEJ in Breast Cancer

1.8.1 Breast Cancer

Breast cancer in the United States is one of the most common cancers among women. It is the second leading cause of cancer death in women, surpassed only by lung cancer (ACS, 2014). Also, breast cancer is the number one cancer killer in women aged 20-59 years old (Ahmedin et al., 2010). There is a chance of one out of eight women that will have an invasive breast cancer some time during their lives. Also, one out of 36 women expected to die in 2015 will do so as a result of breast cancer.

Breast cancer treatment requires multiple approaches. The recommended treatment for most patients with “invasive” breast cancer is surgical removal of primary tumor, systemic chemotherapy and/or hormonal therapy as well as radiotherapy (Buchholz, 2009). Breast irradiation is indicated for most patients who undergo breast-conserving surgery (lumpectomy). Also, radiation therapy is recommended after mastectomy for patients who are at high risk of developing recurrence (Shenkier et al., 2004). The current treatment available for breast cancer has shown to be quite effective in suppressing the breast cancer growth and improving patients’ quality of life (Buchholz, 2009). However, the risk of breast cancer recurrence is still not uncommon. Recurrent breast cancer can occur months or years after the initial treatment. Breast cancer recurrence can reappear as local recurrence at the original tumor site (invasive or noninvasive ipsilateral breast tumor recurrence), as regional recurrence in the axilla, chest muscle, internal mammary lymph nodes or supracavicular fossa lymph nodes, or as distant recurrence (metastasis) in which the tumor cells leave the breast tissue and spread to other sites including bone, lungs, brain and other organs (Millar et al., 2009; Clarke et al., 2005; Bruce et al., 2006). The prognosis of recurrence and metastatic breast cancer is generally poor and associated with high resistance to further treatment and reduced survival rate (Dean-Colomb and Esteva, 2008; Gonzalez-Angulo et al., 2007; Jameel et al., 2004).

1.8.2 The Choice of DSBs Repair Mechanism in Breast Cancer

Breast cancers can be divided into two types; the first type, known as sporadic breast cancer, develops after conception and accounts for 90-95% of breast cancer cases. The other type of breast cancers is familial breast cancer due to mutated genes inherited from one's parents. It accounts for 5-10% of all breast cancers, and about 35 - 45% of familial breast cancer can be attributed to mutation in two different tumor suppressor genes known as BRCA1 and BRCA2 (Rosen et al., 2003; Miki et al., 1994; Wooster et al., 1995). Nevertheless, mutations in either of BRCA1 or BRCA2 occur occasionally in sporadic breast cancer (Futreal et al, 1994; Lancaster et al, 1996). In addition to the role of mutated BRCA1 and 2 in predisposing individuals to breast cancer, these two proteins play an important role in protecting genome stability by responding to DNA damage. Particularly, these genes have been shown to be involved in DSBs repair and are mainly critical for efficient HR but appear to play only a minor role in NHEJ, although BRCA1 may influence NHEJ fidelity (Gudmundsdottir and Ashworth, 2006; Nagaraju and Scully, 2007; H. Wang et al., 2001; Zhuang et al., 2006). Many sporadic breast tumors show allelic loss (Johnson et al., 2002) and/or reduced expression of BRCA1 and BRCA2 (Birgisoittir et al, 2006; Jaspers et al., 2009; Yshikawa et al., 1999; Wilson et al., 1999) suggesting that those tumors would be more dependent on NHEJ. Conversely, breast tumor cells often show upregulation of receptors of the epidermal growth factor (EGFR) family (Johnson et al., 2006), which have been implicated in radioresistance (Contessa, Abell, Mikkelsen et al., 2006; Contessa, Abell, Valerie et al., 2006) and stimulation of NHEJ (Das et al., 2007). Therefore, targeting NHEJ may selectively increase radiosensitivity of many breast tumor cells.

1.8.3 XRCC4-XLF Interaction as a Target for Radiosensitization

Crystal structure studies of XRCC4 and XLF show structural similarity (Figure 1.4 and Figure 1.5) in which both proteins form homodimers and have similar N-terminal head domains and long α helical tails (Li et al., 2008; Andres et al., 2007; Junop et al., 2000). Mutagenesis studies of the head domains of XRCC4

and XLF (Figure 1.5) found residues E55, D58, M61 and F106 of XRCC4, and R64, L65 and L115 of XLF as critical to XRCC4-XLF interaction (Ropars et al., 2011; Malivert et al., 2010). Based on the crystal structures of XRCC4 and XLF, and based on mutagenesis analysis, it has been suggested that these two proteins could form filaments of alternating XRCC4-XLF dimers which could twist a DSB and help to align the ends (Andres et al., 2007). Regardless of the accuracy of the predicted filament formation between XRCC4 and XLF, the interaction between these proteins is essential for NHEJ. Thus, this critical interaction should be susceptible to disruption by small peptides that bind this XLF-interacting region of XRCC4, and such disruption should severely suppress NHEJ.

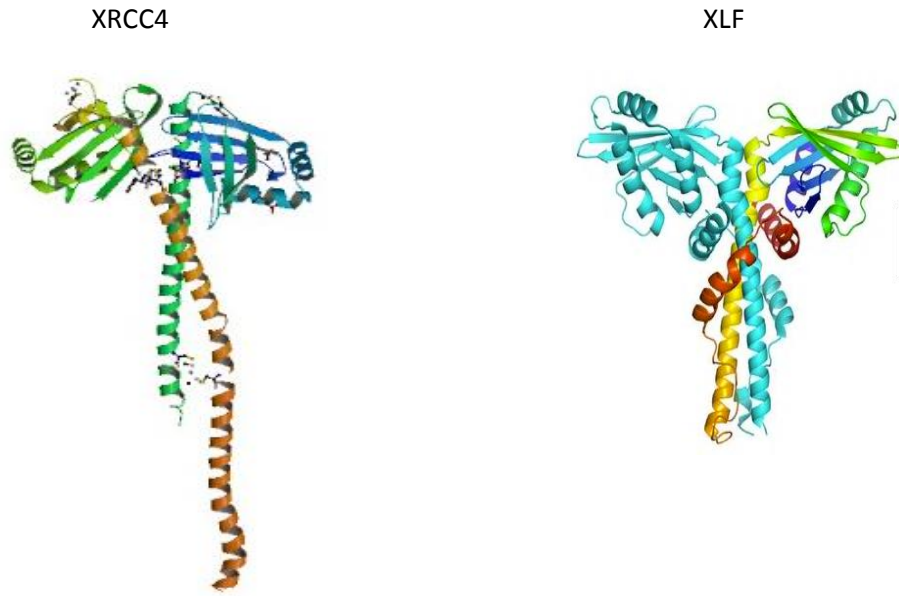


Figure 1.4. Crystal structures of XRCC4 and XLF. Both XRCC4 and XLF have a head domain and long α helix
(Andres et al., 2007)

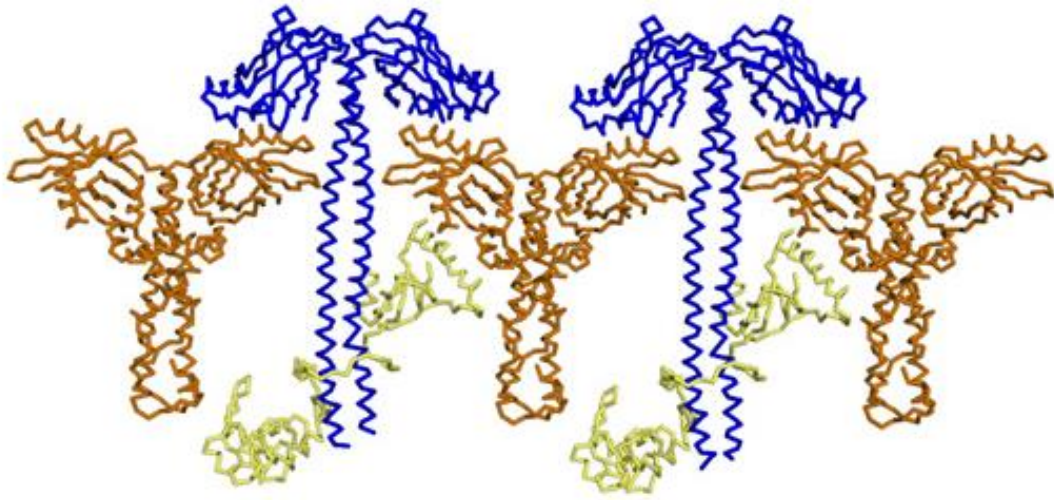


Figure 1.5. Filaments of alternating XRCC4-XLF dimers. Proposed filaments that show the formation of alternating filaments between XLF (orange) and XRCC4 (blue). The binding of XRCC4 to Ligase IV (yellow) is also indicated (Andres et al., 2007).

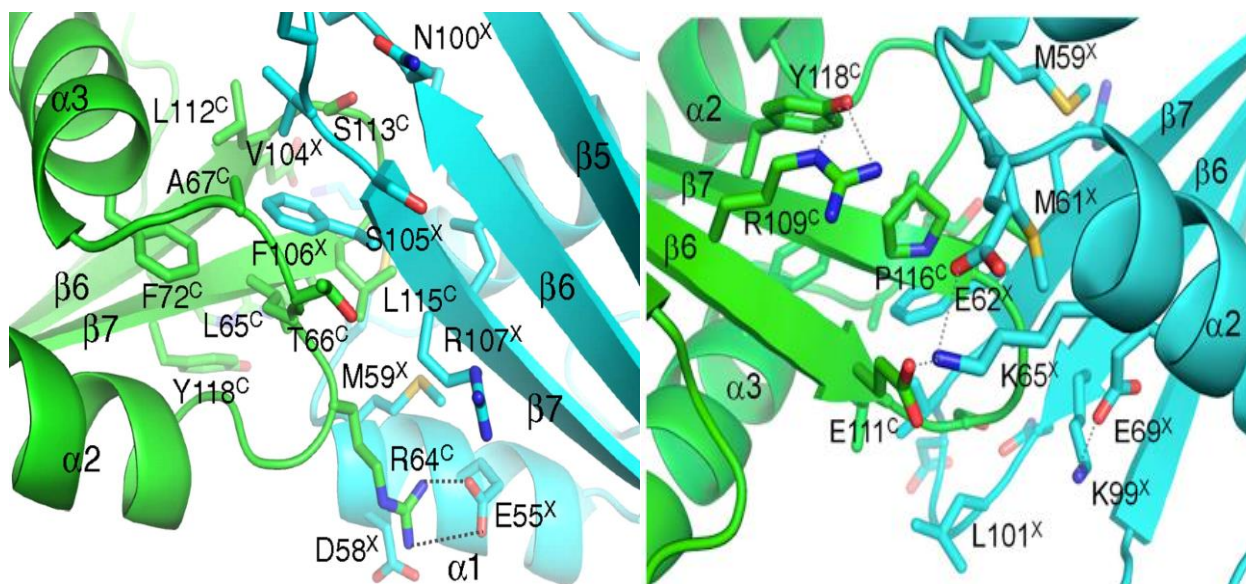


Figure 1.6. Interface of the XRCC4¹⁻¹⁵⁷-XLF¹⁻²²⁴ complex formed by the distal part of their N-terminal head domains. Residues involved in the interface between XRCC44 (cyan) and XLF (green) are shown in a stick representation. Residues are labeled with “X” and “C” superscripts for X4 and Cernunnos (XLF), respectively. Dashed lines indicate inter- and intra-molecular hydrogen bonds and salt bridges between side-chain atoms proposed from Rosetta modeling. (Taken from Ropars et al., 2011)

1.9 XRCC4-XLF Interaction as a Good Druggable Target

Many proteins produce their functions by interacting with other proteins. XRCC4-XLF interaction is one of those which occurs only in NHEJ and this mechanism is highly upregulated in most breast cancers. The nature of the interaction between XRCC4 and XLF that occurs in a distinct region facilitates inhibitor design (Hammel et al., 2011)(Figure 1.7) . Also, the presence of a well characterized binding site with a hydrophobic Leu-lock motif makes this interface a good place to look by high-throughput screening for therapeutic inhibitors.

Peptides have become an interesting class of inhibitors, which can explore large contact surfaces involved in protein-protein interactions. The advantages of peptides include their flexibility, the ability to manipulate the procedure of their development to produce highly specific and tight binders, their small size, and their low toxicity (Higueruelo et al., 2013). There are many techniques available to search for peptides as modulators of protein-protein interactions and mRNA display is one of the best technologies in this field.

1.10 mRNA Display

mRNA display is an *in vitro* selection technology that can be used to synthesize libraries of mRNA-peptide fusions containing up to 10 trillion unique sequences (Roberts & Szostak, 1997). The main idea of this technology is the covalent attachment of the peptide chain to the 3' end of its own mRNA template. The process starts when the mRNA first becomes covalently attached at its 3' end to a puromycin containing short DNA linker via a psoralen photo-crosslink. During an *in vitro* translation, when the ribosome reaches the crosslinked region and translation pauses, puromycin mimics the 3' end of an incoming tRNA by entering the ribosome A-site and accepting the nascent peptide, forming the covalent bond between the mRNA and the peptide it encodes. Using a library of mRNAs transcribed from a synthet-

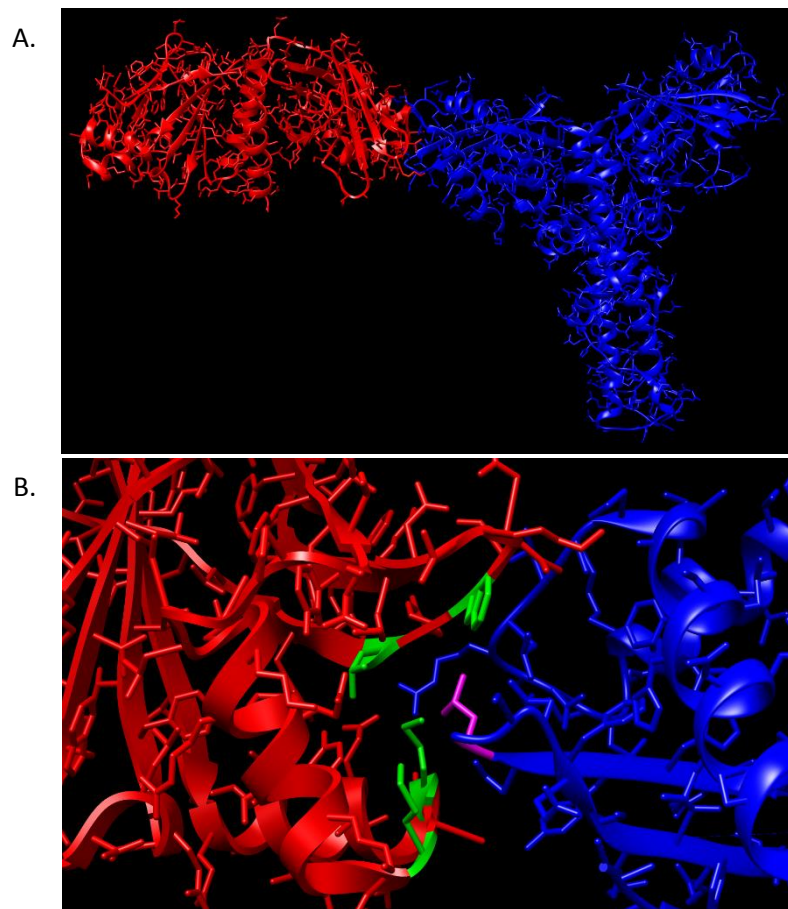


Figure 1.7. XRCC4-XLF interaction interface. A) Shows the interaction between XRCC4 (Red) and XLF (blue) through the head domain of these protein. B) Shows the hydrophobic pocket of XRCC4 where the XLF “Leucine” fits in.

ic DNA template, this process will create large collections of mRNA-peptide fusions. The RNA portion of the mRNA-peptide fusions can be reverse-transcribed and PCR-amplified, which allows for the identification of the functional peptide by DNA sequencing. Several rounds of selection and amplification can be carried out in order to allow for an enrichment of unique sequences with the required properties.

1.11 Advantages of mRNA Display Technique

1.11.1 Removal of non-specific binders:

It is very important to remove nonspecific binders which are sometimes selected as a result of some experimental biases. This requires increase in the stringency during the selection, which is not tolerable for some techniques. For example, the interaction of the peptides with the target occurs in the cell nuclei in the yeast two-hybrid technique (Huang et al., 2007), which prevents the increase in selection stringency. The other technique that cannot tolerate harsh selection condition is ribosome display (Hanes and Plückthun, 1997). While both mRNA display and ribosome display share some similarities such as using cell-free translation system and production of very high diversity library, they differ in the type of bond that links the mRNA and peptide. The mRNA and peptide are linked with stable covalent amide bond in mRNA display while they are linked with a less stable noncovalent bond in ribosome display. Therefore, very rigorous conditions cannot be used during the selection in ribosome display because the genotype is linked to the phenotype with a chemically fragile bond. In contrast, the freedom of using arbitrary selection conditions makes mRNA display advantageous over other techniques.

1.11.2 Development of Large Libraries:

Some of the selection techniques that are used to look for target-binding partners are limited in the abundance of their libraries. For example, phage display, which is an *in vivo* technique produces a library of about 10^8 - 10^{10} (Hammers and Stanley, 2014). Yeast two-hybrid is a cell-based selection

produces a library with about 1 million variants (Huang et al., 2007). However, mRNA display is a completely *in vitro* selection technique which can produce peptide libraries in the range of 10^{12} - 10^{14} unique sequences (Roberts & Szostak, 1997). The development of large library size results in an increase in the binding affinity of the selected peptides as well as an improvement in the specificity.

1.12 Applications of mRNA Display

mRNA display has many applications. For example, this method has been used to identify molecules that bound to TNF- α with a dissociation constant of 20 pM (Xu et al., 2002). Also, this technique was used to select molecules that bind to phosphorylated I κ B α with an affinity of 18 nM (Olson et al., 2008). Moreover, mRNA display was helpful in selecting Bcl-xL inhibitor with an IC₅₀ of 0.9 μ M (Matsumura et al., 2010). In addition, an inhibitor with an IC₅₀ of 2-5 nM has been identified by mRNA display to inhibit a protein-ligand interaction between VEGF and its receptor Flt-1 with 800 Å² of buried interfacial surface area (Getmanova et al., 2006; Wiesmann et al., 1997). Also, mRNA display has been used to develop two unnatural and one natural peptide inhibitors of thrombin with K_d in nanomolar range (Guillen Schilppe et al., 2012). The unnatural peptide inhibitors have K_d of 4.5 and 20 nM while the natural one has a K_d of 1.5 nM. Recently, Hartman's group used mRNA display and discovered the first nonphosphate or phosphonate-containing peptide that binds a (BRCT)₂ domain and blocks the protein-protein interactions of the BRCA1 (BRCT)₂ domain in cell lysates and disrupts HRR (White et al., 2015)

1.13 Specific Aims

- To assess the Tg resistance to DSB repair by examining end joining of defined DSBs with a proximal Tg in a cell extract-based system and the role of XLF in facilitating their repair.
- To develop peptide inhibitors of the XRCC4-XLF interaction in order to radiosensitize breast tumor cells.

2. METHODS

2.1 Production of Wild Type XLF and XLF mutants (L115A and L1145D) Proteins

2.1.1 Construction of XLF Mutants (L115A and L115D)

For expression in *Escherichia coli*, we have a full-length XLF gene cloned into plasmid pQE80L with an N-terminal 6× His tag (gift of Dr. David Chen, University of Texas Southeastern). The L115A and L115D mutants were generated using the QuickChange site-directed mutagenesis kit (Stratagene), and the following primers determined by the QuickChange Primer Design Program (Stratagene):

5'-AAATTCCAATAGAAGGGGGCGCCAGAGAGCTCACTTCG-3' and

5'-CGAAGTGAGCTCTCTGGCGCCCCTTCTATTGGAATTT-3' for L115A and

5'-AAATTCCAATAGAAGGGGTCGCCAGAGAGCTCACTTCG-3' and

5'-CGAAGTGAGCTCTCTGGCGACCCCTTCTATTGGAATTT-3' for L115D.

The mutated residues are highlighted in which the leucine (CTC) was mutated to either alanine (GCC) or to aspartic acid (GAC). Then, each mutant plasmid was transformed into *E. coli*. 5 µL pQE80L-XLF^{L115A} and pQE80L-XLF^{L115D} were transformed into *E. coli* competent (DH5 α) bacterial cells (Stratagene) by heat shock. The DNA and *E. coli* cells were mixed and placed on ice for 30 minutes, placed in a 42°C water bath for 45 seconds and placed on ice for 2 minutes. Following 2 minutes on ice, 1000 µL of LB broth was added followed by 1 hour incubation with agitation at 37°C. In order to grow a mix of colonies, following incubation, 10 µL, 100 µL, 200 µL of the transformation mix were spread on LB agar plates containing 100 µg/ml ampicillin and incubated at 37°C overnight. pQE80L contains an ampicillin resistance gene. Therefore, *E. coli* colonies that contain pQE80L should grow in the presence of ampicillin. Individual

colonies that grew on agar plates were selected using a sterile toothpick and each colony was added to 5 mL of LB medium containing 100 µg/ml ampicillin and incubated at 37°C overnight with gentle agitation. Plasmid DNA from individual colonies were isolated using mini-prep plasmid DNA isolation kit from QIAGEN. Confirmation that the plasmid DNA, isolated from the colonies, contained XLF^{L115A} or XLF^{L115D} and pQE80L was achieved by digesting the purified colonies with *Bam*HI and *Hind*III restriction enzymes and electrophoresis using a 1% agarose gel (Figure 2.1). Furthermore, confirmation was achieved by DNA sequencing (Figure 2.2).

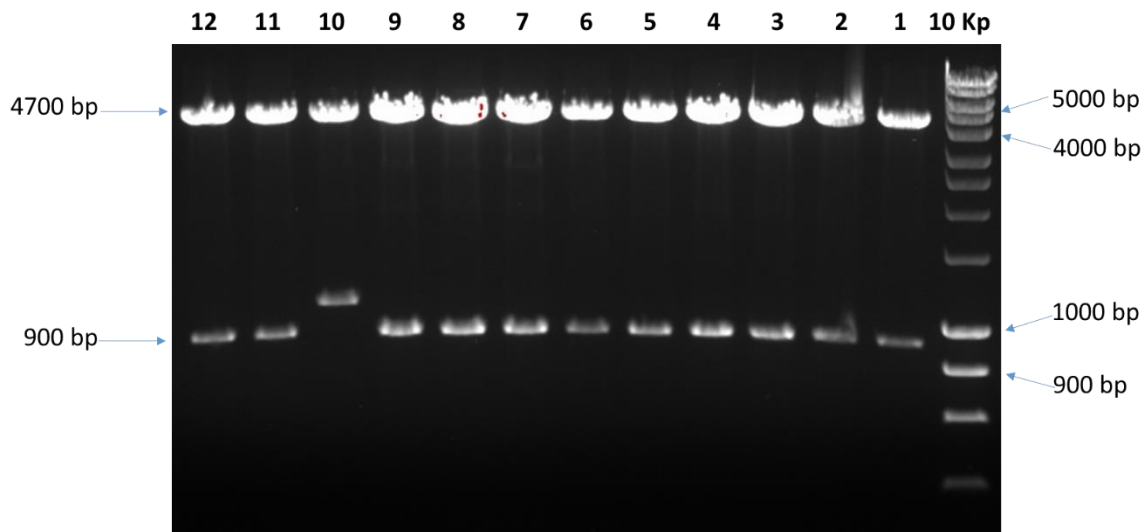


Figure 2.1 The full length XLF^{L115D} cut from pQE80L vector. Then, the XLF^{L115D} was cut out from the pQE80L vector with *Bam*HI and *Hind*III restriction enzymes. Two bands were formed; the upper band is around 4700 bp indicating the pQE80L vector and the lower band is around 900 bp indicating the XLF^{L115D} DNA. The results show that the samples in lanes 1-9 and 11-12 have an insert of the expected size.

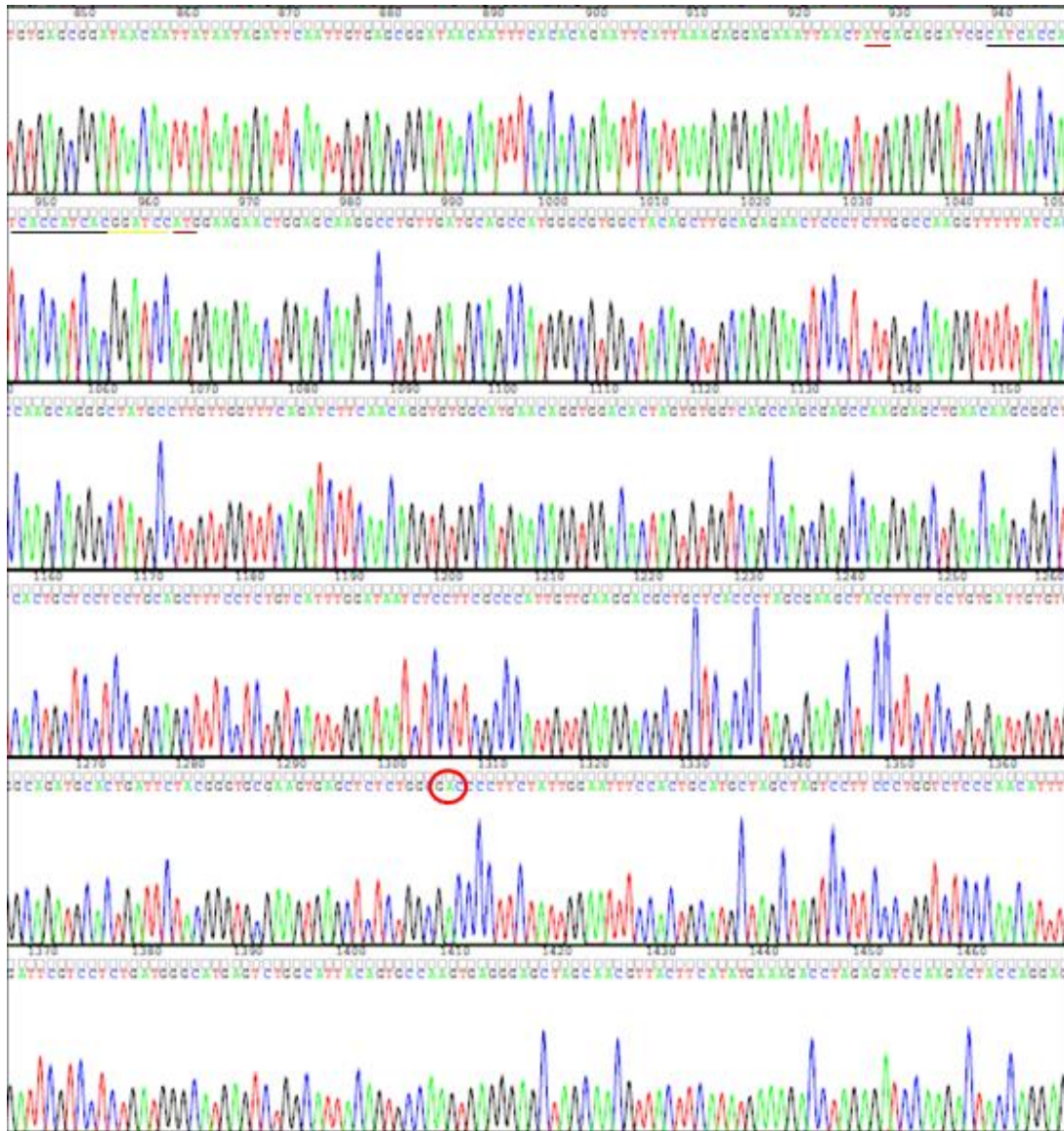


Figure 2.2 XLF^{L115D} sequence. Red circle indicates the site of the mutation inserted in which the Leucine (CAC) was mutated to Aspartic acid (GAC).

2.1.2 Production of Wild-Type XLF, XLF^{L115A} and XLF^{L115D} Proteins

Wild type and mutant plasmids were expressed in *E. coli* BL21 (DE3) competent cells and induced using IPTG. First, single colonies of the plasmids harboring wild-type, XLF^{L115A} or XLF^{L115D} were grown overnight at 37°C with agitation in 5 mL LB medium containing 100 µg/ml ampicillin. Then, 1 ml of the overnight cultures was transferred into four each of 2 L flasks containing 500 mL LB medium (each 500 mL culture contains 5 gm tryptone, 5 gm NaCl, 2.5 gm yeast and 500 µL of 100 µg/ml ampicillin). The four cultures were inoculated at 37°C with agitation and at an optical density (600 nm) of 0.5, IPTG was added to 1 mM for induction. Four hours later, the cells were centrifuged at 4000 rpm and 4°C for 30 minutes, and the dry pellets were stored at – 20°C until use.

2.1.3 Ni-NTA Purification

Cell pellets were left to thaw in ice and the pellet in each bottle was resuspended in 5 ml of freshly prepared Basic Buffer N (50 mM phosphate pH 8, 10% glycerol, 5 mM fresh 2-mercaptoethanol (BME), 20 mM imidazole and 0.5 M NaCl) and 150 µL His-compatible protease inhibitor (Merck, EMD). After that, the cells were transferred into a 50 mL centrifuge tube and sonicated 4X 45 seconds on 30% power (Sonic Dismembrator model 100 from Fisher Scientific). The lysed cells were diluted with 20 mL Basic Buffer N and centrifuged for 15 minutes at 15000 rpm at 4°C. Then, the supernatants were transferred into a 50 mL Falcon tube and mixed with 4 mL Ni-NTA resin (QIAGEN) and gently stirred for 1 hour at 4°C. After that, the mixture was transferred into a 20 mL Econo-Pac Chromatography Columns (Bio-Rad) the flow through was collected by gravity and the resin washed with 20 mL of Basic Buffer N and collected by gravity as well. The protein was eluted by gravity 6 times and each time was with 1 mL of Ni-NTA elution buffer (50 mM NaH₂PO₄, 300 mM NaCl and 250 mM imidazole; pH 8). All six fractions were analyzed by SDS-PAGE electrophoresis (Figure 2.3), and peak fractions were dialyzed against 20 mM Tris-HCl pH 8.0 overnight. XLF wild-type and mutants proteins were filtered (0.22 µm), loaded on a MonoQ FPLC column

(Pharmacia) and eluted with a gradient of 0–0.8 M NaCl in 20 mM Tris–HCl pH 8.0 over 20 minutes. Fractions were collected and analyzed by SDS–PAGE (Figure 2.4). XLF-containing fractions eluted at ~0.75 M NaCl and were stored at –20°C in the elution buffer plus 50% glycerol. Final concentration of the protein was determined using Pierce BCA assay with BSA as standard.

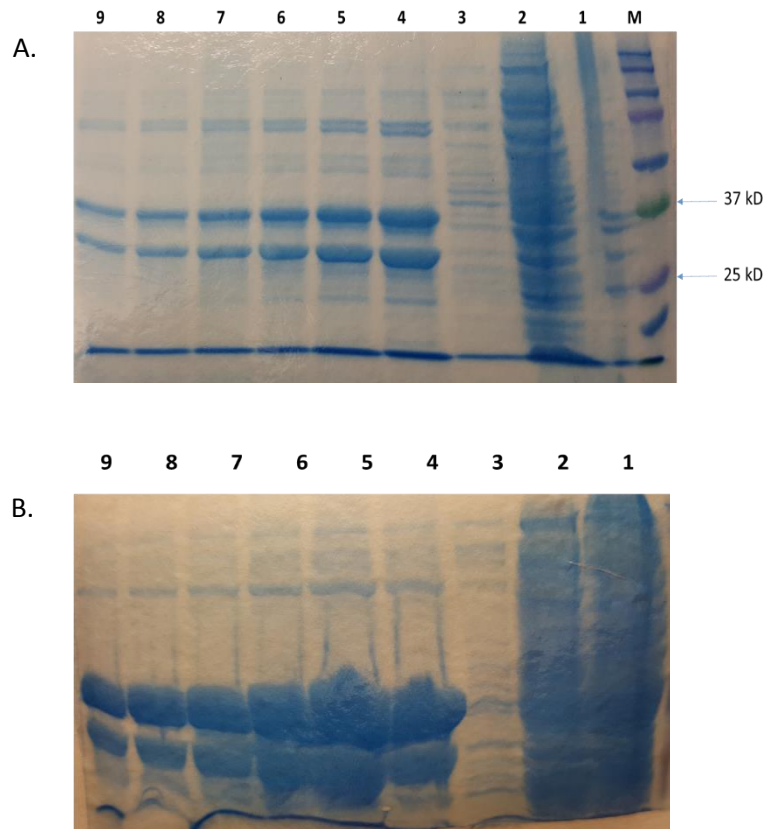


Figure 2.3 Protein composition of A) WT XLF and B) XLF^{L115D} after Ni-NTA purification as determined by SDS-PAGE. A) and B) 10% polyacrylamide gradient gel stained with coomassie blue. Lane 1: 30 µL of lysate was loaded (out of 5 mL). Lane 2: 30 µL of flow through was loaded (out of 5 mL). Lane 3: 30 µL of washes (out of 20 mL). Lane 4-9: 30 µL of different protein elutions (each elution was 1 mL). The results show that the samples in lanes 4-9 have the XLF protein on the expected size.

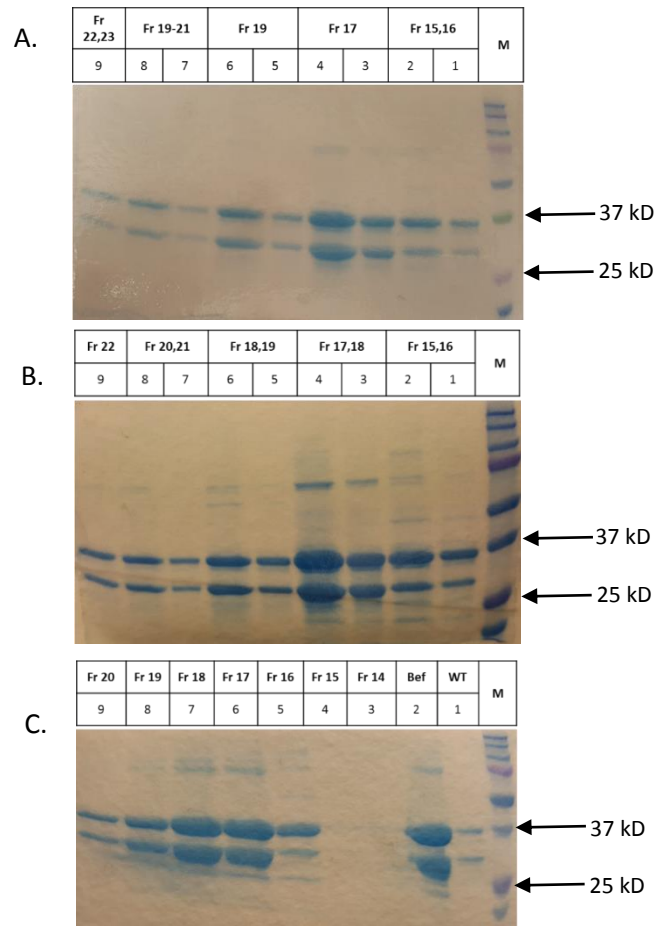


Figure 2.4 Protein composition after FPLC purification as determined by SDS-PAGE. Different fractions of each protein were collected and run on 10% polyacrylamide gradient gel stained with coomassie blue. (A) WT XLF and (B) XLF^{L115A}. Lane 1,3,5,7: 10 μ L of different fractions (each was 1 mL) was loaded. Lane 2,4,6,8,9: 30 μ L of different fractions (each was 1 mL) was loaded. (C) XLF^{L115D}. Lane 1: 30 μ L of WT XLF was loaded. Lane 2: 30 μ L of XLF^{L115D} protein before FPLC was loaded. Lane 3-9: 30 μ L of different fractions (each was 1 mL) was loaded.

2.2 Substrate

Plasmid pUC19 (34 µg) was cut with BstAPI and KasI and the larger 2.6-kb fragment was agarose gel-purified and electroeluted. The 25-mer ATGCGGATCGCGTTGTCT (50 pmoles), either unmodified or with Tg as the 3'-terminal base, was 5'-³²P end-labeled with T4 polynucleotide kinase (PNK) in a volume of 10 µl. After inactivation for 3 min at 90°C, it was annealed to 50 pmole of pAGACAACGCGATCCGCATATG by heating to 80°C followed by slow cooling to 10°C, resulting in a duplex with a 3-base -ATG 3' overhang that is complementary to the -CAT 3' overhang of the BstAPI site (Figure 2.5). Thus, 8 pmole of the duplex was ligated to 2 pmole of the BstAPI/KasI fragment by treatment with 12,000 units (4 µl) units T7 DNA ligase for 2 hr at 25°C in 130 µl of the buffer provided by the vendor (66 mM Tris-HCl, 10 mM MgCl₂, 1 mM ATP, 1 mM dithiothreitol, 7.5% polyethylene glycol, pH 7.6). Under these conditions, blunt-end ligation by T7 ligase is negligible (Doherty et al., 1996), so that the dominant product was a double-length plasmid joined tail-to-tail at the KasI sites, with the labeled duplex linked to each end (Figure 1A). This product was cut with SmaI and the final 2.1-kb substrate with one modified and one unmodified blunt end was gel-purified. Substrates with Tg as the second base (terminal sequence -TTGC-Tg-C), third base (-TTG-Tg-CT) or fifth base (-T-Tg-GTCT) from the 3' end, were similarly constructed.

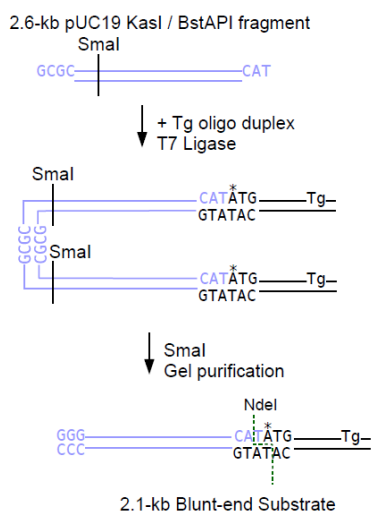


Figure 2.5. Tg-containing DSB substrates. Construction of modified substrates from short, end-labeled (*) Tg-containing duplexes and a fragment of pUC19. .

2.3 End Joining Reactions

Reactions in extracts contained 50 mM triethanolammonium acetate pH 7.5, 1 mM ATP, 1 mM dithiothreitol, 50 µg/ml BSA, 1.3 mM magnesium acetate and dNTPs (or ddNTPs) at 100 µM each. Typically, a 16-µl reaction contained 10 µl of extract, resulting in a final concentration of 8 mg/ml protein, 66 mM potassium acetate and 16% glycerol, and an effective Mg^{++} concentration of 1 mM (taking into account ~0.3 mM EDTA from the extract). Buffer components were first mixed with cell extract at 22°C. Recombinant proteins (XLF and/or Artemis) were then added, followed immediately by the substrate (20 ng). The reaction was again mixed by pipetting, and placed in a 37°C water bath, usually for 6 h. Samples were then deproteinized as described (Doherty et al., 1996), ethanol-precipitated in the presence of 1 µl GlycoBlue coprecipitant (Invitrogen), cut with NdeI and PstI (20 units each) for 3 hr in 40 µl of NEB CutSmart buffer (50mM potassium acetate, 20 mM Tris-acetate, 10 mM magnesium acetate, 100 µg/ml BSA, pH 7.9) and analyzed on 20% polyacrylamide DNA sequencing gels. Storage phosphor screens were exposed to frozen polyacrylamide gels for 40 hr, and images were analyzed with ImageQuant 5.1 software. For some experiments, samples were treated with *E. coli* endonuclease III (EndoIII) to cleave Tg-containing products. For treatment prior to restriction cleavage, half of each deproteinized, precipitated sample was treated with 20 units EndoIII for 2 hr at 37°C in 20 µl of the buffer provided by the vendor (20 mM Tris-HCl, 1 mM EDTA, 1 mM dithiothreitol, pH 8), followed by EndoIII inactivation for 20 min at 65°C and addition of NdeI, PstI and CutSmart buffer. In other experiments, after NdeI/PstI cleavage, sodium acetate was added to 0.3 M along with a 44-base oligomer (100 nM) complementary to the expected Tg-containing strand of a blunt-end ligation product. The sample was denatured at 90°C and then annealed by slow cooling to 10°C. Samples were then ethanol-precipitated and treated with EndoIII as above, and again precipitated prior to denaturing gel electrophoresis.

2.4 Polyacrylamide Gel Electrophoresis

Polyacrylamide gels (20x30x0.08cm) for electrophoretic separation contained 20% acrylamide:

bisacrylamide in a ratio of 20:1 with urea added to a final concentration of 8.3 M for electrophoretic separations. After the urea dissolved, the mixture was cooled to room temperature before adding 0.075% (w/v) ammonium persulfate and 0.03% (v/v) TEMED (N', N',N',N'-tetramethylethylene diamine). The gel was allowed to polymerize for 1 hour. Samples then loaded into the wells of the gel and electrophoresed at constant power of 42 watts for 3-4 hours in 1X TEB running buffer.

2.5 Statistics

Error bars represent standard error of mean (SEM) for at least three independent experiments.

Unpaired two-tailed t-tests were performed and the data were reported as significant for P values <0.05.

2.5 mRNA Display and *In Vitro* Selection

2.5.1 DNA library Synthesis

Five different DNA libraries have been synthesized (by Dr. Hartman) and used in the selection process. Briefly, each library encodes a fixed cysteine at the N-terminus and another cysteine after 2, 4, 6, 8, or 10 random amino acids in order to produce different cyclic sizes of peptides. The DNA sequence of the random library is:

TAATACGACTCACTATAGGGTTAACTTTACTAAGGAGGACAGCTAAATGTGCNNSNNSNNSNNSNNSNNSNNSNN
SNNSNNSNNSNNSNNSGGTAGCGGCTCCTTAGGCCACCATCACCATCACCAACGGCTATAGGTAGCTAG

The detailed sequence composition of each library is as follows:

- 1- TAATACGACTCACTATA: T7 promoter, followed by GGG with the first “G” as the transcription start.
- 2- TTAAC TT TAG: Epsilon enhancer.
- 3- TAAGGAGG: Shine-Dalgarno sequence, also known as the ribosome binding site.
- 4- ACAGCTAA: the Spacer between ribosome binding site and the start codon, with “AA” at end.

5- ATGTGCNNS'sTGCNNS's: translation start codon for methionine (ATG) and the codon for the fixed cysteine (TGC), followed by a mix of random NNS codons and another fixed cysteine at the site indicated above. We used the NNS (S=C/G) codon in the random region to decrease the prevalence of stop codons as compared to NNN (A=A/T/G/C). The translated peptides have the sequence of MCX2CX10GSGSLGHis6, MCX4CX8GSGSLGHis6, MCX6CX6GSGSLGHis6, MCX8CX4GSGSLGHis6, or MCX10CX2GSGSLGHis6, where X can be one of the natural amino acids.

6- GGCTCCGGTAGCTTAGGC: codons for GlySerGlySer- LeuGly, the flexible linker with two out-of-frame stop codons.

7- CACCATCACCATCAC: codons for His5 tag. The sixth His of His6 tag is in the following sequence.

8- CACCGGCTAT: hybridization region for the Psoralen crosslinker (XL-PSO oligonucleotide, see below). The CAC encodes the sixth His of the intact His6 tag.

9- AGGTAGCTAG: 3' -UTR to allow those non-crosslinked peptides to release at the in-frame TAG stop codons.

2.5.2 PCR Amplification of Library DNA

The DNA libraries were synthesized in reverse orientation. For example, CTAGCTACCTATAGCCGGTGGTGATGGTGATGGTGGCCTAAGGAGCCGCTACCSNNSNNSNNSNNSNNSNNSNNSNNSNNSNNSNNGCACATTTAGCTGTCCTCCTTAGTAAAGTTAACCTATAGTGAGTCGTATTA. Then, the DNA libraries were amplified by PCR using the following primers 5'-TAATACGACTCACTATAGGGTTAACTTTACTAAGGAGGACAG-3' and the 5'-CTAGCTACCTATAGCCGGTGGTGATGGTGATGGTGGCCTAAGGAGCCGCTACC-3'. Each PCR reaction contained 12 nM of DNA library, 0.5 μ M of each primer, 1X ThermoPol buffer, 100 μ M of dNTP's and 5 U of Taq polymerase. The PCR reaction started by an initial heating of 94°C for 2 minutes followed by 18 cycles of 94°C for 15 seconds, 60°C for 30 seconds, and 72°C for 45 seconds followed by 72°C for 5

minutes. PCR product amplified was mixed with sample buffer and resolved on a 2% agarose gel containing ethidium bromide for visualization using UV (Figure 2.6). PCR product was cut from the gel and gel purified by QIAquick Gel Extraction Kit from QIAGEN.

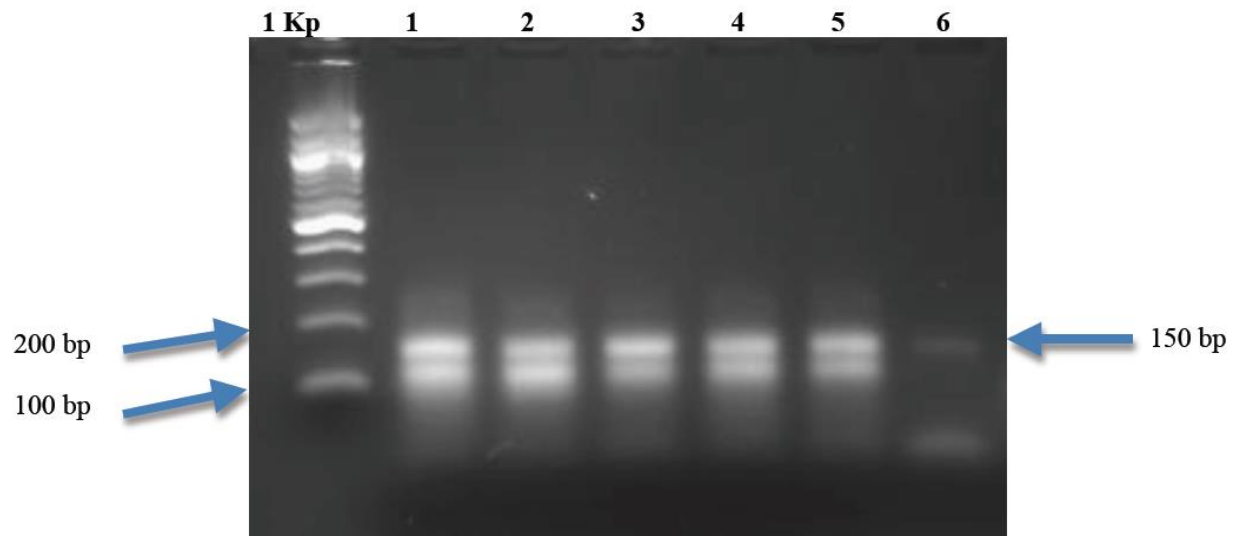


Figure 2.6 DNA library on 2% agarose gel. Lane 1: CX2CX4 DNA library. Lane 2: CX4CX8 DNA library. Lane 3: CX6CX6 DNA library. Lane 4: CX8CX4 DNA library. Lane 5: CX10CX2 DNA library. Lane 6: no template. The upper bands were cut and gel purified.

2.5.3 StrataClone Cloning and Sequencing

The PCR product was ligated to StrataClone vector (Stratagene). The ligation product was transformed into StrataClone SoloPack competent cells following the StrataClone PCR Cloning Kit from Stratagene. After that, the transformation product was plated onto LB plates containing 20 mg/ml kanamycin and the plates were incubated overnight at 37°C. Then, 96 single colonies were selected and sent for sequencing to ensure that the libraries were synthesized as designed (Figure 2.7).

```

CX2CX10 NTTHYRVNFTKEDS*MCVFCLSLMLSWLRGGSGSLGHHHHHHRL*VA
CX2CX10 NTTHYRVNFTKEDS*MCWT CRAHFRWTD FSGSGSLGHHHHHHRL*VA
CX2CX10 NTTHYRVNFTKEDS*MCPCWCMISRVYPEVTGSGSLGHHHHHHRL*VA
CX2CX10 NTTHYRVNFTKEDS*MCSCACNFCVLVRAVWGSGLGHHHHHHRL*VA
CX2CX10 NTTHYRVNFTKEDS*MCVFCLSLMLSWLRGGSGSLGHHHHHHRL*VA
CX4CX8  NTTHYRVNFTKEDS*MC GGVD CYGGALRGLGSGSLGHHHHHHRL*VA
CX4CX8  NTTHYRVNFTKEDS*MC GLVOC TFFEC ECGSGSLGHHHHHHRL*VA
CX4CX8  NTTHYRVNFTKEDS*MC AVWGC GRSD EDRGSGSLGHHHHHHRL*VA
CX4CX8  NTTHYRVNFTKEDS*MC SLRGC PIVRE KFMGSGSLGHHHHHHRL*VA
CX4CX8  NTTHYRVNFTKEDS*MC PQVAC GDGRM CRHGSGLGHHHHHHRL*VA
CX4CX8  NTTHYRVNFTKEDS*MC LAISC PTTCR PLCGSGSLGHHHHHHRL*VA
CX6CX6  NTTHYRVNFTKEDS*MC TRYGWAC MYQPYGGSGSLGHHHHHHRL*VA
CX6CX6  NTTHYRVNFTKEDS*MC RLRGSHC SVLCYRGSGSLGHHHHHHRL*VA
CX6CX6  NTTHYRVNFTKEDS*MC HSQYRMC METWYSGSGSLGHHHHHHRL*VA
CX6CX6  NTTHYRVNFTKEDS*MC WLARSRC AGFYPRGSGSLGHHHHHHRL*VA
CX6CX6  NTTHYRVNFTKEDS*MC RLRGSHC SVLCYRGSGSLGHHHHHHRL*VA
CX8CX4  NTTHYRVNFTKEDS*MC VLLTSQYCC LHVP GSGSLGHHHHHHRL*VA
CX8CX4  NTTHYRVNFTKEDS*MC RGLSITAC CENGSGSLGHHHHHHRL*VA
CX10CX2 NTTHYRVNFTKEDS*MC PASSRILSNKCTWGSGLGHHHHHHRL*VA
CX10CX2 NTTHYRVNFTKEDS*MC PVNTYLLMTLCHEGSGSLGHHHHHHRL*VA
CX10CX2 NTTHYRVNFTKEDS*MC MGCRVLPNNICLP GSGSLGHHHHHHRL*VA
CX10CX2 NTTHYRVNFTKEDS*MC PGYNAGPTSR CGMGSGLGHHHHHHRL*VA

```

Figure 2.7: DNA libraries sequence. Each library was PCR-amplified and sample clones were sequenced.

The predicted amino acid sequence from each clone is shown. The sequences of the libraries were analyzed by using Bio-Edit software

2.5.4 Transcription and Purification of mRNA

Each library was transcribed by setting up a 1 ml transcription reaction that contains 0.1 μ M DNA library, 0.6 μ M T7 primer, 40 mM/0.1% Tris/Triton solution, 2.5 mM spermidine, 25 mM MgCl_2 , 10 mM DTT, 5 mM CTP, 5 mM UTP, 5 mM ATP, 9 mM GTP, 0.2 U/ μ l RNase inhibitor, 1 U/ μ l inorganic pyrophosphatase and 1 U/ μ l T7 RNA polymerase (MA & Hartman, 2012). Then, the reaction was incubated overnight at 37°C in an incubator chamber. After that, the transcription reaction was removed from the incubator and 50 μ L of Turbo DNase (Invitrogen) was added and the reaction was incubated for 15 minutes at 37°C. After incubation, 7.5 M urea was added and mixed well and the reaction was loaded on Urea PAGE by setting up a large 65 SequaGel (20 cm X 20 cm) on an Owl P10DS Dual Gel System. The gel was pre-run for 20–30 min by using constant power at 25 W supplied by EC Apparatus electrophoresis power supply EC 600. Then, the urea was flushed out from well and the sample was loaded. The gel was run at constant power of 25 W for 60-90 minutes until the bromophenol blue reaches the bottom of the gel. After that, the gel was transferred from the glass plates to Saran wrap on both sides and the mRNA band was visualized by UV shadowing and the band cut out with a fresh razor blade.

After that, the mRNA was eluted by using the Whatman Elutrap electroelution System. First, the gel slice was put into the chamber, and mashed into small pieces and the chamber filled with 0.5X TBE buffer until the gel is covered. The electroelution was run for 2 h at 300 V on a Bio-Rad PowerPac basic power supply. At the end of running, the electrodes switched and run backwards for 1 min at 300 V. Then, the solution between membranes was collected and ethanol precipitated with 0.1 volume of 3 M KOAc and 3 volumes of 100% ethanol. The sample was mixed well and chilled at –20°C for 30 minutes. After that, the sample was centrifuged at 16,000 Xg for 20 minutes at 4°C. The supernatant was discarded and the pellet washed with 500 μ L of 70% ethanol and centrifuged again at 16,000 xg for 1 min. The supernatant was discarded and the pellet air-dried for 5–10 min at room temperature. The mRNA was dissolved in ddH₂O and an absorbance at 260 nm was measured on a spectrophotometer. The

concentration was calculated by using the online software Oligonucleotide Properties Calculator (<http://www.unc.edu/~cail/biotool/oligo/index.html>). Then, the mRNA was stored at -20°C.

2.5.5 Psoralen Photo-Crosslinking

The five mRNA libraries were mixed together with a final concentration of 2 μ M in order to be photo-crosslinked with an XL-PSO oligonucleotide. The sequence of the XL-PSO oligonucleotide is 5'-PsoC6-(UAGCCGGUG)2'-OMe-15xA-2xSpacer9-ACC-Puro-3'. Spacer9 is triethyleneglycol (TEG) phosphoramidites and it is used to tether 5'-dCdC-puromycin to the 3'-end. The Psoralen photo-crosslinking reaction contains 20 mM HEPES-KOH, pH 7.6, 7.5 μ M XL oligo, 100 mM KCl, 1 mM spermidine, 1 mM EDTA and the mixture of the mRNA libraries. The reaction was mixed well and transferred into PCR tubes with 100 μ l in each tube. The PCR tubes were placed in a PCR machine, heated to 70°C for 5 min, then cooled to 25°C over 5 min (0.1°C/s). After this, each sample was transferred to a crosslink plate, 100 μ L per well. A 365 nm UV lamp was used to irradiate the plate for 20 minutes at 4°C. The samples were collected in 1.5 ml eppendorf tube and ethanol precipitated as previously described. The pellet was resuspended in the required volume.

2.5.6 *In Vitro* Translation

A 5-mL translation reaction was prepared, which contained 8 mM putrescine, 1mM spermidine, 5 mM potassium phosphate, 95 mM potassium chloride, 5 mM ammonium chloride, 5 mM magnesium acetate, 0.5 mM calcium chloride, 1mM dithiothreitol, 1 μ g/ml inorganic pyrophosphatase, 4 μ g/ml creatine kinase, 1.1 μ g/mL nucleotide diphosphate kinase, 30 μ M (6R,S)-5,10-formyl-5,6,7,8-tetrahydrofolic acid, 93 μ g/mL myokinase, 10 mM creatine phosphate, 2 mM ATP, 2mM GTP, 2.4 mg/ml *E. coli* total tRNA, 0.2 μ M MTF, 1.0 μ M IF1, 0.3 μ M IF2, 0.7 μ M IF3, 3.2 μ M EF-Tu, 0.6 μ M EF-Ts, 0.5 μ M EF-G, 0.3 μ M RF1, 0.4 μ M RF3, 0.1 μ M RRF and 0.5 μ M ribosomes. In addition, the reaction contained 18 natural amino acids (200 μ M each), 10 μ M cysteine, 10 μ M methionine and 20 aminoacyl tRNA

synthetases (0.1 μ M MetRS, 0.3 μ M LeuRS, 0.6 μ M GluRS, 0.2 μ M ProRS, 1.0 μ M GlnRS, 1.0 μ M HisRS, 0.25 μ M PheRS A294G, 1.5 μ M TrpRS, 0.2 μ M SerRS, 0.2 μ M IleRS, 0.4 μ M ThrRS, 0.6 μ M AsnRS, 0.6 μ M AspRS, 0.5 μ M TyrRS, 0.5 μ M LysRS, 0.4 μ M ArgRS, 0.2 μ M ValRS, 0.2 μ M AlaRS, 0.5 μ M CysRS, and 0.06 μ M GlyRS). 0.3 μ M of 35 S-Met is added to isotopically label the peptides. The translation mix was incubated for 15 minutes at 37°C. Then, the 2 μ M photo-crosslinked mRNA was added to the translation mix and incubated for 1 hour at 37°C. After that, the translation reaction was quenched with 550 mM KCl and 50 mM MgCl₂ followed by an incubation for 90 minutes at 37°C. Then, the translation reaction was chilled overnight at -80°C.

2.5.7 Oligo(dT) Purification and Cyclization

The goal of oligo(dT) purification and cyclization is to remove all non photo-crosslinked mRNA-peptide fusions and to produce cyclic peptides at the same time (Figure 2.8). The translation reaction was thawed and vortexed and 5 μ L removed for scintillation counting to determine the total radioactivity of 35 S-Met added to the translation reaction. Then, 100 mg Oligo(dT)-cellulose Type 7 powder (GE Healthcare) was added into each of five 20 mL Bio-Rad Econo-Pac columns (BioRad) and rinsed once with 5 ml ddH₂O to swell cellulose and twice with oligo(dT) binding buffer (20 mM Tris-HCl, pH 7.8, 10 mM EDTA, 1 M NaCl, 0.2% Triton X-100, and 0.5 mM fresh TCEP). Then, each one ml of the translation reaction was added to one column and the reaction was brought up to 4 mL with the binding buffer. The columns were placed on a rocking platform shaker in 4°C cold room and shaken for 30 min. After that, the flow-through was removed and the beads were rinsed twice with the oligo(dT) binding buffer. Then, 4 mL of cyclization buffer (20 mM Tris-HCl, pH 7.8, 0.66 M NaCl, 3 mM α,α' -dibromo- *m* -xylene (Sigma-Aldrich/Fluka), 33% acetonitrile (v/v), 0.5 mM fresh TCEP) was added to each reaction and rocked for 30 minutes at room temperature. Then, the flow-through was removed and each column was washed twice with 4.5 mL oligo(dT) wash buffer (20 mM Tris-HCl, pH 7.8, 0.3 M NaCl, 0.1% Triton X-100); first wash was

with 5 mM fresh BME and the other wash was with 0.5 mM fresh TCEP. Then, the columns were eluted 8 times with ddH₂O and filtered to remove residual Oligo(dT)-cellulose in the fusion solution. One μ L of each eluent was counted in a scintillation counter and the fractions with significant radioactivity were combined and ethanol precipitated using 0.3 volume of 3 M KOAc, pH 5.2, 0.002 volume of glycogen (5mg/mL) (Applied Biosystems), and 3 volume of 100% ethanol. Then, the pmole amount of the mRNA-peptide fusion was calculated based on the scintillation counts and the pellet re-dissolved in ddH₂O so that the final concentration of the fusion is 100 nM (0.1 pmole/ μ L).

2.5.8 Reverse Transcription

The goal of reverse transcription (RT) is to convert the single-stranded mRNA portions of the fusions to heteroduplex of RNA/DNA in order to eliminate any unwanted RNA secondary structures and render the nucleic acid portion of the fusion more stable. The RT reaction was carried out following the Superscript III First Strand Synthesis Kit (Invitrogen). In a microcentrifuge tube, the 100 nM mRNA-peptide fusions were added to 0.5 mM dNTPs and 0.5 μ M RT-primer TTTTTTTTTTTTTTTGTGATGGTGGTGGCCT-AAGC. The tube was incubated for 5 minutes at 65 °C in a heating block. After five minutes, the tube was immediately placed on ice and incubated for at least 1 minute. Then, the following reagents were added in a final concentration of 5 mM MgCl₂, 1 mM DTT, 2 U/ μ L RNaseOUT (Invitrogen), 5 U/ μ L Superscript III (Invitrogen). The RT reaction was incubated for 15 minutes at 55°C for elongation, then 15 minutes at 70°C to inactivate the Superscript III. At the end of the RT reaction, 0.5 μ L of each RT reaction was counted in a scintillation counter in order to calculate how much of mRNA-peptide fusions were recovered.

2.5.9 Ni-NTA Purification

Ni-NTA purification was performed in order to remove any truncated peptide fusions (Figure 2.9). The following buffers were prepared for Ni-NTA purification under denaturing condition:

<u>Denaturing Binding buffer, pH 8</u>	<u>Wash buffer, pH 8</u>	<u>Elution buffer, pH 8</u>
100 mM NaH ₂ PO ₄	100 mM NaH ₂ PO ₄	50 mM NaH ₂ PO ₄
10 mM Tris HCl	300mM NaCl	300mM NaCl
6 M guanidinium HCl	0.2% Triton X-100	250mM imidazole
0.2% Triton X-100	5 mM BME (fresh)	0.2% Triton X-100
5 mM BME (fresh)		5 mM BME (fresh)

First, 100 µl of Ni-NTA agarose was added into spin filter tube. Then, the RT reaction was diluted 5 fold with the Ni-NTA denaturing binding buffer and transferred into filter tube. The peptide fusion was bound to the Ni-NTA for one hour at 4°C in a tumbler in a cold room. After that, the flow through was removed by centrifuging at 5900 rpm for 1 minute. The resin was washed 3 times with Ni-NTA wash buffer and centrifuged at each time. Then, the peptide fusion was eluted 6 times with portions of 50 µL Ni-NTA elution buffer and 0.5 µL of each eluent was counted in a scintillation counter to measure how much of mRNA-peptide fusions recovered. All eluents with high counts were combined and dialyzed against 1 L pre-cooled selection buffer (50 mM Tris-HCl, pH 8.0, 150 mM NaCl, 4 mM MgCl₂, 0.25% Triton X-100, 0.1 mg/ml BSA). The overnight-dialyzed peptide fusions were collected and 1 µL was counted in a scintillation counter.

2.5.10 *In Vitro* Selection

The selection process started by an overnight incubation of two proteins with Pierce Magnetic Glutathione beads (Thermo Fisher Scientific). The first sample contains GST protein only for negative selection (pre-clearing) (Figure 2.10) and the second sample contains GST-XRCC4¹⁵⁷ fusion for selection. 50 µL of Pierce Magnetic Glutathione beads per 1 mL translation reaction was transferred into two 1.5 mL eppendorf tubes and washed three times with 400 µL GST beads wash buffer (125 mM Tris-HCl, pH 8.0,

150 mM NaCl); each time the magnetic beads were mixed gently and the supernatant was removed by using Magnetic separation stand (Invitrogen). 130 µg of each protein was mixed with 400 µL GST beads wash buffer and transferred to the tubes with magnetic beads and incubated at 4°C for overnight with rotation on a tube rotator. In the next day, the magnetic beads with GST protein were pelleted briefly and the supernatant was removed using the magnetic stand. The beads were washed twice with 400 µL GST beads wash buffer and once with 400 µL selection buffer. Then, the dialyzed mRNA-peptide fusions from the previous step were added to the tube and a final concentration of 0.1 mg/mL BSA was added. The tube was incubated at 4°C for 2 hours with rotation. After that, the supernatant was collected and the beads washed three times with 200 µL selection buffer. The beads from this step and 10 µL from the supernatant and washes were counted in a scintillation counter. Then, the remainder of the supernatant and the three washes were transferred to the other tube that contained the GST- XRCC4¹⁵⁷ fusion. The tube was incubated at 4°C for 2 hours with rotation. Then, the supernatant was removed and the beads were washed three times with 400 µL of the selection buffer. Then, the beads were suspended in 100 µL of the selection buffer and 5 µL was counted in a scintillation counter. After that, the mRNA-peptide fusions that attached to the GST-XRCC4¹⁵⁷ were amplified by PCR directly from the beads as described below.

2.5.11 PCR Amplification of Selected Fusions

The PCR reaction was carried out directly from the beads. First, a test of 100 µL PCR reaction was done with 5 µL of the suspended beads in order to find the optimum conditions for PCR. The PCR reaction was performed as previously described with the following primers 5'-TAATACGACTCACTATAGGGTAACT-TTACTAAGGAGGACAGCTAAATG-3' and the 5'-CTAGCTACCTATAGCCGGTGGTGATGGTGATGGTGGCCTAAG-GAGCCGCTACC-3'. Starting in cycle 14, 5 µL was taken out of the PCR tube after the elongation step (step 4, at 72°C). The PCR machine was paused at 44 seconds of this step and 5 µL was taken from the PCR

reaction. This was done for even numbered PCR cycles 14-32. The PCR product was checked on 2% agarose gel and the intensity of DNA bands was analyzed to find out the optimum conditions of the PCR. Then, large-scale PCR was set up using multiple PCR tubes and all suspended beads were used to amplify the selected fusions. After PCR, the reaction mixtures were combined and an equal volume phenol:chloroform:isoamyl alcohol (25:24:1) (Sigma-Aldrich) was added. The sample was vortexed and centrifuged at 4000 rpm for 2 minutes in a cold room. The upper layer was transferred to a new tube and an equal volume of CHCl_3 was added to the tube and spun down again. The aqueous layer was transferred to new tube and ethanol precipitated as previously described. The resulting precipitate was dissolved into a final volume of 100 μL ddH₂O, and passed over a NAP-5 column (GE Healthcare) to de-salt. The final volume from NAP-5 was 500 μL . This was the template for the next round of selection.

DNA Library

mRNA Library

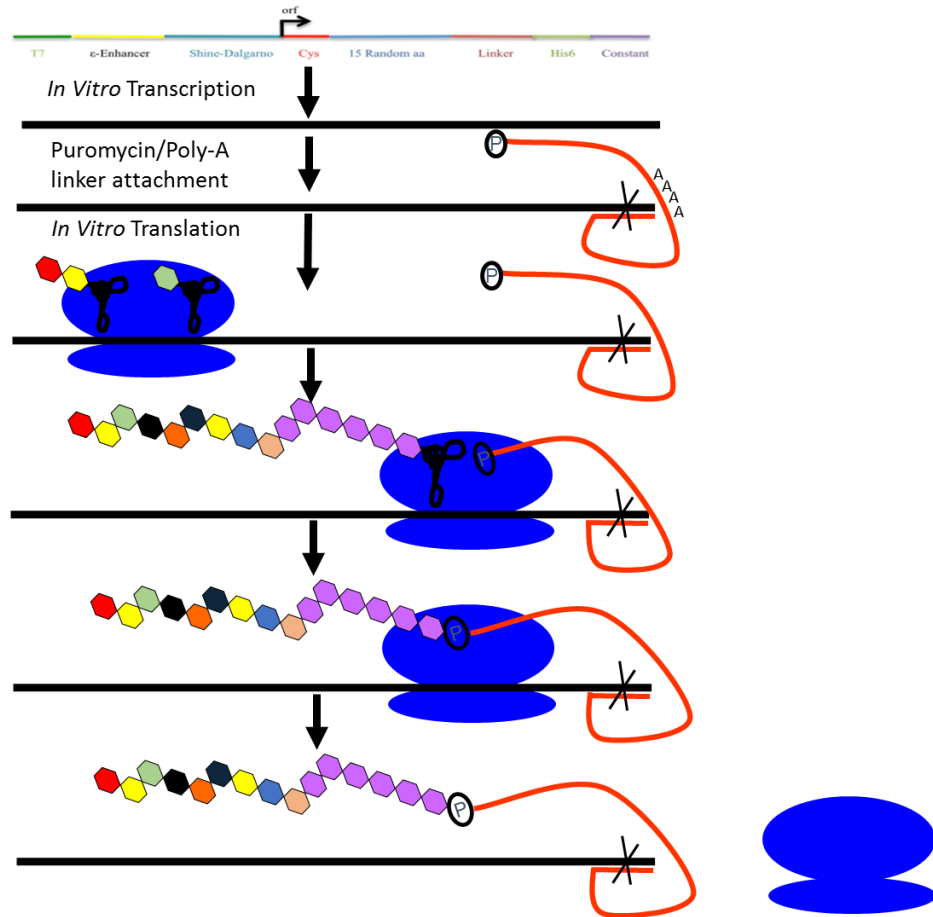


Figure 2.8 *In vitro* transcription, photo cross-linking and *in vitro* translation

Purification of the mRNA-peptide fusions

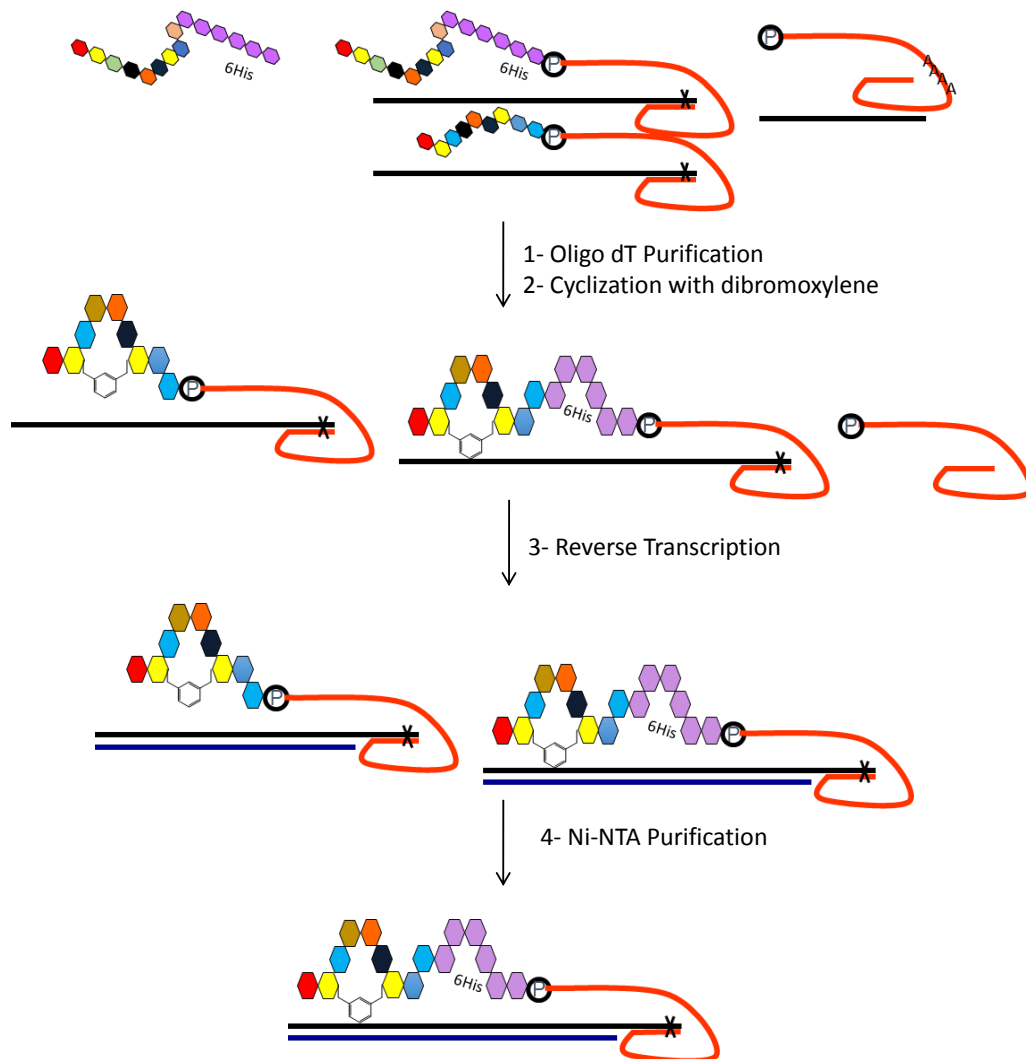


Figure 2.9 mRNA-peptide fusions purification steps.

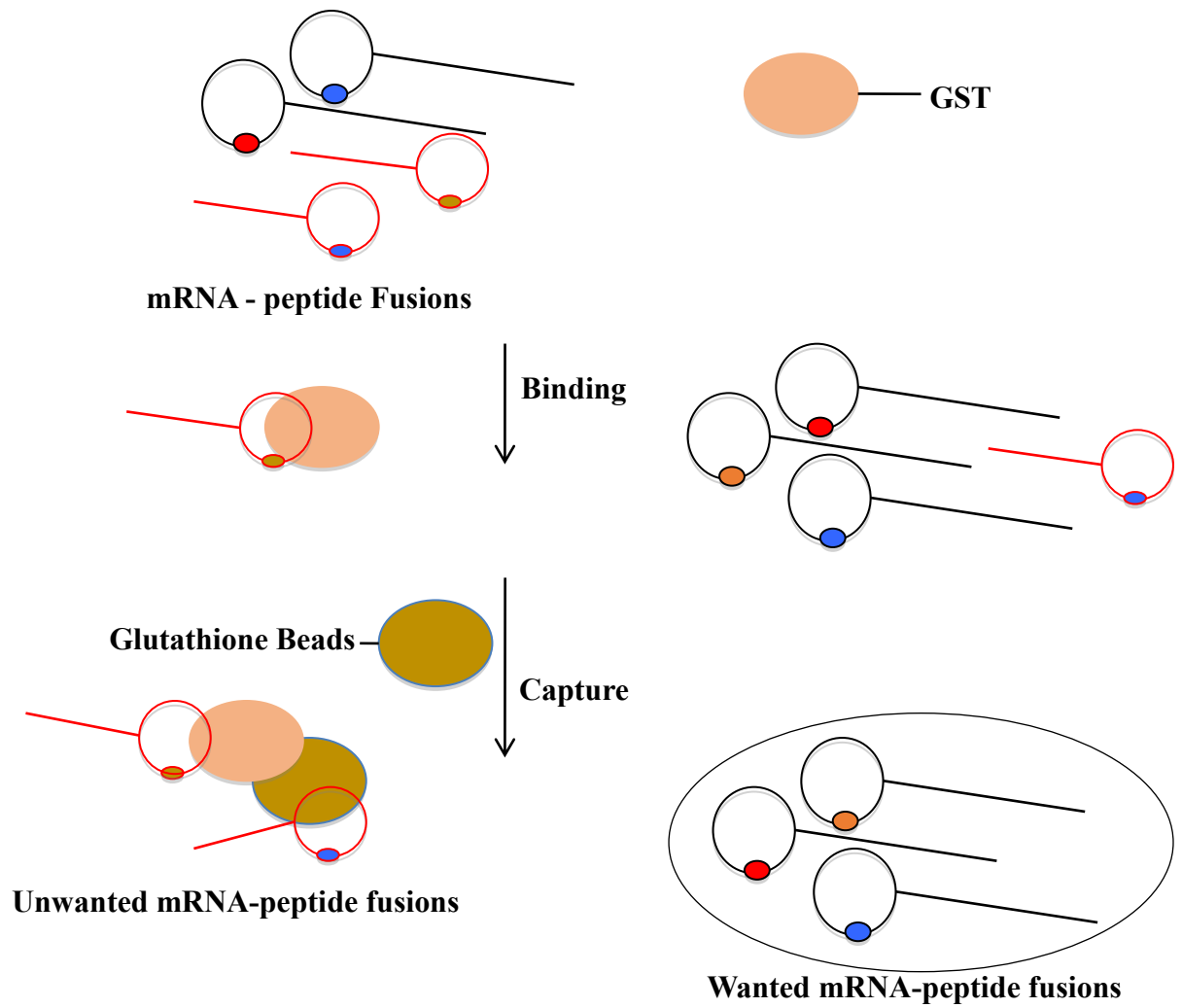


Figure 2.10. Pre-clearing (negative selection) with GST protein only immobilized on magnetic beads

2.6 Peptide Synthesis

2.6.1 Solid Phase Peptide Synthesis

Standard Fmoc-based solid phase peptide synthesis was used to synthesize the peptides on a Liberty Automated Microwave Peptide Synthesizer (CEM). The peptides were made on a Fmoc-Rink amide MBHA Resin (0.65 mmol/gm). After each coupling step a capping step was performed using 20% acetic anhydride (Fisher Certified ACS), but no capping was performed on the final N-terminal amino acid to leave the amine free for labelling. The formation of the peptides were confirmed by MALDI-TOF.

2.6.2 Labeling with 5(6)-Carboxyfluorescein

The peptides were labeled using 600 μ mole 5(6)-carboxyfluorescein (FAM) (Sigma-Aldrich), 600 μ mol DCC, 600 μ mole HOBt and 30 μ mol peptide resin in DMF. The labeling was confirmed by Ninhydrin test (Sigma-Aldrich) as well as on MALDI-TOF. The resin was collected on a fritted peptide synthesis filter and washed with DCM, Methanol and air-dry.

2.6.3 Cleavage of the Peptide from the Resin

The peptide was cleaved from the resin using trifluoroacetic acid (TFA) (Chem Impex)/ triisopropylsilane (TIS) (Sigma)/ 3,6-dioxa-1,8-octanedithiol (DODT) (Sigma)/water (92.5:2.5:2.5:2.5) with incubation at RT for 4 hours, and the resin was filtered off. The filtrate containing the crude peptide was precipitated with cold ether, and collected by centrifugation. The supernatant was discarded and the peptide was dissolved in CH₃CN (Fisher HPLC Grade) and water with 10% acetic acid (Fisher certified ACS PLUS) (1:1) followed by freezing and lyophilization.

2.6.4 Purification by HPLC

The lyophilized peptide generally dissolved in 50 % CH₃CN or DMSO and purified by reverse phase HPLC using a Shimadzu Prominence system. For small scale, the purification was performed under

analytical condition: column, Vydac 218TP5410 4.6 × 100 mM; Solvents: A=water/0.1% TFA, B=CH₃CN/0.1% TFA) flow rate, 0.44 mL/min; gradient, 10 min at 10 % B, 30 min at 10–100 % B. Injection occurred at 5 minutes and the absorbance was monitored at 443 nm. For large-scale purification we used **semi-preparative column** following conditions: column, Vydac 218TP52210 22 × 100 mm; flow rate, 10 mL/min; the other parameters are similar to the ones used for the analytical column. HPLC fractions were analyzed on MALDI-TOF. Fractions with the desired product were collected, frozen and lyophilized.

2.6.5 Cyclization with α - α' -dibromo-*m*-xylene in Solution

A reaction of a 50 mL final volume was set up in a 100 mL oven-dried flask, which was charged with water (15 mL) and acetonitrile (15 mL) and was deoxygenated by bubbling Argon for 10 min. Then, 20 mM ammonium bicarbonate (5 mL of 200 mM, pH 8.6), 200 μ M tris-carboxyethylphosphine (TCEP) (10 mL of 1 mM) in water and peptide (10 mg, 3.5 μ mol) were added and the reaction was kept under argon. After 60 min, 1.1 mM of α - α' -dibromo-*m*-xylene linker (5 mL of 11 mM) in CH₃CN was added. The reaction was incubated at RT and monitored by MALDI-TOF. After the cyclization is completed, the reaction was frozen and lyophilized. The resulting white powder was dissolved in the appropriate solvent and purified by reverse phase HPLC as described above.

2.6.6 Cysteine Protecting Group Removal to Prepare for Cyclization on the Solid Phase

For this part we used Fmoc-S-tert-butylthio-L-cysteine as building block instead of Fmoc-(L)-Cysteine(Trt)-OH during the synthesis of the peptides on SPPS. To remove the protecting group: in a 15 mL falcon tube, we added 100 mg of dried peptide, 5.1 mL DMF, 100 mM NH₄HCO₃ (600 μ L of 1M in water), and 50 mM DTT (300 μ L of 1M in DMF) and the reaction was deoxygenated by bubbling Argon for 2 minutes. The reaction was allowed to proceed for 2.5 hours at 55 °C and the resin was collected on a fritted peptide synthesis filter tube, the solution of the reaction was removed using vacuum, washed three times with DCM and methanol, and air-dried for 5 min. The completion of the reduction was monitored

by analytical test cleavage and MALDI-TOF. 0.5 – 1 mg of the above resin was transferred into a 0.6 μ L microcentrifuge tube and 100 μ L of a cleavage cocktail containing trifluoroacetic acid (TFA) (Chem Impex)/ triisopropylsilane (TIS) (Sigma)/ 3,6-dioxa-1,8-octanedithiol (DODT) (Sigma)/ water (92.5:2.5:2.5:2.5) was added. The tube was tumbled for 40 minutes at RT. The resin was filtered off by using Pasteur pipette glass with cotton. The filtrate containing the crude peptide was precipitated with 200 μ L of cold ether, and collected by centrifugation for 5 min at 10,000 \times g at RT. The supernatant was discarded and the peptide was dissolved in an appropriate solvent and analyzed by MALDI-TOF.

2.6.7 Cyclization of the Peptide with α , α' -dibromo-*m*-xylene on the Resin

In a 15 mL test tube with a final volume of 5 mL DMF, 50 mg of dried peptide resin that has two fully deprotected cysteine residues, 20 mM of $(\text{NH}_4)_2\text{CO}_3$ (40 μ L of 2.5 M in water), 200 μ M of TCEP (125 μ L of 8 mM), and 11 mM of α , α' -dibromo- *m*-xylene (1.375 mL of 40 mM in DMF) were added. The reaction was allowed to proceed for 1-2 hours at 55 $^\circ$ C. The cyclization reaction was monitored by analytical cleavage and MALDI-TOF as above and the resin was collected and washed as above. Then, the peptide was labeled with 5(6)-carboxyfluorescein, cleaved and HPLC purified as described above.

2.7 MALDI-TOF Analysis

Samples were prepared for analysis by 1:1 dilution in a 1:0.99:0.01 $\text{CH}_3\text{CN}:\text{H}_2\text{O}:\text{TFA}$ solution containing 10 mg/mL α -cyano-4-hydroxy-cinnamic acid (CHCA). After spotting on the sample plate, samples were allowed to co-crystallize by slow evaporation at RT. Samples resulting from translation reactions were desalted and concentrated with ZipTipC18 Pipette Tips (Millipore) according to the manufacturer's protocol.

2.8 K_D Determination Using Bead Capture of *In Vitro* Translated Peptides.

^{35}S -Met labeled peptide was incubated with GST-XRCC4¹⁵⁷ with different concentrations in 20 μ L binding/

wash buffer (125 mM Tris, 150 mM NaCl, pH 8) at room temperature for 1 hour. Each solution was then added to 40 μ L pre-equilibrated glutathione magnetic beads (Pierce) and tumbled at room temperature for 1 hour. The supernatant was removed and the beads were washed with binding/wash buffer (2 x 40 μ L). The radioactivity of the supernatant and wash solutions was measured by scintillation counting as unbound fractions. 40 μ L glutathione elution buffer (250mM Tris pH 8.8, 500mM NaCl, 100mM glutathione, 1% Triton X-100) was added to each tube and tumbled for 1 hour. The supernatant was removed and the beads were washed with 40 μ L binding/wash buffer. The radioactivity of the supernatant and this wash solution was measured by scintillation counting as bound fractions. To account for nonspecific binding to the beads, the measured radioactivity of the fraction containing no GST- XRCC4¹⁵⁷ was subtracted as background from the measured radioactivity of the trials containing GST- XRCC4¹⁵⁷. The subsequent background-corrected bound value was divided by the total counts (bound + unbound fractions) to determine the percent of peptide bound to GST- XRCC4¹⁵⁷ for each trial. Results were analyzed using SigmaPlot software and the K_D was determined using a dynamic curve fit.

3. RESULTS

3.1 NHEJ is Tolerant of a Substrate Containing Tg Near a DSB End

Tg is a major product of free radical damage to DNA, and will often occur at or near the terminus of a radiation-induced DSB. Because Tg is nonplanar, it induces severe distortion in DNA structure (Aller et al., 2007). Classical NHEJ, however, is capable of joining mismatched overhangs as well as a variety of other noncomplementary end structures (Gu et al., 2007; Tsai et al., 2007). To determine whether Tg poses a barrier to ligation in the context of NHEJ, internally labeled blunt-ended substrates were constructed (Figure 3.1) with Tg as the first, second or third base from the 3' terminus of one DNA end (Tg1, Tg2 and Tg3, respectively); the opposite end was blunt but unmodified. End joining of these substrates was detected by subsequent cleavage with *NdeI* and *PstI*, which release labeled and unlabeled fragments, respectively, from opposite ends of the substrate. For Tg-containing samples, the 19-mer corresponding to unjoined substrate migrates as a doublet, reflecting different stereoisomers of Tg.

To assess whether Tg was a barrier to NHEJ, each of the four blunt-end substrates was incubated in whole-cell extracts of XLF-deficient Bustel fibroblasts (note: this work of Figure 3.2 was done by Duaa Bafail (a former Master student)). For the unmodified, blunt-ended substrate, end joining was completely dependent on addition of purified recombinant XLF, and the only detectable products were the expected 44-base head-to-tail and 36-base head-to-head products of direct blunt-end ligation, each of which precisely comigrated with synthetic markers of the same sequence (Figure. 3.2A, lanes 22-28). Unexpectedly, the Tg3 substrate (lanes 15-21) yielded, in addition to apparent 36- and 44-base products, a third product migrating as a slightly diffuse band above the 36-mer band (labeled as 36Tg). Treatment

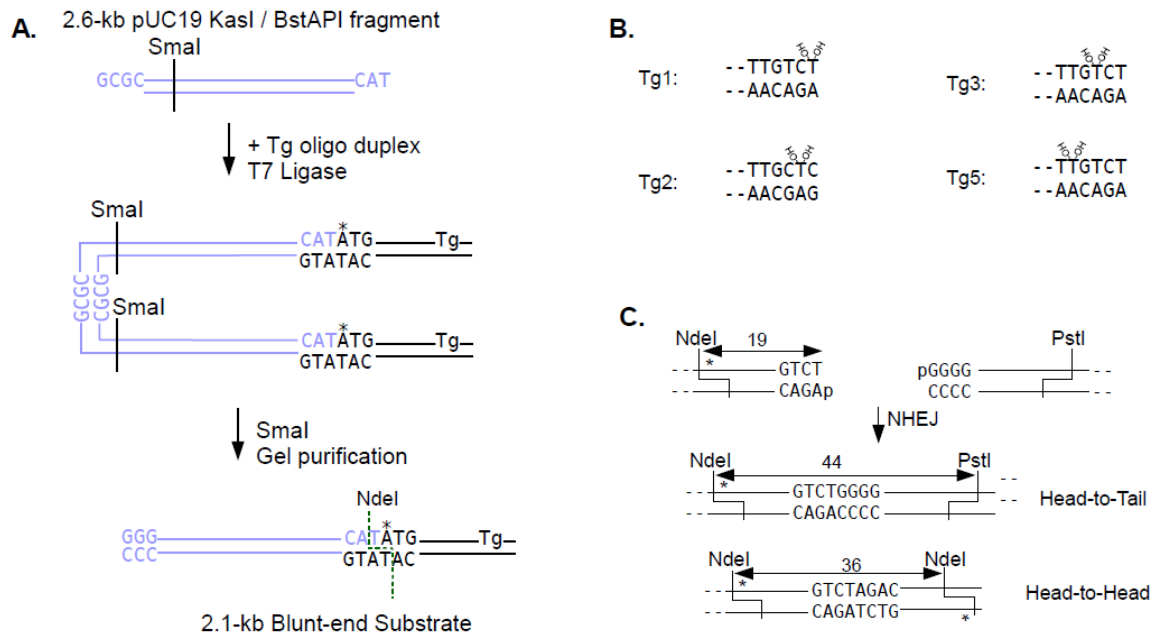


Figure 3.1. Tg-containing DSB substrates. A. Construction of modified substrates from short, end-labeled (*) Tg-containing duplexes and a fragment of pUC19. B. Terminal structures and sequences of the substrates. C. Formation of head-to-tail and head-to-tail end joining products, and their detection as fragments of NheI/PstI cleavage.

of the DNA with EndoIII after incubation in extracts but before NdeI/PstI cleavage (lane 18) eliminated most of this band, suggesting that it represents a 36-base head-to-head ligation product in which Tg is still present. This Tg-containing 36-mer migrates more slowly than the unmodified 36-base product, which migrates anomalously fast because it is palindromic and can snap back into a hairpin upon denaturation/renaturation. The Tg apparently disrupts hairpin formation and thereby decreases the electrophoretic mobility, providing a convenient indication of the extent to which head-to-head end joining products still contained the Tg base.

In addition, EndoIII treatment eliminated about half of the 44-base product, suggesting that, as with the 36-base product, Tg was still present in some but not all of the ligated 44-base products. As further confirmation that some of the Tg had been excised and replaced with thymine, the experiment was performed with ddTTP added to the extracts in place of dTTP, to arrest excision repair as a nonligatable intermediate. For samples with ddTTP, the unsubstituted 36-base product from Tg3 was largely eliminated, confirming that it arose from excision repair of a Tg-containing ligation product (lane 21). The unmodified and Tg3 substrates yielded approximately the same level of 44-base product (22.1% vs 19.2%), and the sum of the Tg-substituted and unsubstituted 36-base products from Tg3 (6.3% and 5.9%, respectively) was equal to the yield of single 36-base product from the unmodified substrate (11.6%), indicating that overall, Tg at the third position from a DNA end conferred little or no inhibition of NHEJ.

3.2 Tg as the Terminal or Penultimate Base at the 3' End of a DSB is a Barrier to NHEJ

In contrast to the efficient blunt-end ligation seen with the Tg3 substrate, the Tg1 and Tg2 substrates yielded only a trace of 44-base product, approximately 1-2% of the total substrate or about tenfold less than Tg3 (Figure 3.2A, lanes 1-14). Moreover, Tg1 and Tg2 yielded no detectable 36-base head-to-head joining product. These results indicate that Tg as the terminal or penultimate base consti-

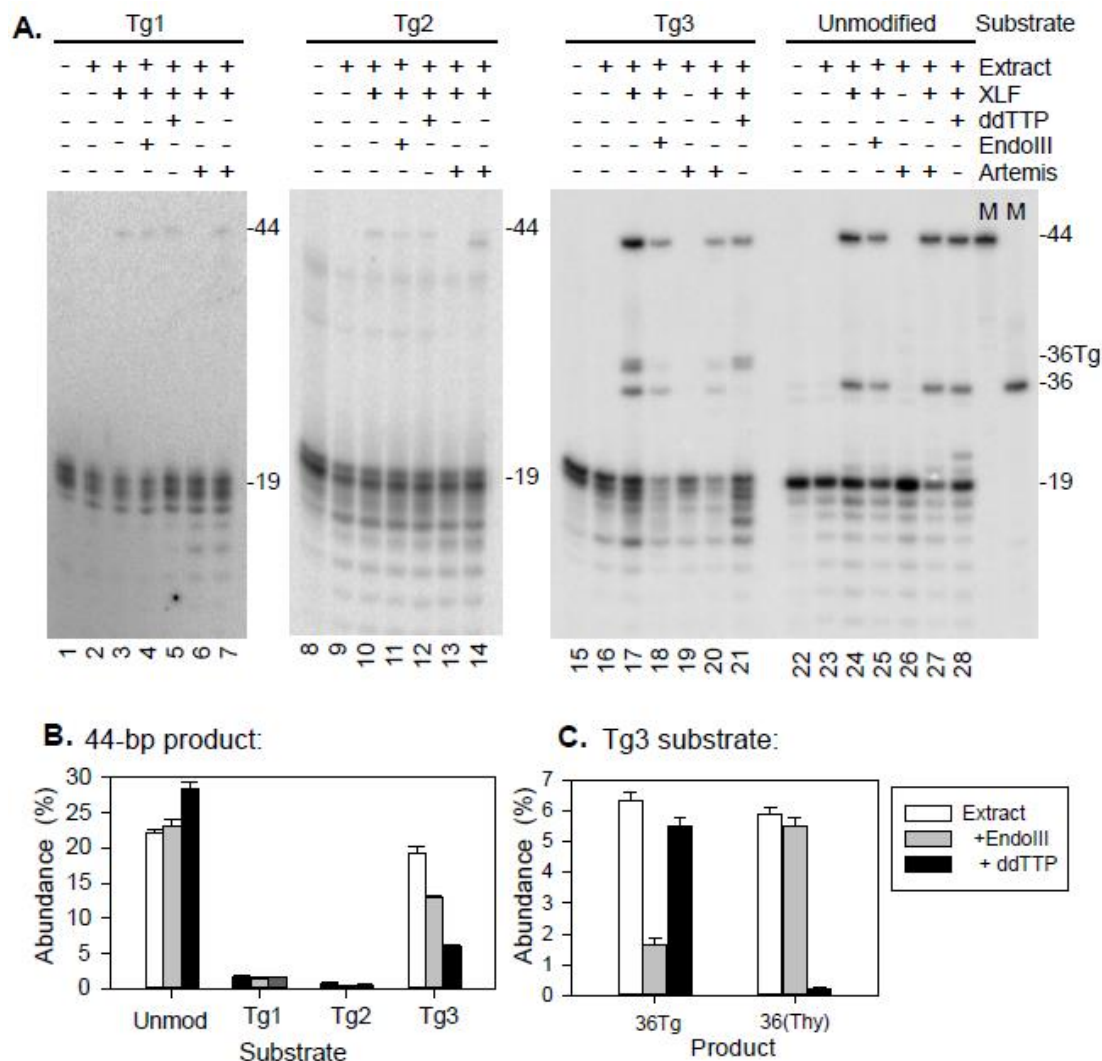


Figure 3.2. Effect of Tg on joining of blunt-ended substrates by NHEJ. The site-specifically labeled (*) substrates shown, either unmodified or containing Tg at the first, second or third position from the terminus of the labeled end, were incubated in XLF-deficient BuS extracts, supplemented with XLF (100 nM), Artemis (80 nM), and/or ddTTP in place of dTTP as indicated, for 6 hr at 37°C. The samples were deproteinized, in some cases treated with EndoIII, then cut with NdeI and PstI and analyzed on denaturing gels. Lanes marked “M” contain 5'-end-labeled 36- and 44-base oligomers of the sequence expected for blunt-end ligation products. Bar graphs show yield of specific products of the indicated substrates and error bars indicate mean \pm SEM for 4 replicate experiments.

(Note: this work of Figure 3.2 was done by Duaa Bafail (a former Master student))

tutes a major barrier to blunt-end ligation in NHEJ when present at one end of a DSB, and an absolute barrier when present at both ends. One possible mechanism for resolution of such a barrier would be trimming of the Tg by Artemis, an endonuclease that associates with DNA-PK and is activated by that association. As shown previously, there is insufficient Artemis in whole-cell extracts to trim canonical Artemis substrates such as 3' overhangs of DSBs. For the Tg-containing substrates, added Artemis did not detectably increase trimming beyond the low level already seen in the unsupplemented extracts (Figure 3.2A, lanes 7, 14, 20 and 26). Nevertheless, for the Tg2 substrate only (lane 14), addition of Artemis resulted in a twofold increase in the yield of ligated product ($1.48 \pm 0.08\%$ vs. $0.77 \pm 0.07\%$, $N=3$), accompanied by a slight decrease in its length (~ 2 bases, based on its mobility). These results suggest that Tg near a DSB 3' terminus can be trimmed by Artemis, albeit inefficiently.

3.3 Ligation of Tg-Containing Substrates Does Not Require Prior Tg Removal

For the Tg3 substrate, EndoIII treatment prior to restriction nuclease digestion reduced the yield of 44-base product, but for the Tg1 substrate in particular (Figure 3.2B), EndoIII appeared to have little if any effect. Although this result could be explained by a replacement of Tg by normal thymine in all the Tg1 ligation products, an alternative possibility is that only the Tg-containing strand was ligated, and the remaining nick in the opposite strand prevented EndoIII from acting. To assess the presence of Tg without regard to the status of the complementary strand, end joining products generated in extracts containing either dTTP or ddTTP were cut with NdeI and PstI, then denatured, and annealed to an excess of a 44-base oligomer complementary to the expected ligation product of the labeled, Tg-containing strand. The annealed products were finally treated with EndoIII (Figure 3.3). Under these conditions, EndoIII reduced the yield of 44-base product from the Tg1 and Tg2 substrates by half, and from the Tg3 substrate by 30%. Thus, the NHEJ machinery was clearly capable of ligating all three Tg-containing substrates, albeit inefficiently, even ligating a 3'-terminal Tg to a blunt end. These results also exclude the possibility that

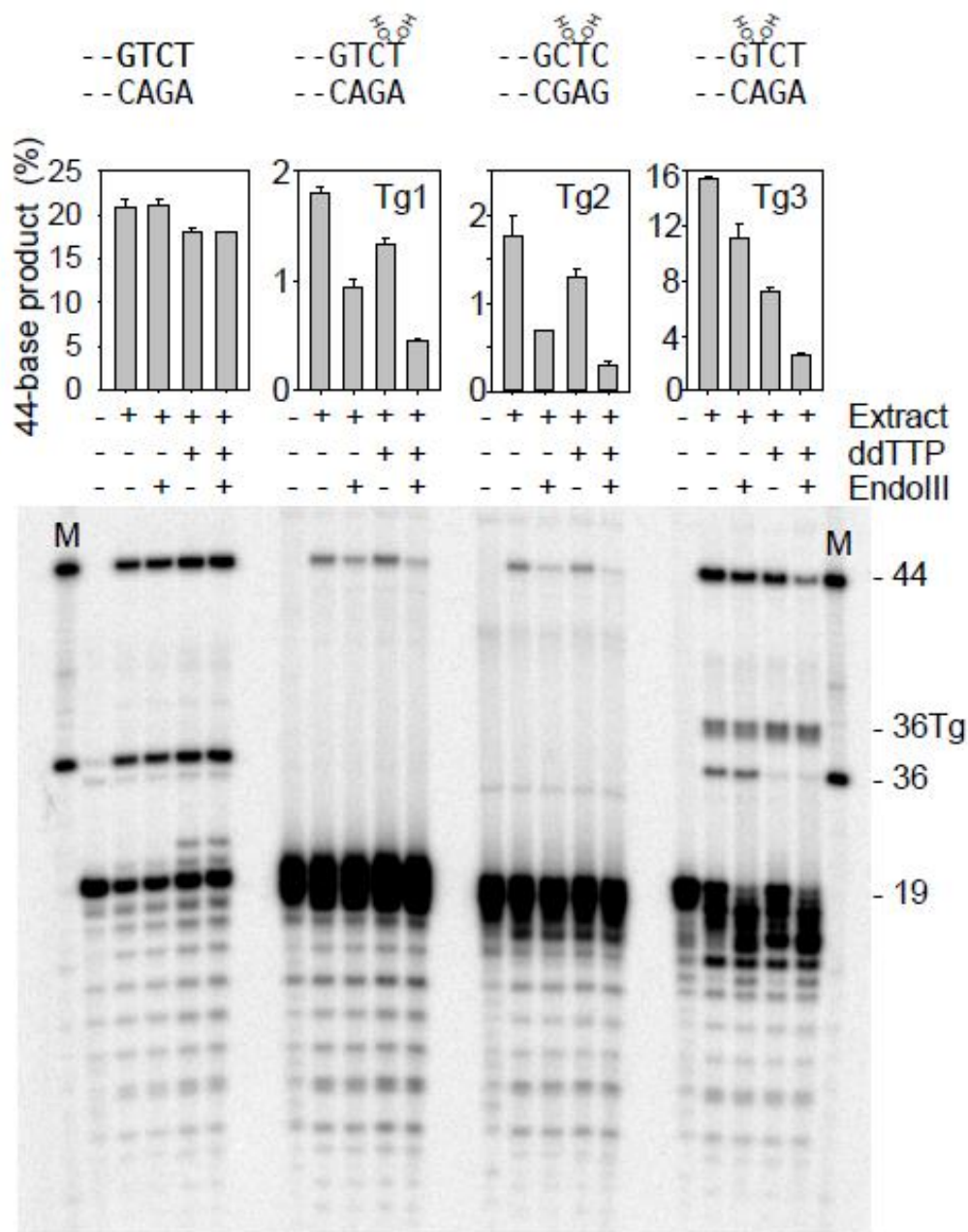


Figure 3.3 Presence of Tg in end joining products. Tg-containing or unmodified substrates were incubated for 6 hr in Bustel extracts supplemented with XLF and ddTTP as indicated. Samples were deproteinized and cut with NdeI and PstI, then denatured and annealed to 44-base complements of the expected head-to-tail ligation products and treated (or not) with EndoIII prior to denaturing gel electrophoresis. Bar graphs show the yield of 44-base products in each case (mean \pm SEM for 3 independent experiments).

the apparent ligation of Tg1 and Tg2 substrates was the result of contamination with a small fraction of the corresponding unmodified substrates. As expected, EndoIII had no effect on yield of products from the unmodified substrate. For all of the Tg-containing substrates, substitution of ddTTP for dTTP likewise reduced the yield of ligation products dramatically, and also eliminated most of the EndoIII-resistant ligation products (Figure 3.3); the remainder may be due to some residual dTTP in the extracts. This result shows that Tg was sometimes excised and replaced with thymine, although it does not distinguish whether such replacement occurred before or after blunt-end ligation of the DSB. In the case of the Tg3 substrate, this question was addressed by substituting ddCTP for dCTP during incubation in the extracts. If Tg were either trimmed off by a nuclease or removed by base excision repair prior to ligation of the DSB, the two 3'-terminal bases attached to it would presumably be lost as well, so that a blunt-end ligation product could only be formed by re-synthesis with dCTP and dTTP. Thus, the finding that ddCTP did not reduce the yield of blunt-end ligation product (Figure 3.4A, lane 9 and Fig 3.4B, lane 8) suggests that most if not all ligations of the Tg3 substrate occurred with Tg still present.

3.4 An Initial Delay in Ligation is Dependent on Tg Position

To further investigate the order of Tg excision and DSB ligation, samples were taken at various times after addition of substrate to the extract. For the Tg3 substrate, ligated products began to accumulate rapidly after an initial delay of about 30 min, but the Tg-containing 36Tg fragment accumulated much faster than the thymine-containing 36-base fragment (Figure 3.4A and 3.4C). These data are consistent with a mechanism wherein ligation preceded Tg removal and replacement, so that at later times continuing ligation was approximately balanced by slow excision of Tg from the ligated product, resulting in a steady-state level of the 36-base Tg-containing ligation product (36Tg). Thus, this result lends further support to the inference, from ddCTP trapping experiments, that ligation precedes Tg removal and replacement in formation of the unmodified (thymine-containing) 36-base product. There

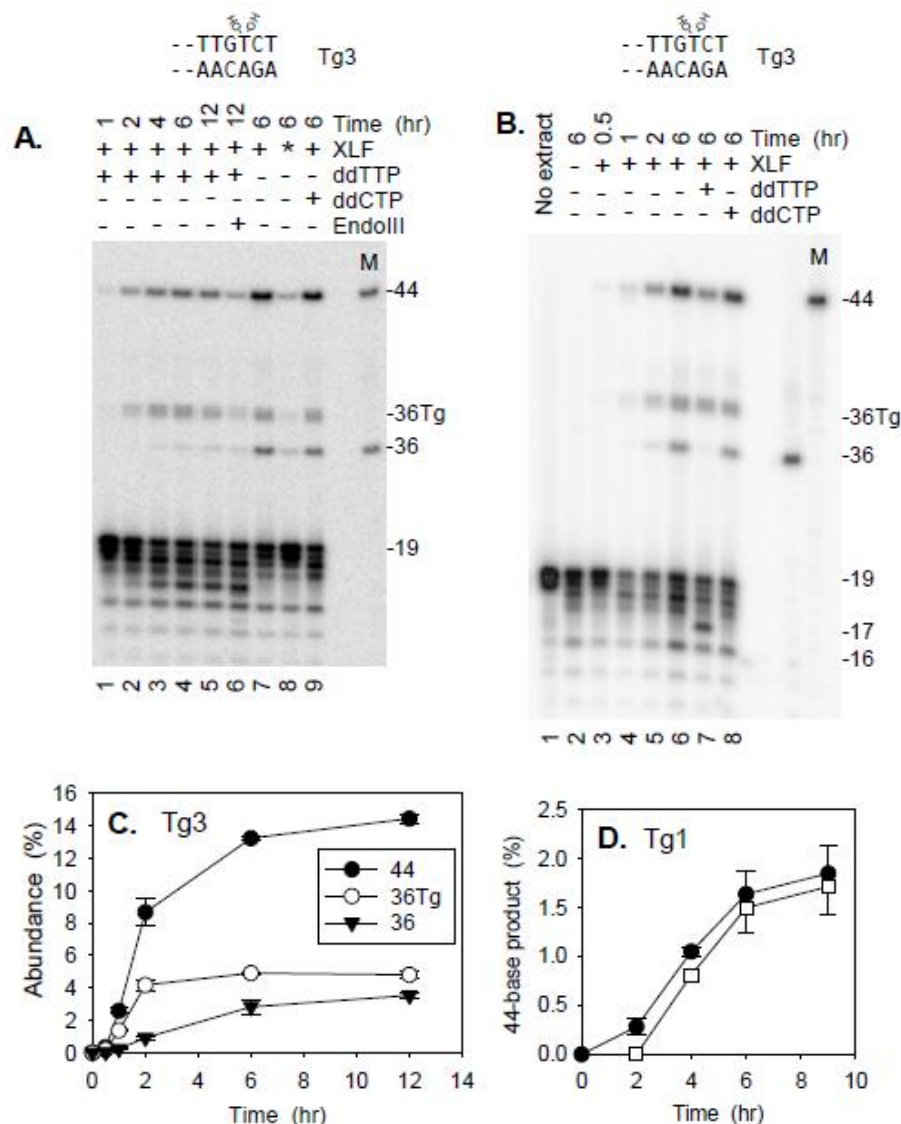


Figure 3.4. Time course for Tg3 and Tg1 end joining and effect of dideoxynucleotides. A. and B. Tg3 was incubated in extracts containing ddTTP, ddCTP and/or XLF for the times indicated, then cut with NdeI and PstI and analyzed as in Fig. 2. One sample in (A.) was treated with EndoIII prior to NdeI/PstI cleavage, as in Fig. 3.2. Asterisk (*) indicates addition of a mutant XLF with an L115A mutation. C. Quantitative analysis of Tg3 ligation in the presence of dNTPs, derived from three replicates of the experiment shown in (B.). D. Time course of formation of end joining for Tg1. The Tg1 substrate was incubated in extracts, with XLF added either at the start of the reaction (●) or after 2 hr incubation (□). Reaction conditions were as in Fig. 3.2.

was, however, an initial delay of about 30 min before a significant level of end joining products appeared (Figure 3.4C). For the Tg1 substrate, a longer delay of nearly 2 hr was seen (Figure 3.4D). However, when extract and substrate were preincubated for 2 hr in the absence of XLF, end joining began immediately upon XLF addition, suggesting that there was some prejoining process that did not require XLF but that either proceeded more slowly with the Tg1 substrate, or was only essential for the Tg1 substrate.

3.5 Mutations in XLF at its Interface with XRCC4 Reduce or Eliminate Ligation

Previous X-ray crystallography shows that XLF binds to XRCC4 via a “leucine lock” motif wherein Leu115 of XLF slips into a hydrophobic pocket in XRCC4 (Hammel et al., 2011; Ropars et al., 2011). Moreover, an L115A mutation eliminates detectable XLF-XRCC4 binding, suggesting that the leucine lock is essential for this interaction. To assess whether disruption of XRCC4-XLF interaction would differentially influence end joining of Tg-containing substrates, each of the substrates were incubated in extracts containing no XLF, wild-type XLF, or XLF wherein Leu115 was replaced with either Ala or Asp (Figure 3.5). The L115A mutation decreased ligation of all substrates, by roughly seven-fold, reducing ligation of Tg1 and Tg2 to near the lower limit of detection; nevertheless, a trace of ligation of the Tg1 substrate could be seen. A less conservative L115D mutation completely eliminated ligation of all five substrates. These results suggest that XLF-XRCC4 interaction is essential for end joining but that the L115A mutant still retains some interaction with XLF. However, there was no evidence that mutations in XLF differentially affected ligation of Tg-containing substrates. Moreover, the 14-mer band corresponding to Tg excision from the Tg5 substrates was equally intense with or without added XLF, suggesting that the putative XLF-XRCC4 filament did not protect Tg in the unligated substrate from excision by BER.

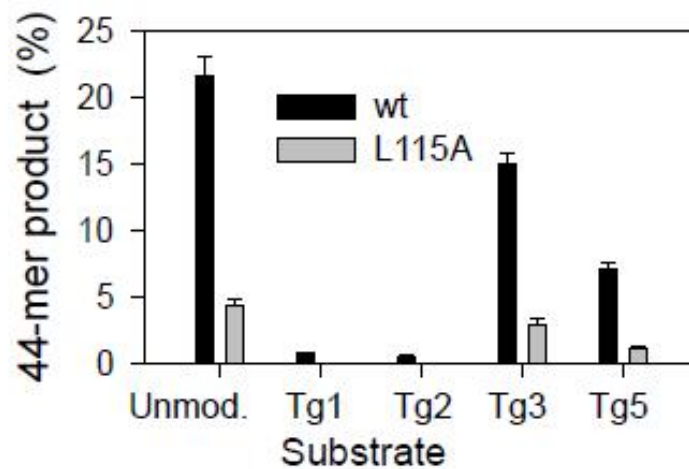
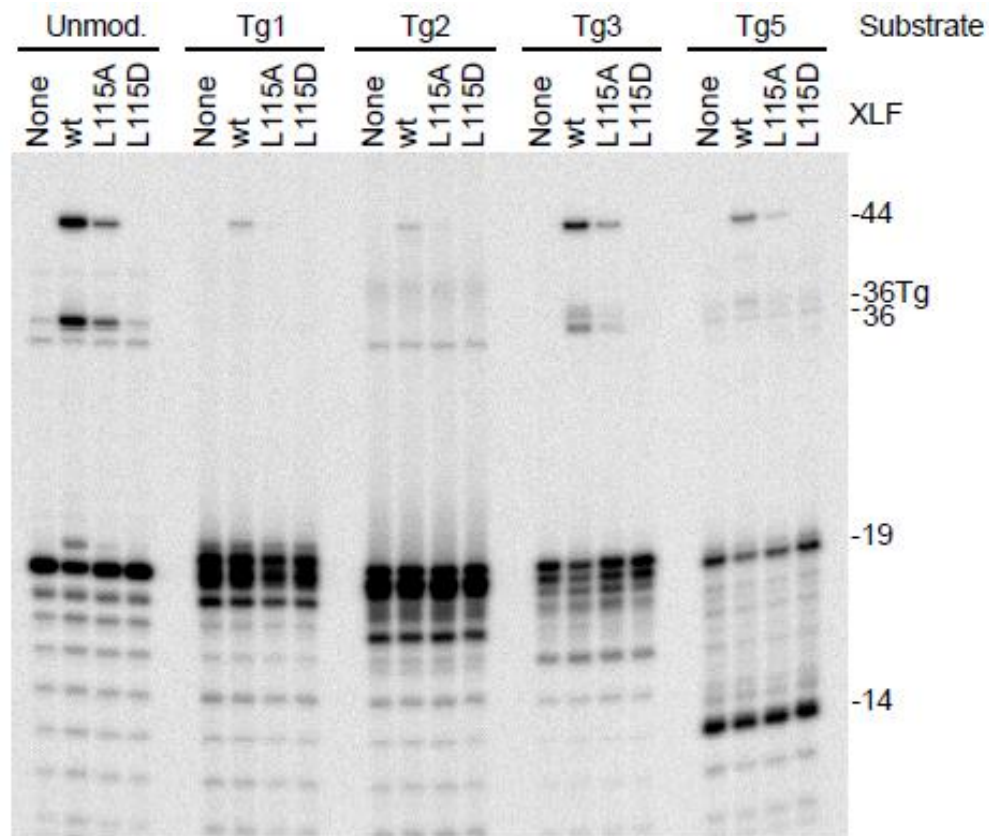


Figure 3.5. Effect of L115 mutations in XLF on end joining. Tg-containing substrates were incubated in extracts complemented with the indicated normal or mutant XLF proteins (100 nM) for 6 hr, cut with NdeI and BstI and analyzed on denaturing gels. Graph shows abundance of the 44-base head-to-tail ligation product. There was no detectable product in samples containing either no XLF or the L115D mutant.

3.6 Development of a Diverse Peptide Libraries Composed of Cyclic Peptides to Inhibit XRCC4-XLF Interaction

We used the mRNA display technique to synthesize libraries of mRNA-peptide fusions to inhibit the XRCC4-XLF interaction (Roberts & Szostak, 1997). In order to find tight-binding peptides, we designed five libraries to contain cyclic sequences of a variety of ring sizes. The complete structure of each DNA library is summarized in Figure 3.6. The libraries were constructed to contain a 12 random amino acids region with two fixed cysteines at different positions to ensure that we have cyclic peptides with different ring sizes. This will allow XRCC4¹⁵⁷ to “choose” the most appropriate scaffold with which to bind. Also, we used the NNS (S=C/G) codon in the random region to decrease the prevalence of stop codons as compared to NNN. For cyclization, we focused on the well-established and robust bis-bromomethylbenzene chemistry, which covalently cyclizes peptides with two cysteines (Dewker et al., 2009; Guillen Schlippe et al., 2012; Timmerman et al., 2005).

3.6.1 *In Vitro* Selection

The formation of mRNA display natural cyclic peptide library started by transcription of five DNA templates that encode peptides with 12 random amino acids interspersed with two cysteine residues (Figure 3.7). Following transcription, the five mRNA libraries were combined together and photo cross-linked to an oligonucleotide containing puromycin at its 3' end. Then, the combined mRNA libraries were translated on a 5 mL translation scale in the PURE translation system (Shimizu et al., 2001) with 20 natural amino acids. After that, mRNA peptide fusions were immobilized on an oligo-dT column and cyclized using dibromoxylene. In addition to giving a simple means for cyclization, these two processes were performed to remove peptides that were not conjugated to their mRNAs, and mRNAs that were not photocrosslinked by psoralen. After that, the peptide-fusions were reverse transcribed to create cDNA for PCR and to eliminate any unwanted RNA secondary structures. Then, the mRNA-peptide fusions were purified using

Library Construction

mRNA	ATG TGC NNS NNS TGC NNS NNS NNS NNS NNS NNS NNS NNS NNS NNS GGC TCC GGT AGC TTA GGC CAC CAT CAC CAT CAC CAT CGG CTA
Peptide	Met Cys X X Cys X X X X X X X X X X Gly Ser Gly Ser Leu Gly His His His His His His Arg Leu
mRNA	ATG TGC NNS NNS NNS NNS TGC NNS NNS NNS NNS NNS NNS NNS NNS GGC TCC GGT AGC TTA GGC CAC CAT CAC CAT CAC CAT CGG CTA
Peptide	Met Cys X X X X Cys X X X X X X X X X Gly Ser Gly Ser Leu Gly His His His His His His Arg Leu
mRNA	ATG TGC NNS NNS NNS NNS NNS NNS TGC NNS NNS NNS NNS NNS NNS GGC TCC GGT AGC TTA GGC CAC CAT CAC CAT CAC CAT CGG CTA
Peptide	Met Cys X X X X X X X Cys X X X X X X X Gly Ser Gly Ser Leu Gly His His His His His His Arg Leu
mRNA	ATG TGC NNS NNS NNS NNS NNS NNS NNS NNS NNS NNS TGC NNS NNS NNS GGC TCC GGT AGC TTA GGC CAC CAT CAC CAT CAC CAT CGG CTA
Peptide	Met Cys X X X X X X X X X X Cys X X X Gly Ser Gly Ser Leu Gly His His His His His His Arg Leu

Figure 3.6 DNA libraries structure. The peptide sequence encoded by the library (shown above) has an N-terminal fixed cysteine and another cysteine after a random region of 2, 4, 6, 8 or 10 amino acids encoded by a degenerate codon NNS (S=C, or G). It has a flexible linker with two out of frame stop codons; GlySerGlySer-LeuGly. It has 6xHis tag at the C-terminus for Ni-NTA purification.

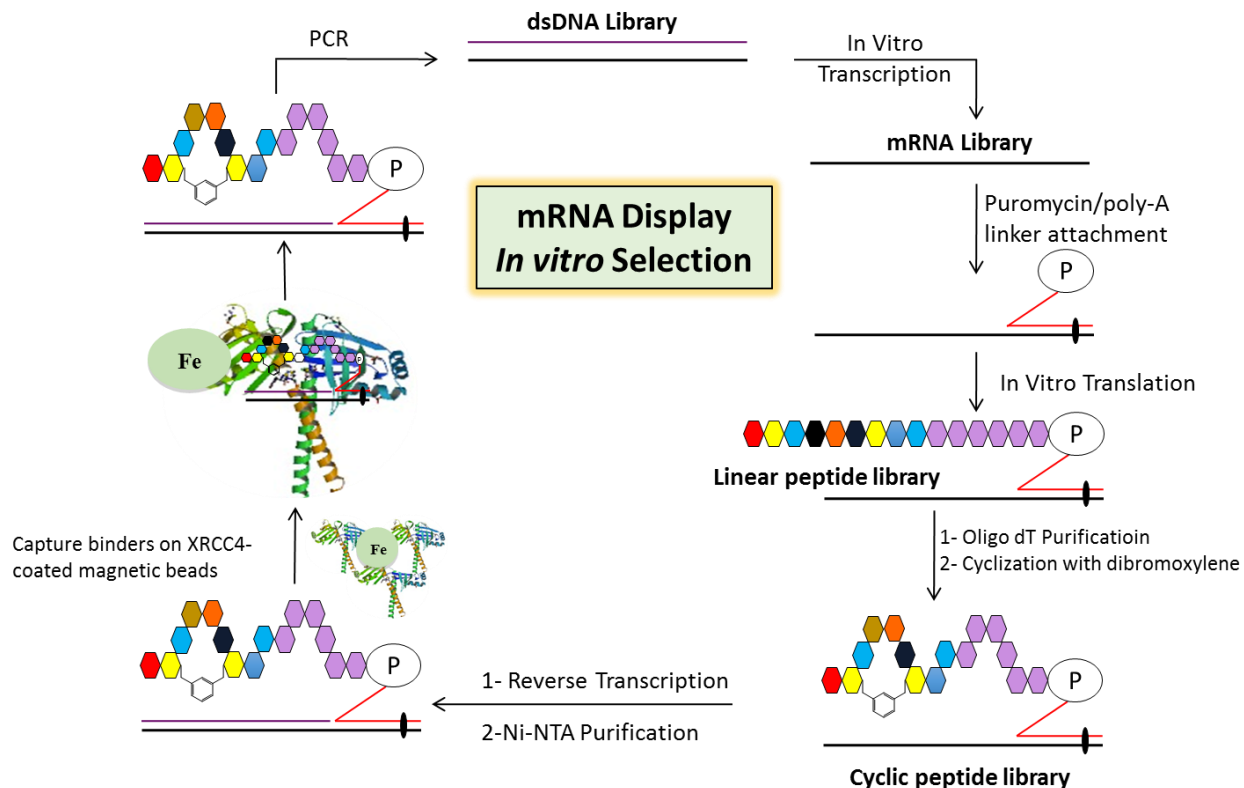


Figure 3.7. *In vitro* selection process search for XRCC4-XLF inhibitors. We started with DNA libraries as described in Figure 3.6. After mRNA–peptide fusion formation, peptides were cyclized with dibromoxylene. Purified mRNA–peptide fusions were reverse transcribed and purified on Ni-NTA beads before being selected for binding to GST-XRCC4¹⁵⁷ fusion immobilized on magnetic beads. Unbound peptides were washed away, and bound peptides were PCR amplified, and carried through the subsequent round of selection.

a Ni-NTA column in order to remove the truncated mRNA peptide fusions which were dialyzed into selection buffer. After this procedure, 1.44 pmols of peptides library were created, corresponding to a diversity of 870 billion unique peptide sequences.

In the selection step of the first round, we first incubated our library with GST protein (not fused to XRCC4) on magnetic beads in order to remove all non-specific peptide inhibitors that bind to the GST or glutathione magnetic beads. Then, the flow through and washes with high counts were collected and bound to WT GST-tagged XRCC4¹⁵⁷ fragment. This fragment includes the complete head domain known to contain the XLF interface but lacks the C-terminal DNA ligase IV-binding region that could interact with the mRNA component of our mRNA-peptide fusions. Those peptides that bound to WT GST-XRCC4¹⁵⁷ were captured on the glutathione magnetic beads. Then, the beads were washed and suspended in selection buffer and the percentage of the ³⁵S-labeled peptides bound to the resin was measured to be 2.1% (0.03 pmole). The DNA-mRNA duplex fused to the XRCC4-captured peptides was amplified by PCR. This signifies the end of the first round and the resulting DNA from this round was *in vitro* transcribed and then new mRNA-peptide fusions were formed to take through the subsequent rounds. The recovery was calculated at the end of each round (Figure 3.8). From round five, we started to increase the stringency of washing during the selection by using a technique known as Continuous-Flow Magnetic Separation (Olsen et al., 2011). After binding the peptide-fusions to the immobilized protein, we continuously washed with washing buffer at a rate of 0.5 mL per minute for 10 minutes in order to remove those peptides which are not very tight binders and leave those with high binding affinity to the protein.

A.

	First Rd	Second Rd	Third Rd	Fourth Rd	Fifth Rd	Sixth Rd	Seventh Rd
Purification (input)	1.44 pmole	0.35 pmole	0.49 pmole	0.18 pmole	0.436 pmole	0.21 pmole	0.53 pmole
GST-XRCC4¹⁵⁷ (output)	0.03 pmole (2.08%)	0.004 pmole (1.14%)	0.011 pmole (2.24%)	0.022 pmole (12.2%)	0.051 pmole (11.7%)	0.022 pmole (10.48%)	0.021 pmole (3.96%)

B.

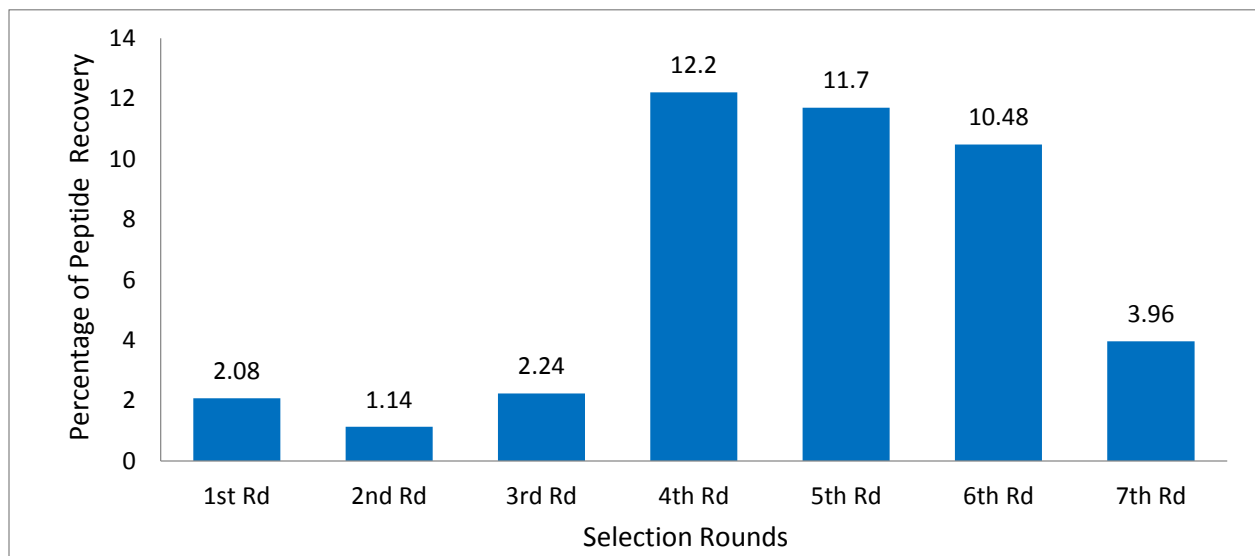


Figure 3.8. *In vitro* selection results. Progress of the selection measured by the percentage of the total ³⁵S-Met labeled peptides. A) Shows the amount of peptide fusions after purification added to the selection step (input) compared to the remained bound to the beads. B) Graphical representation of percentage recovery from (A). Note: the decrease in the percentage of the recovery after round seven was due to bead lost during the washing step.

3.7 Sequencing

After the seventh and final round, cDNAs corresponding to the selected mRNA–peptide fusions were sequenced. The sequencing result shows that the peptides could be arranged into five families, which we named 7.1-7.5 based on their relative abundance (Figure 3.9). To ensure the winners of the seventh round were present and enriched during the selection from round to round, we sequenced cDNA from round 3 to 6 using Second Generation Sequencing (Figure 3.10 and Figure 3.11). Indeed, the Second Generation Sequencing result showed that the winners of round seventh were present from the beginning and were enriched especially from round 4 to 5 and from round 5 to 6. However, they were not the winners of round three and did not enrich very well from 3 to 4; nevertheless, the number of sequences of these peptides were high in these rounds. The reason why we see significant enrichment from round 4 to 5 and 5 to 6 is because at round five we started to increase the stringency of washing during the selection (Olsen et al., 2011). The fact that these peptides survived the continuous washes suggests that the winners of round seven are high affinity binders.

MCWEVVGELCVWSL
 MCWEVVGELCVWSL
 MCWEVVGELCVWSL
 MCWEVVGELCVWSL
 MCWEVVGELCVWSL
 MCWEVVGELCVWSL
 MCWEVVGELCVWSL
 MCWEVVGELCVWPL
 MCWEVVGELCVWSL
 MCREVVGELCVWSL
 MCREVVGELCVWSL
 MCWEVVGELYVWSL

[illegible]

MCWEVVGILLCARAN
MCWEVVGISLCARAN
MCWEVVGISLCARAN

Figure 3.9. Sequencing result. After round seven, cDNA from the library pool was cloned and sequenced giving the 81 sequences shown. Similar sequences were arranged into five families.

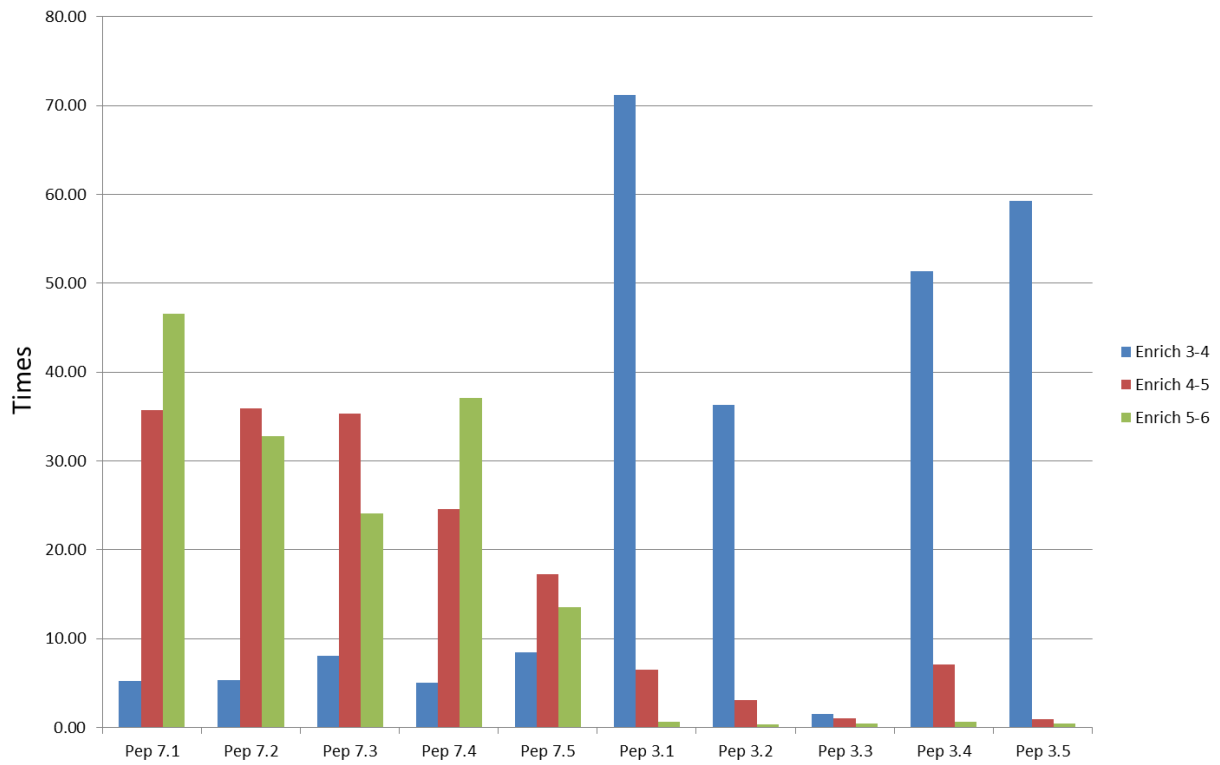


Figure 3.10. Second generation sequencing result. cDNA from round 3, 4, 5 and 6 were sequenced by Second Generation Sequencing. The graph shows the enrichment of the selected peptides from round to round.

Round Three	Round Four	Round Five	Round Six
MCRGARSTTPVEHRR*	MCRGARSTTPVEHRR*	MCRGARSTTPVEHRR*	MCLCGTRRRRGARRGAV
MCRKTQTVCPVVRNNGS	MCAVCPATWLCVMREGS	MCGLPMTTELVCPCRMGS	MCSWMWRIETCGMILGS
MFCDGFIYACYMDVSGS	MCRVLKRRALSSCLVGS	MCAVCPATWLCVMREGS	MCWEVVGEILCVWSLGS
MCGLPMTTELVCPCRMGS	MCRKTQTVCPVVRNNGS	MCRKTQTVCPVVRNNGS	MCGVGVRVCRQRGGS
MCRVLKRRALSSCLVGS	MCGLPMTTELVCPCRMGS	MCWKCQCMCLHGILRGS	MCRGARSTTPVEHRR*
MCAVCPATWLCVMREGS	MCRYFSLWLHEPTGCAGGS	MCLCGTRRRRGARRGAV	MCGLPMTTELVCPCRMGS
MCKFIKFFNFYRHRGSGS	MCWKCQCMCLHGILRGS	MCWEVVGEILCVWSLGS	MQLDVAHRDVRDDPR*
MCWKCQCMCLHGILRGS	MCAVCPVTCVSFCSSV	MCRVLKRRALSSCLVGS	MCAVCPATWLCVMREGS
MCLVTYVVCPMTRESGS	MWRMCLCPAAASSV	MCSWMWRIETCGMILGS	MCGKMEGRSVKRA*RGs
MCLCGTRRRRGARRGAV	MCRYFSLWLHEPTGCAGS	MCAVCPVTCVSFCSSV	MCWEVVGILLCARANGS
MWRMCLCPAAASSV	MCQMNIERMENR*GTV	MCRGARSTTPVEHRW*	MCWEFMGRSPCLWARGs
MCSWMWRIETCGMILGS	MCFCAIKVAQRSSADVPGS	MCAVCPATSLSLIVTGS	MCRKTQTVCPVVRNNGS
MCAVCPVTCVSFCSSV	MCRGARSTTPVEHRW*	MCQMNIERMENR*GTV	MCLCGTRRRRGARRGVV
MCWEVVGEILCVWSLGS	MCRGLTCCTLLAAKKGS	MWRMCLCPAAASSV	MCWEVVGISLCARANGS
MCPKFMLNVC PFVRLWV	MCRVLKRRALSSCLVV	MCGVGVRVCRQRGGS	MCVPCKGRSVKRA*RGs
MCQMNIERMENR*GTV	MCAVCPATSLSLIVTGS	MCRGARSATPVEHRR*	MCCWWVLIFAAACGAV
MCRGLTCCTLLAAKKGS	MCAT*ICLIQRRLENGs	MCWEFMGRSPCLWARGs	MCWKCQCMCLHGILRGS
MCAT*ICLIQRRLENGs	MCWVCPQTR*SMKWFGS	MCWEVVGILLCARANGS	MCRVLKRRALSSCLVGS
MCGVGVRVCRQRGGS	MCPKFMLNVC PFVRLWV	MCWVCPQTR*SMKWFGS	MCWEVVGEILCVWSMGs
MCAVCPPELDYLVGGS	MCLVTYVVCPMTRESGS	MCRGLTCCTLLAAKKGS	MC*LTGCWEVWGTWYGS
MCRCCRWLWTGEANMGs	MCW*R*RECPCSNSNGs	MCRYFSLWLHEPTGCAGGS	MCDRLMVWSICFVRAV
MCCSGGCTNHCMCLQGS	MFCDGFIYACYMDVSGS	MCRGARSTTPVEQRR*	MCRGARSTTPVEHRW*
MCW*R*RECPCSNSNGs	MCLCGTRRRRGARRGAV	MCAT*ICLIQRRLENGs	MCRQCGRSAATTRGV
MCRGARSTTPVEHRW*	MCRCCRWLWTGEANMGs	MCRVLKRRALSSCLVV	MCNVEKLRQVCIRPGR*
MCWEVVGILLCARANGS	MCWEVVGEILCVWSLGS	MCRGARSTTPVEHRRE	MCSWMWRIETCGMILGS
MCWVCPQTR*SMKWFGS	MCKFIKFFNFYRHRGSGS	MRRGARSTTPVEHRR*	MCWEVVGEILCVWSLV
MCEKTQCMSSRLRLMGs	MCAVCPPELDYLVGGS	MCGLPMTTELVCPCRMV	MCSWMWRIETCGMVLGs
MCCRL*RLCQRIRYSGs	MCWGEDLEGDC*KWRR*	MCRYFSLWLHEPTGCAGS	MCAVCPVTCVSFCSSV
MCPWKNSKKGCELEEGs	MCRGARSATPVEHRR*	MCGKMEGRSVKRA*RGs	MCWEALRGANCVVIGs

Figure 3.11. Top 30 sequences of round 3, 4, 5, and 6 after second generation sequencing. The highlighted sequences are the winners of round seven.

3.8 Synthesis of the Selected Peptides

We selected a representative peptide from each family of round seven (7.1 – 7.5) as well as two winner's peptides from round 3 (3.2 and 3.3) to be synthesized on solid phase peptide synthesis (SPSS). The synthesis of the peptides is summarized in Figure 3.12. The goal is to prepare m-dibromoxylene cyclized, 5(6)-Carboxyfluorecin labeled and HPLC purified peptides (Figure 3.13 and 3.14). The progress of the peptides synthesis is summarized in Table 3.1. The cyclization is because we have used cyclic peptides during the selection for XRCC4 binders. However, we prepared linear forms as well to see the differences between the cyclic and linear peptides in term of binding affinity to XRCC4 protein and inhibition of NHEJ in cell extract assay. However, we had challenges during the preparation of our peptides.

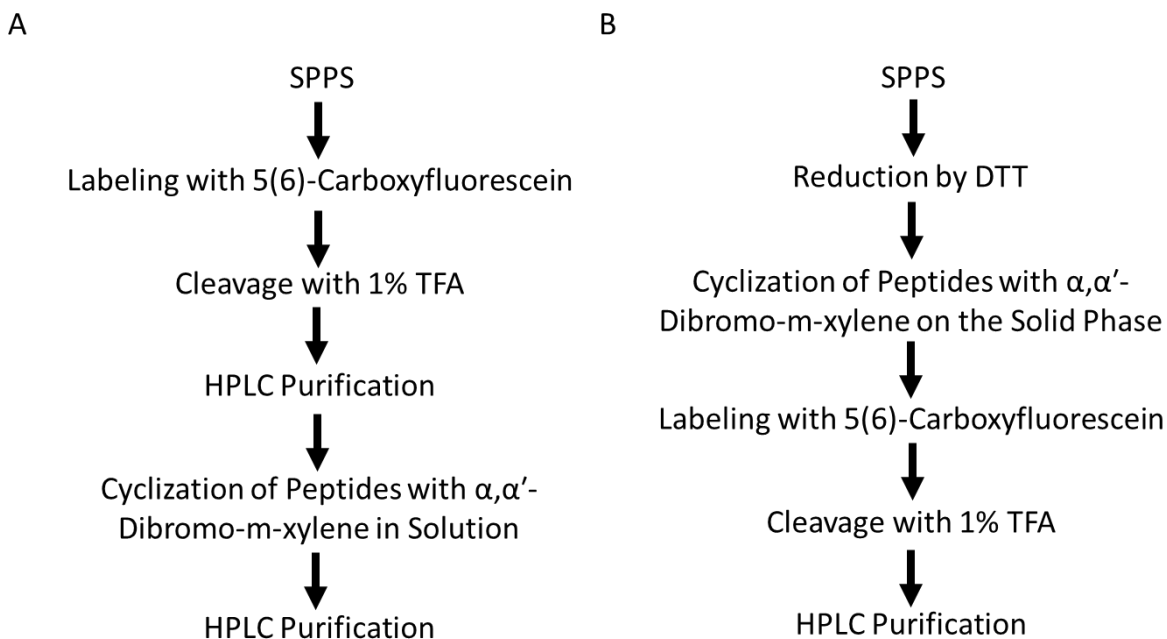


Figure 3.12. Peptide synthesis approaches. Synthesis of the peptides that involved (A) cyclization in solution or (B) cyclization on the resin.



Figure 3.13. HPLC spectrum of Pep 7.4

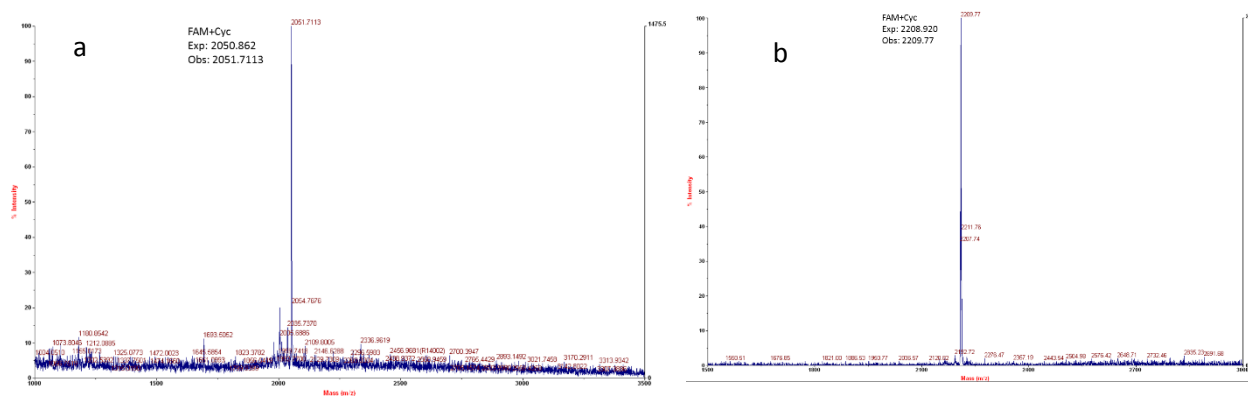


Figure 3.14 MALDI-TOF analysis of Pep 7.4 and Pep 3.2. After synthesis on the solid phase, a) Pep 7.4 and b) Pep 3.2 were labeled, cyclized and purified by HPLC and analyzed by MALDI-TOF. Expected (Exp) masses are $[M + H]^+$ peaks.

Peptides	Sequences	SPPS	Labeling	Reduction	Cyclization	HPLC (Linear)	HPLC (Cyclic)
7.1	MCSWMWRIETCGMIL	Yes	Not complete	Not complete	No	Yes	No
7.2	MCLCGTRRRGARRGAVAAP	Yes	Complete	Complete	Yes	Yes	Yes
7.3	MCWEVVGEILCVWSL	Yes	Not complete	Not complete	No	No	No
7.4	MCGVGVRVCRQRG	Yes	Complete	Complete	Yes	Yes	Yes
7.5	MCWEVVGISLCARAN	Yes	Not complete	Not complete	No	No	No
3.2	MCRKTQTVCPVVRN	Yes	Complete	Complete	Yes	Yes	Yes
3.3	MFCDGFYACYMDVGS	No	Not complete	Not complete	No	No	No

Table 3.1. Summary of peptides synthesis.

3.8.1 Challenges

Peptides 7.1, 7.3, 7.5 and 3.3 are highly hydrophobic as shown in Table 3.2, and presumably as a consequence these peptides presented severe difficulties in synthesis and purification, as shown for Pep 7.1 in Figure 3.15. Also, we could not get pure product of crude peptide 3.3 which might be due to the presence of aspartic acid followed by glycine (X-Asp-Gly-X) in its sequence in which these two amino acids are difficult to be coupled. Since this peptide was not one of the winners of round seven and we were not successful in getting pure product, we stopped working with it. To overcome the hydrophobicity of these peptides, we replaced m-dibromoxylene with 1,3-bis(bromomethyl)benzyl 2-[2-(2-methoxyethoxy)ethoxy]acetate which was prepared by attaching a hydrophilic linker (2-[2-(2-methoxyethoxy)ethoxy]acetic acid) to 1,3,5-tris(bromomethyl)benzene (Figure 3.15) using the procedure outlined by Dewkar and Hartman (2009). This substitution helped to some extent but not very significantly. The other approach that we have used to increase the solubility of these peptides is to attach

a poly arginine (R9) with a GS linker at the C-terminus of each peptide (Table 3.3) and to this product attach an 6-Aminohexanoic acid to the N-terminus of these peptides as a linker to improve the efficiency of labeling with 5-FAM. We also made truncated peptides. All of that was helpful but still not enough to get a soluble cyclic peptide of 7.1, 7.3 and 7.5 that can be purified by HPLC.

Peptides	Sequences	Hydrophilic residues	Hydrophobic residues	Net Hydrophobicity (%)
7.1	MCSWMWRIETCGMIL	RE	MWMWIMIL	40.00
7.2	MCLCGTRRRGARRGAVAAP	RRRRR	MLV	-6.67
7.3	MCWEVVGEILCVWSL	EE	MWVVILVWL	46.67
7.4	MCGVGVRVCRQRG	RRR	MVVVV	13.33
7.5	MCWEVVGISLCARAN	ER	MWVVIL	26.67
3.2	MCRKTQTVCPVVRN	RKR	MVVV	6.67
3.3	MFCDGFYACYMDVGS	DD	MFFYYMV	33.33

Table 3.2. Percentage of the hydrophobicity of each peptide.

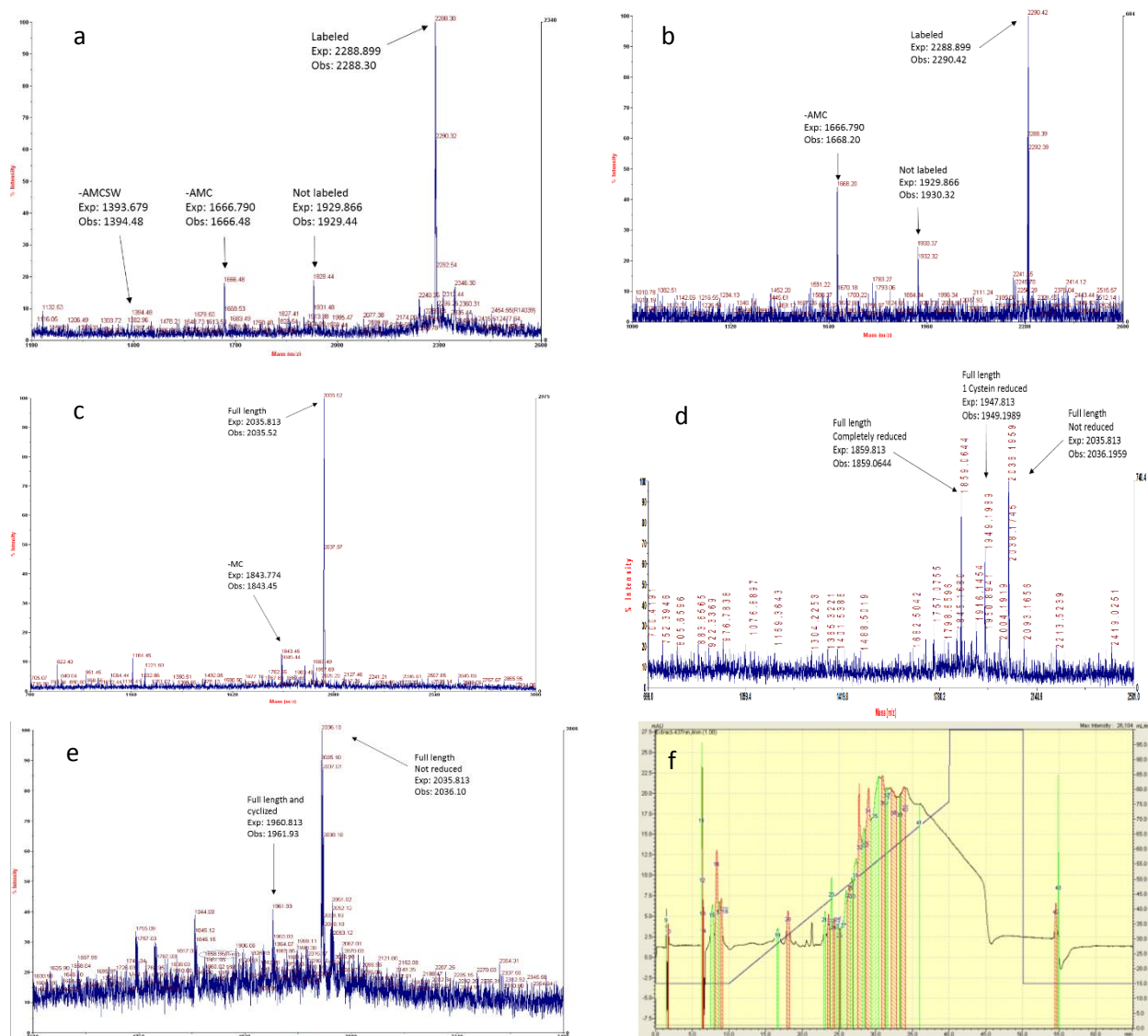
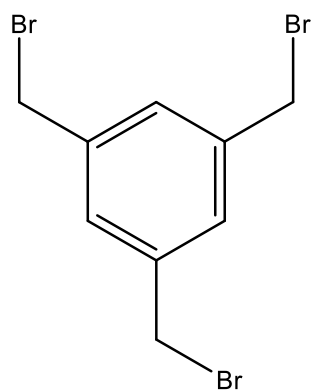
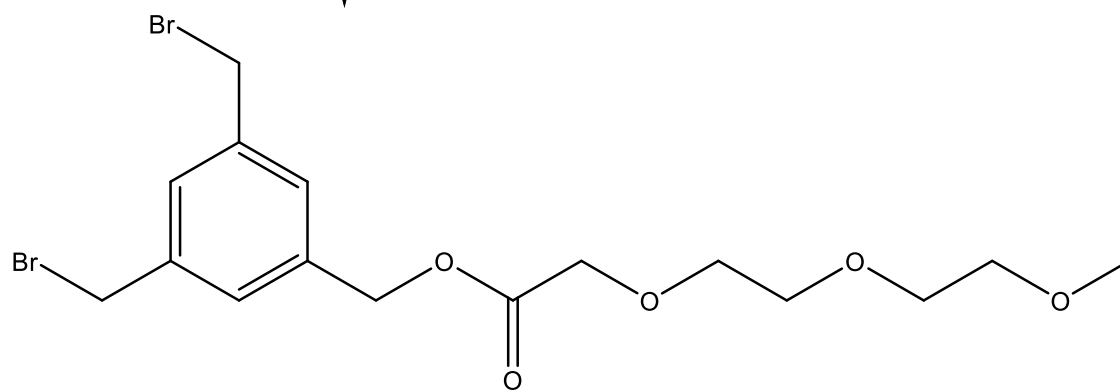
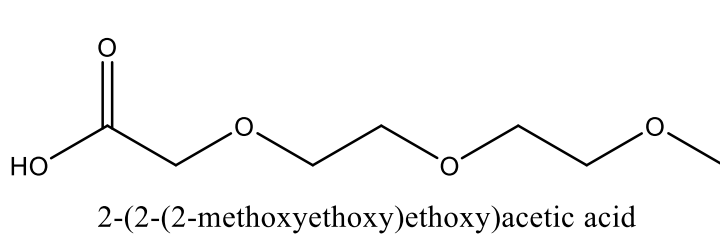


Figure 3.15. MALDI-TOF analysis of Pep 7.1 (MCSWMWRIETCGMIL). a) Analysis of linear Pep 7.1 after labeling with 5-FAM. Beta-alanine was attached at the N-terminus as a linker to facilitate labeling. It shows that not all of the peptide was labeled and it shows some truncations. b) Analysis of labeled Pep 7.1 after HPLC. The spectrum shows impure peptide. c) Analysis of linear Pep 7.1 in which we used Fmoc-S-tert-butylthio-L-cysteine as building block instead of Fmoc-(L)-Cysteine(Trt)-OH. d) Reduction of the thiol groups of the cysteines of Pep 7.1 while it is on the resin with 50 mM DTT and 100 mM NH_4HCO_3 . e) Cyclization of Pep 7.1 (d) on resin with α, α' -dibromo- m-xylene. f) HPLC for linear Pep 7.1 labeled with 5-FAM. All expected (Exp) masses are $[M + H]^+$ peaks.



1,3,5-Tris(bromomethyl)benzene



3,5-bis(bromomethyl)benzyl 2-(2-(2-methoxyethoxy)ethoxy)acetate

Figure 3.16. The Synthesis of 1,3-bis(bromomethyl)benzyl 2-[2-(2-methoxyethoxy)ethoxy]acetate. Note: the linker was synthesized by Dr. Hartman

	Full length peptides	Truncated peptides
7.1	6-AminoHex-MCWMWRIETCGMIL-GS-RRRRRRRRR	6-AminoHex-CSWMWRIETC-GS-RRRRRRRRR
7.3	6-AminoHex-MCWEVVGEILCVWSL-GS-RRRRRRRRR	6-AminoHex-CWEVVGEILC-GS-RRRRRRRRR
7.5	6-AminoHex-MCWEVVGISLCARAN-GS-RRRRRRRRR	6-AminoHex-CWEVVGSLC-GS-RRRRRRRRR

Table 3.3. Modification of the peptides to increase their solubility. Full length and truncated Pep 7.1, 7.3 and 7.5 were synthesized on SPPS. GSRRRRRRRRR was attached to the C-terminus. 6-Aminohexanoic acid was attached to the N-terminus of these peptides.

3.9 Determination the Binding Affinity of the Selected Peptides to XRCC4 Protein

3.9.1 Fluorescence Polarization

We used a fluorescence polarization (FP) assay to determine the K_d of our peptides. Generally, the concentration of the fluorescently labeled peptides was kept constant and incubated with an increasing protein concentration. FP requires high protein concentrations to produce a full binding curve. The K_d of the linear Pep 7.1 and Pep 7.2 were 16.78 μ M and 18.77 μ M, respectively Figure 3.17. Unfortunately, the reported results of the above peptides could not be reproduced. The cyclic Pep 7.2, 7.4 and 3.2 failed to show any binding affinity to XRCC4 protein. We could not measure the binding affinity of the cyclic Pep 7.1, 7.3 and 7.5 because we could not synthesize full length, cyclize, labeled and HPLC purified of these peptides

3.9.2 Scintillation-Based K_d Determination

The other approach we have used to determine the binding affinity of our peptides is by translating our peptides *in vitro* and measuring the K_d based on the scintillation count of 35 S-methionine-labeled peptides (Railey et al., 2015; Horiya et al., 2014). We have saved clones in glycerol stocks in 96 well plate when we sent the cDNA after round seven for sequencing. Therefore, we picked up some clones, sent for sequencing, *in vitro* transcribed and *in vitro* translated with 35 S-methionine (Figure 3.18). The translation yields and the input count of the selected peptides were not high and could not generate binding results of this experiment (Figure 3.19). Then, we ordered DNA templates of these peptides with an optimization of the N-terminus, but it did not help. One possible reason is that Pep 7.1, 7.3 and 7.5 are highly hydrophobic which might lead to aggregation and prevent the His tag from binding to Ni-NTA. We have tried detergent to prevent such aggregation. Unfortunately, it did not improve the translation yield significantly.

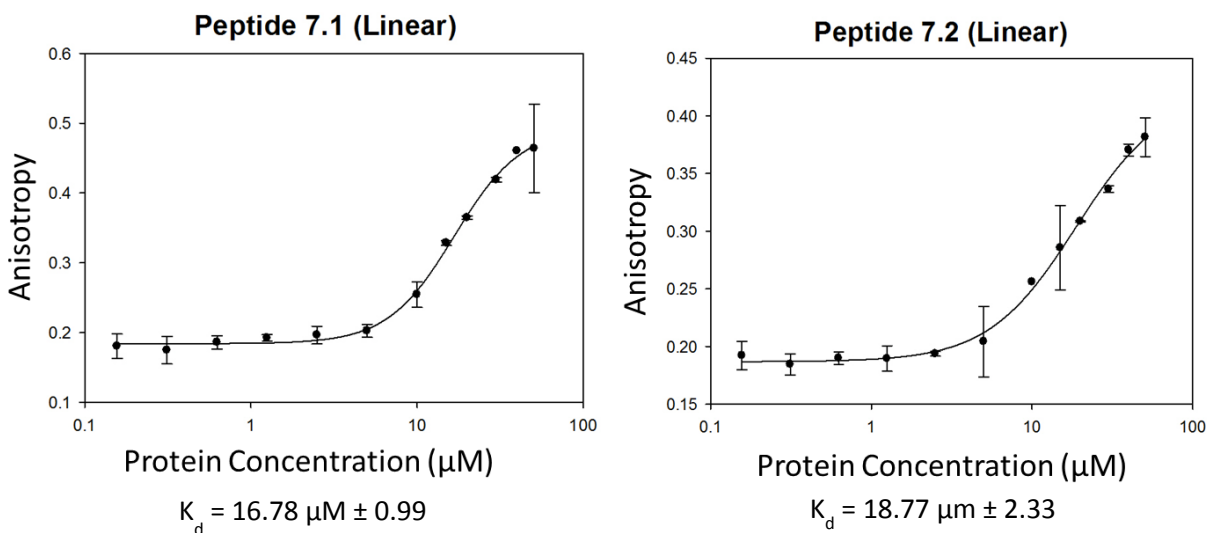
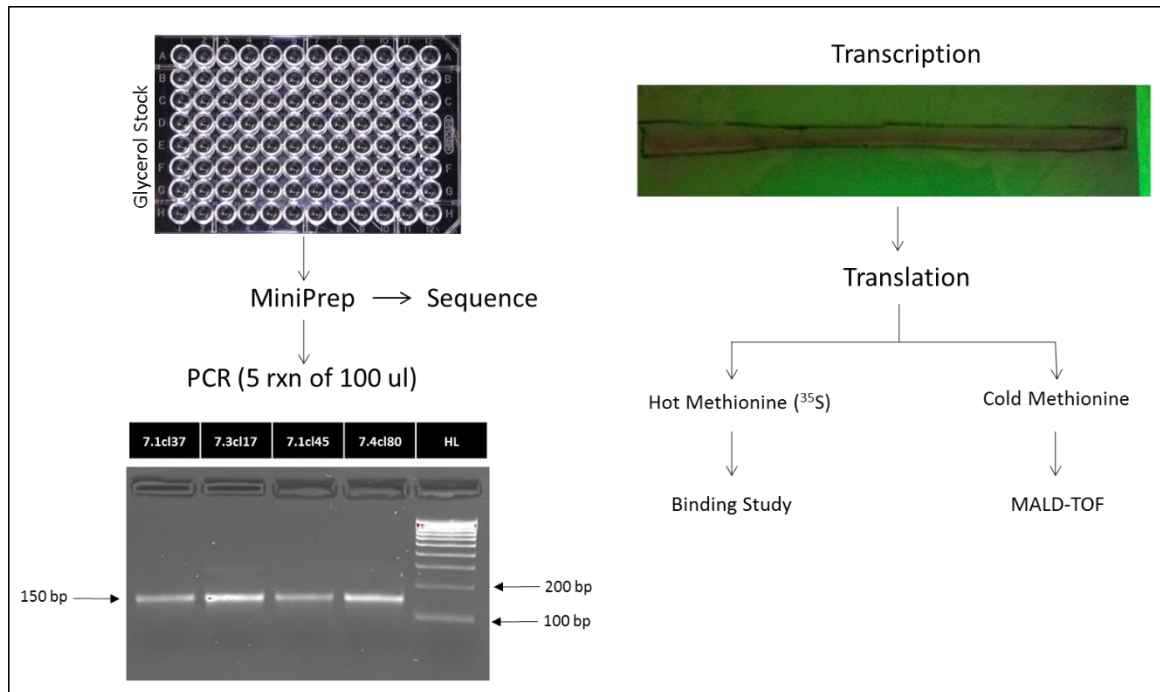


Figure 3.17. Fluorescence polarization data of Pep 7.1 and Pep 7.2. Anisotropy measurements were analyzed in Sigma Plot where curves were fit to the Four Parameter Logistic Curve to determine the K_d values. Each reaction contained 20 nM FAM-labeled peptides incubated with different XRCC4¹⁵⁷ protein concentrations. Error bars denote the standard deviation from the mean of duplicate experiment in a single plate.

A



B

7.1	NTTHYRVNFSKEDS*MC	SWMWRIETCGMILGSGSLGHHHHHHRL*VA
	NTTHYRVNFSKEDS*MC	SWMWRIETCGMILGSGSLGHHHHHHRL*VA
	NTTHYRVNFSKEDS*MC	SWMWRIETCGMILGSGSLGHHHHHHRL*XX
	NTTHYRVNFSKEDS*MC	SWMWRIETCGMILGSGSLGHHHHHHRL*VA
	NTTHYRVNFSKEDS*MC	SWMWRIETCGMILGSGSLGHHHHHHRL*VA
	NTTHYRVNFSKEDS*MC	SWMWRIETCGMILGSGSLGHHHHHHRL*VA
7.3	NTTHYRVNFSKEDS*MC	WEVVGEILCVWSLGSGLGHHHHHHRL*VA
7.4	NTTHYRVNFSKEDS*MC	GVGVVRVCRQRGGSGSLGHHHHHHRL*VAX

Figure 3.18. Preparation for scintillation-based K_d determination. A) General scheme that shows how the clones are picked up and prepared for binding study. B) Sequence verification for the selected clones.

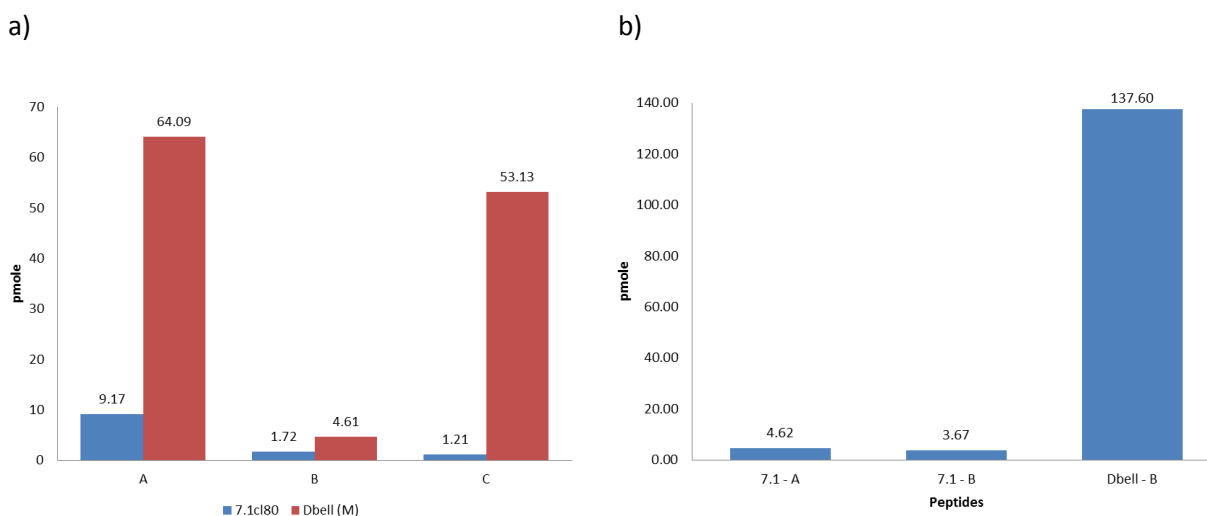
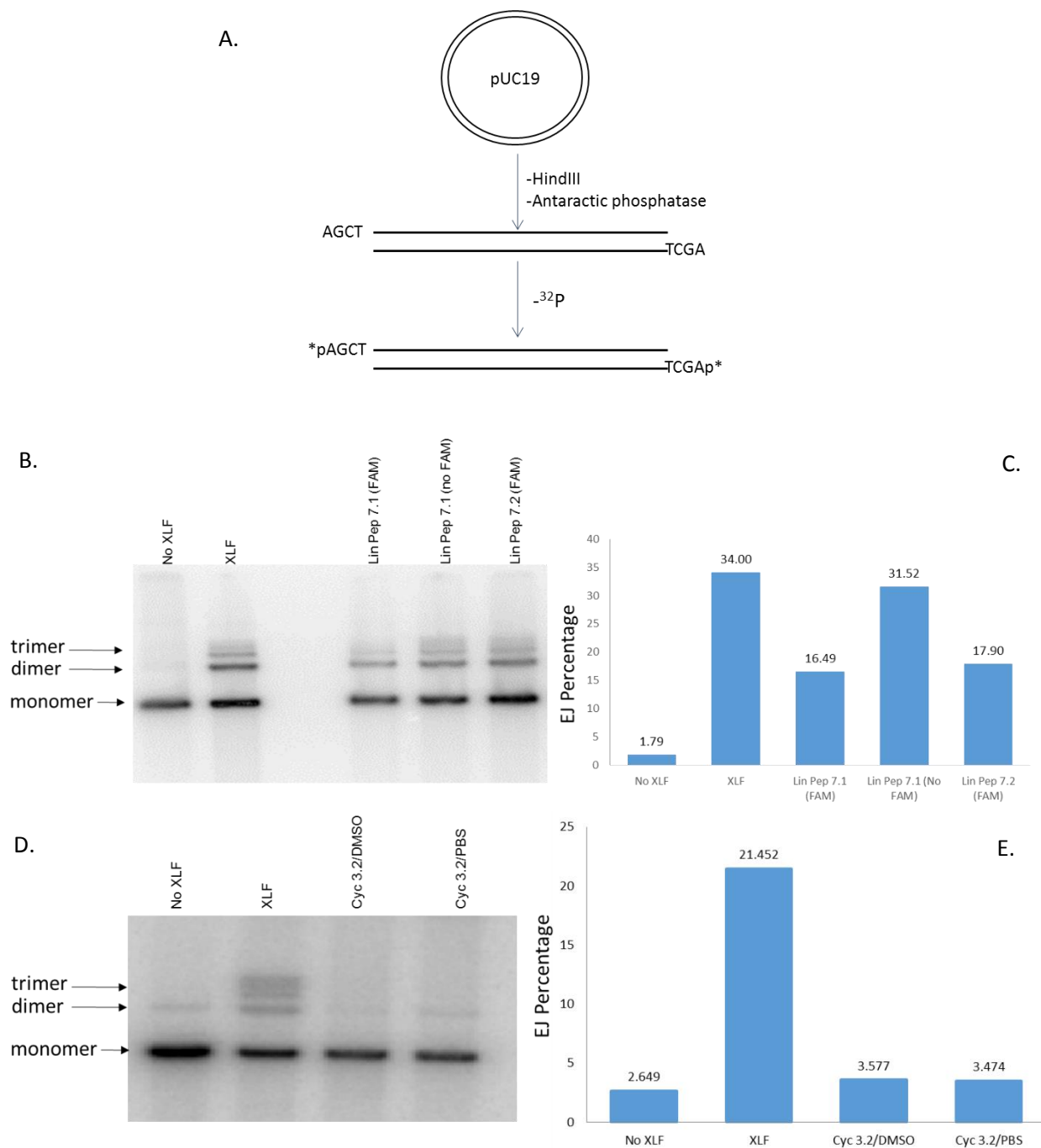


Figure 3.19. *In vitro* translation of Pep 7.1. a) *In vitro* translation of Pep 7.1 (from clone number 80) compared to that of a high-yielding peptide Dbell in three different conditions: A. Bind under denaturing condition and wash and elute under native conditions. B. Suspend the peptide with DMSO on the column and transfer to new tube; then wash and elute under native condition. C. Bind and wash with Tris-buffered saline (TBS) and elute with 1%TFA. b) *In vitro* translation of Pep 7.1 (from ordered DNA template). 7.1-A and Dbell-B. Binding under denaturing condition and wash and elute under native condition. 7.1-B. Bind and wash with TBS + 0.2% Triton and elute with 1%TFA + 0.2% Triton.

3.10 Inhibition of NHEJ in Cell Extracts

It has been shown that whole-cell extracts isolated from any of several patients with XLF mutations could not rejoin a simple-restriction cut plasmid, and about 10% of the end joining was detected when the cell extract prepared from patient cells was transfected with XLF cDNA (Buck et al., 2006). However, we have used extracts with high protein concentration and were able to detect about 2% of end joining even in an extract with XLF deficiency (Konstantin et al., 2009). Moreover, the end joining was stimulated as much as 75-fold by complementing the cell extract with XLF protein. This suggests that NHEJ efficiency depends on XLF protein for repairing even simple DSBs with no requirement for end processing. As pointed out before, XRCC4/XLF interaction is essential in NHEJ, and mutagenesis studies (Ropars et al., 2011; Malivert et al., 2010) showed that this interaction is disrupted by a single mutation on the interface between these two proteins. As pointed out in section 3.5, XLF L115D mutant completely inhibits EJ of modified and unmodified substrates in cell extract. Therefore, the cell extracts study is an excellent model to test the ability of our peptides to inhibit the interaction between XRCC4 and XLF.

We tested the linear form of Pep 7.1 and Pep 7.2 and cyclic form of Pep 3.2 using a simple restriction cut plasmid in cell extract (Figure 3.20). Initially, they showed significant inhibition to the end joining. Linear Pep 7.1 reduced the EJ by about 50%, linear Pep 7.2 by about 40% and cyclic Pep 3.2 by about 80%. However, these results could not be reproduced and cyclic Pep 7.2 and cyclic 7.4 did not show inhibition to the EJ. The initial result that we have seen could be due to an aggregation in the extract that prevent the EJ rather than an actual effect of the peptides.



3.20. EJ inhibition assay. A) Construction of a labeled plasmid bearing cohesive 3' overhangs (–GTAC/–GTAC). B) The labeled plasmid was incubated with Pep Lin Pep 7.1 or Lin Pep 7.2 for 6 hours in BuS extracts supplemented with XLF. D) Similar to B except that we used Cyc Pep 3.2 that either dissolved in DMSO or PBS buffer. C) and E) Graph representation of B and C, respectively.

4. DISCUSSION AND FUTURE DIRECTION

In mammalian cells, repair of DSBs induced by ionizing radiation, as judged either by pulsed-field gel electrophoresis of cellular DNA (Stenerlow et al., 2003) or by the emergence and dissolution of γ H2AX foci (Leatherbarrow et al., 2006), is typically biphasic. Whereas the majority of breaks are rejoined within 1 hour, the remaining 10-20% require several additional hours. Although most of the slow component of repair likely represents DSBs in heterochromatin (Goodarzi et al., 2008), the finding that DSBs formed by high-LET radiation are also rejoined rather slowly (Shibata et al., 2011), suggests that the chemical complexity of a DSB is an additional factor in increasing the time required for its repair. Slower repair in turn could increase the probability that DSB ends become physically separated, leading to lethal or carcinogenic chromosome breaks and rearrangements.

Complex DSBs can reasonably be assumed to comprise random combinations of fragmented sugars and any of a multitude of oxidatively modified bases, spread over 10-20 bp of DNA (Ward, 1988; Hutchinson, 1985). Once terminal blocking groups, primarily 3'-phosphates and 3'-phosphoglycolates, are removed, religation of otherwise compatible ends may still be prevented by base damage, especially structure-distorting base lesions very close to the termini. Tg, one of the most common oxidative lesions in DNA (Evan et al., 2004), is nonplanar, resulting in severe local perturbation of DNA structure (Aller et al., 2007), potentially rendering DSBs resistant to repair. Although in principle these damaged ends could be trimmed off by the NHEJ-associated Artemis nuclease, previous work indicates that presence of Tg near a DSB end does not promote such trimming, but on the contrary inhibits trimming of structures that would otherwise be favored Artemis substrates, such as 3' overhangs (Mohapatra et al., 2013). On the other hand X4L4 can ligate diverse nonmatching ends that are not substrates for other ligases, and its

tolerance for mismatched ends is enhanced by XLF (Gu et al., 2007; tsai et al., 2007). To determine the tolerance of NHEJ for modified structures that would occur in complex, free radical-mediated DSBs, joining of ends harboring Tg at various distances from the 3' terminus was examined in Bustel whole-cell extracts. End joining of all substrates in this system is completely dependent on the presence of XLF as well as DNA-PKcs, and is blocked by a DNA-PKcs inhibitor (Baumann and West, 1998; Akopiants et al., 2009; Povirk et al., 2007), suggesting that it reflects exclusively classical NHEJ. Moreover, inasmuch as these extracts can carry out all steps of NHEJ with very high efficiency (as much as 30-50% of free ends rejoined), they likely contain ample concentrations of core NHEJ proteins Ku, DNA-PKcs, X4L4 and XLF, and possibly additional factors that remain to be identified.

Tg as the third base from a blunt end (Tg3 substrate) had only a small inhibitory effect on ligation of blunt ends by the combination of X4L4, XLF and Ku, and almost no effect on ligation in extracts. The significant proportion of head-to-head ligations derived from this substrate indicates that such ancillary damage was tolerated even when present at both ends of a break. Although Tg in this substrate was eventually replaced with thymine, presumably via BER, DSB ligation usually if not always preceded Tg excision, as indicated by the rapid accumulation of ligated Tg-containing products. In the unligated substrate, there appeared to be minimal processing by BER, as there was little accumulation of the 2-base-shorter fragment that would result from BER in the presence of ddTTP.

The unligated Tg1, Tg2 and Tg3 substrates appeared to be poor substrates for BER, as judged by the low levels of cleavage at Tg sites, even in the presence of ddTTP (Figure 3.3). Since the Tg1 and Tg2 products were also poor substrates for NHEJ-mediated ligation as well as for Artemis-mediated trimming, such lesions when formed in cells could be quite persistent, increasing the probability of either misjoining to the end of a different DSB, or of a collision with a replication fork or transcription complex. This is particularly true for breaks with base damage at both ends. With the Tg1 and Tg2 substrates, there was

not under any condition any detectable head-to-head ligation of such DSBs. In S and G2 phase, the unrepaired break could be 5'-resected by Mre11 and CtIP and thereby channeled into HRR. However, the damaged 3' end would still have to be resolved at some point in order to prime the synthesis required for completion of HRR. Mre11/CtIP may also carry out more limited 5' resection in G1 (Averbeck et al., 2014; Quennet et al., 2011), perhaps exposing enough undamaged 3' overhang to promote trimming by Artemis, finally yielding an end more compatible with NHEJ.

Despite the structural evidence for the importance of the leucine lock motif in stabilizing XLF-XRCC4 interaction (Hammel et al., 2011; Ropars et al., 2011), disparate results have been obtained for the XLF L115A mutant. This mutant protein showed no apparent binding to XRCC4 and little or no stimulation of X4L4-mediated ligation of mismatched ends (Andres et al., 2007), yet fully complemented an XLF-deficient HCT116 cell line in terms of both V(D)J coding joint formation and end joining of a transfected substrate (Fattah et al., 2014). The less conservative L115D mutant on the other hand has yielded uniformly negative results in all assays (Hammel et al., 2011; Ropars et al., 2011; Malivert et al., 2010), but the two mutants have never been compared in the same study. The present results clearly show that the two mutations are not equivalent and that the L115A mutant retains some residual activity in promoting end joining, which appears to be sufficient to phenocopy wild-type XLF in intact cells.

4.1 Therapeutic potential of suppressing DSB repair by targeting XRCC4/XLF interaction

Induction of DNA damage by a radio- or chemotherapeutic agent is still a key element in cancer therapy. However, the dose of DNA damaging agent that can be delivered to the cancer cells is limited due to the toxic side effects produced by such agents. Exposure to cytotoxic agents also results in the activation of accurate or inaccurate DNA repair mechanisms that allow the survival of cancer cells leading to inadequate tumor response to radio- or chemotherapy (Bolderson et al., 2009). Therefore, targeting the DNA repair mechanisms that are required for cancer cell survival will increase the efficiency of radio-

or chemotherapy. Furthermore, since cancer cells often have disrupted DNA damage and repair responses, they may be more susceptible than normal cells to interference with normal repair mechanisms.

The majority of ionizing radiation-induced DSBs are repaired by NHEJ in mammalian cells, which has raised the possibility of directly targeting the NHEJ proteins and their interactions for the purpose of radiosensitization of tumor cells. DNA-PK has been shown to be a good target for radiosensitization of tumor cells, in that cells deficient in Ku70/80 or the DNA-PKcs are sensitive to DSBs induced by IR. The use of NU7441, a DNA-PK inhibitor, has shown an increase in the radiosensitivity of different cell lines and in xenograft models in preclinical trials (Zhao et al., 2006). However, inhibitors of DNA-PK will also interfere with its roles in telomere maintenance (Gilley et al., 2001; Goytisolo et al., 2001) and immune functions (W. Chu et al., 2000; Dragoi et al., 2005). Therefore, finding a more selective inhibitor is required.

Inhibition of XRCC4 is a particularly attractive target for overcoming tumor radioresistance because its only known function is in NHEJ (Schaue & McBride, 2005). Also, it has been shown that breast tumor cells can be radiosensitized by adenovirus-mediated overexpression of a fragment of XRCC4 that binds ligase IV but does not support NHEJ (Jones et al., 2005). In addition, the interaction between XRCC4 and XLF should be a much more susceptible target for radiosensitization because, whereas XRCC4 and ligase IV form a tight complex in cells, the XRCC4-XLF interaction is transient. With any radiosensitizer, there will undoubtedly be some sensitization of normal tissues, and whether inhibition of NHEJ will ultimately improve therapeutic index is difficult to predict and will only be determined by future preclinical and clinical studies. However, as many breast tumor cells have partial deficiency in HRR and/or upregulated NHEJ (Gudmundsdottir and Ashworth, 2006; Nagaraju and Scully, 2007; H. Wang et al., 2001; Zhuang et al., 2006), raising the possibility that they may indeed be sensitized more than surrounding tissue when NHEJ is suppressed. Furthermore, when breast tumors treated with radiation metastasize,

the subsequent tumors are often highly radioresistant due to upregulation of these downstream pathways (Johnston et al., 2006; Das et al., 2007) raising the possibility that the therapeutic index with metastasized tumors could be even greater.

Therefore, in order to inhibit the interaction between XRCC4 and XLF, a powerful technique such as mRNA display should be implemented. This technique has been used to find inhibitors of protein-protein and protein-ligand interactions (Railey et al., 2015, Schilppe et al., 2012; Getmanova et al., 2006). We chose mRNA display over the other selection techniques available because it possesses several advantages. For example, the presence of the covalent bond between the peptide and mRNA makes it highly stable compared to a non-covalent bond linkage in other techniques such as the ribosome display (Hui and Rihe, 2011). Therefore, in mRNA display the selection process can be performed under stringent conditions in order to optimize the selection of specific binders from non-specific ones. Another advantage of mRNA display is the ability of producing large libraries of different unique sequences. mRNA display is totally an *in vitro* selection technique that can produce as many as 10^{12} - 10^{14} unique sequences while other techniques that rely on an *in vivo* process have limitations that produces diverse sequences of up to 10^{10} only. Another advantage of mRNA display includes the easy removal of abundant sequences from the starting library increasing the chance of selection non-abundant sequences.

Therefore, we produced WT GST-XRCC4¹⁵⁷ protein in order to use it for the selection of the peptide inhibitors of the XRCC4/XLF interaction. We used truncated XRCC4 because this fragment includes the complete head domain known to contain the XLF interface but lacks the C-terminal DNA ligase IV-binding region that could interact with the mRNA component of our mRNA-peptide fusions (Ropars et al., 2011; Malivert et al., 2010).

Five DNA libraries have been synthesized and we have sequenced sample clones of each library to find that they have the sequences as they were designed. About a trillion mRNA-peptide variants went

to the selection in the first round. We were expecting about 10 trillion unique peptide fusions to start the selection; nevertheless, the amount we obtained should be sufficient to find selective inhibitors. After seven rounds of selection, we sent cDNA for sequencing and found a homology of five families we named 7.1 to 7.5. Second Generation Sequencing of DNA after round 3, 4, 5 and 6 showed that the selected peptides were present in the first rounds and were not randomly selected in the last round. The peptides were significantly enriched from round 4 to 5 and 5 to 6 which could be attributed to the increase in the stringency of washing during the selection. Interestingly, the selected peptides except Pep 7.2 have the second cysteine after 8 amino acids which indicates that this ring size is the most appropriate scaffold for the XRCC4 protein to bind with. The goal is to synthesize a representative peptide from each family of round seven as well as two peptides from round 3. The process of synthesis of Pep 7.1, Pep 7.3 and 7.5 was not easy. These peptides are rich in hydrophobic residues. The selection of hydrophobic peptides might be a good sign that our peptides are attached to the hydrophobic pocket of XRCC4 protein which has the interface where XLF binds. Also, Pep 7.1, Pep 7.3 and Pep 7.5 have leucine residue in their sequences indicating the importance of leucine in binding with XRCC4.

One approach to improve the synthesis of the hydrophobic peptides is to express them on a superfolder green fluorescent protein (sfGFP). It is a stable protein and produces efficient fluorescent chromophore that can be utilized to measure the binding affinity of the peptides by FP. We also may start the *in vitro* selection again using XLF protein to discover peptides that can bind to the XRCC4 interface and inhibit their interaction.

REFERENCES

- Abbott, D.W. and J.T. Holt, 1999. Mitogen-activated Protein Kinase Kinase 2 Activation Is Essential for Progression through the G2/M Checkpoint Arrest in Cells Exposed to Ionizing Radiation. *Journal of Biological Chemistry*, 274 (5): 2732-2742.
- Abbott, D.W., M.E. Thompson, C. Robinson-Benion, G. Tomlinson, R.A. Jensen and J.T. Holt, 1999. BRCA1 Expression Restores Radiation Resistance in BRCA1-defective Cancer Cells through Enhancement of Transcription-coupled DNA Repair. *Journal of Biological Chemistry*, 274 (26): 18808-18812.
- Ahnesorg, P., P. Smith and S.P. Jackson, 2006. XLF Interacts with the XRCC4-DNA Ligase IV Complex to Promote DNA Nonhomologous End-Joining. *Cell*, 124 (2): 301-313.
- Akopian, K., R. Zhou, S. Mohapatra, K. Valerie, S.P. Lees-Miller, K. Lee, D.J. Chen, P. Revy, J. de Villartay and L.F. Povirk, 2009. Requirement for XLF/Cernunnos in alignment-based gap filling by DNA polymerases λ and μ for nonhomologous end joining in human whole-cell extracts. *Nucleic Acids Research*, 37 (12): 4055-4062.
- Aller, P., M.A. Rould, M. Hogg, S.S. Wallace and S. Doublié, 2006. A structural rationale for stalling of a replicative DNA polymerase at the most common oxidative thymine lesion, thymine glycol. *Proc. Natl. Acad. Sci. U. S. A.*, 104 (3): 814-818.
- American Cancer Society. What are the key statistics about breast cancer? , 2015 (7/15/2015).
- Andres, S.N., M. Modesti, C.J. Tsai, G. Chu and M.S. Junop, 2007. Crystal Structure of Human XLF: A Twist in Nonhomologous DNA End-Joining. *Mol. Cell*, 28 (6): 1093-1101.
- Aspinwall, R., D. Rothwell, T. Roldan-Arjona, C. Anselmino, C. Ward, J. Cheadle, J. Sampson, T. Lindahl, P. Harris and I. Hickson, 1996. Cloning and characterization of a functional human homolog of *Escherichia coli* endonuclease III. *Proc. Natl. Acad. Sci. U. S. A.*, 94 (1): 109-114.
- B. Boudaïffa, D. Hunting, P. Cloutier, M.A. Huels and L. Sanche, 2000 Sep. Induction of single- and double-strand breaks in plasmid DNA by 100-1500 eV electrons. , 76 (9): 1209-1221.
- Bahmed, K., K.C. Nitiss and J.L. Nitiss, 2010. Yeast Tdp1 regulates the fidelity of nonhomologous end joining. *Proc. Natl. Acad. Sci. U. S. A.*, 107 (9): 4057-4062.
- Bellon, S., N. Shikazono, S. Cunniffe, M. Lomax and P. O'Neill, 2009. Processing of thymine glycol in a clustered DNA damage site: mutagenic or cytotoxic. *Nucleic Acids Res.*, 37 (13): 4430-4440.

- Bertocci, B., A. De Smet, J. Weill and C. Reynaud, 2006. Nonoverlapping Functions of DNA Polymerases Mu, Lambda, and Terminal Deoxynucleotidyltransferase during Immunoglobulin V(D)J Recombination In Vivo. *Immunity*, 25 (1): 31-41.
- Bjorge, J.D., C. Bellagamba, H. Cheng, A. Tanaka, J.H. Wang and D.J. Fujita, 1995. Characterization of Two Activated Mutants of Human pp60c-src That Escape c-Src Kinase Regulation by Distinct Mechanisms. *J. Biol. Chem.*, 270 (41): 24222-24228.
- Bolderson, E., D.J. Richard, B.S. Zhou and K.K. Khanna, 2009. Recent Advances in Cancer Therapy Targeting Proteins Involved in DNA Double-Strand Break Repair. *Clinical Cancer Research*, 15 (20): 6314-6320.
- Bork, P., K. Hofmann, P. Bucher, A.F. Neuwald, S.F. Altschul and E.V. Koonin, 1997. A superfamily of conserved domains in DNA damage-responsive cell cycle checkpoint proteins. *The FASEB Journal*, 11 (1): 68-76.
- Bryans, M., M.C. Valenzano and T.D. Stamato, 1999. Absence of DNA ligase IV protein in XR-1 cells: evidence for stabilization by XRCC4. *Mutat. Res. /DNA Repair*, 433 (1): 53-58.
- Buchholz, T.A., 2009. Radiation Therapy for Early-Stage Breast Cancer after Breast-Conserving Surgery. *N. Engl. J. Med.*, 360 (1): 63-70.
- Buck, D., L. Malivert, R. de Chasseval, A. Barraud, M. Fondanèche, O. Sanal, A. Plebani, J. Stéphan, M. Hufnagel, F. le Deist, A. Fischer, A. Durandy, J. de Villartay and P. Revy, 2006. Cernunnos, a Novel Nonhomologous End-Joining Factor, Is Mutated in Human Immunodeficiency with Microcephaly. *Cell*, 124 (2): 287-299.
- Cai, M., D.C. Williams, G. Wang, B.R. Lee, A. Peterkofsky and G.M. Clore, 2003. Solution Structure of the Phosphoryl Transfer Complex between the Signal-transducing Protein IIA_{glucose} and the Cytoplasmic Domain of the Glucose Transporter IICB_{glucose} of the Escherichia coli Glucose Phosphotransferase System. *Journal of Biological Chemistry*, 278 (27): 25191-25206.
- Callebaut, I. and J. Mornon. From BRCA1 to RAP1: a widespread BRCT module closely associated with DNA repair. *FEBS Lett.*, 400 (1): 25-30.
- Cathcart, R., E. Schwiers, R.L. Saul and B.N. Ames, 1984. Thymine glycol and thymidine glycol in human and rat urine: a possible assay for oxidative DNA damage. *Proc. Natl. Acad. Sci. U. S. A.*, 81 (18): 5633-5637.
- Chen, L., C.J. Nievera, A.Y. Lee and X. Wu, 2008. Cell Cycle-dependent Complex Formation of BRCA1·CtIP·MRN Is Important for DNA Double-strand Break Repair. *Journal of Biological Chemistry*, 283 (12): 7713-7720.
- Chu, K., N. Teele, M.W. Dewey, N. Albright and W.C. Dewey, 2004. Computerized Video Time Lapse Study of Cell Cycle Delay and Arrest, Mitotic Catastrophe, Apoptosis and Clonogenic Survival in Irradiated 14-3-3 σ and CDKN1A (p21) Knockout Cell Lines. *Radiat. Res.*, 162 (3): pp. 270-286.

- Chu, W., X. Gong, Z. Li, K. Takabayashi, H. Ouyang, Y. Chen, A. Lois, D.J. Chen, G.C. Li, M. Karin and E. Raz, 2000. RETRACTED: DNA-PKcs Is Required for Activation of Innate Immunity by Immunostimulatory DNA. *Cell*, 103 (6): 909-918.
- Ciccia, A. and S.J. Elledge, 2010. The DNA Damage Response: Making it safe to play with knives. *Mol. Cell*, 40 (2): 179-204.
- Clarke M., Collins R., Darby S., Davies C., Elphinstone P., Evans V., Godwin J., Gray R., Hicks C., James S., MacKinnon E., McGale P., McHugh T., Peto R., Taylor C. and Wang Y. Effects of radiotherapy and of differences in the extent of surgery for early breast cancer on local recurrence and 15-year survival: an overview of the randomised trials. *The Lancet*, 366 (9503): 2087-2106.
- Contessa, J., A. Abell, R. Mikkelsen, K. Valerie and R. Schmidt-Ullrich, 2006. Compensatory ErbB3/c-Src signaling enhances carcinoma cell survival to ionizing radiation. *Breast Cancer Res. Treat.*, 95 (1): 17-27.
- Contessa, J.N., A. Abell, K. Valerie, P. Lin and R.K. Schmidt-Ullrich, 2006. ErbB receptor tyrosine kinase network inhibition radiosensitizes carcinoma cells. *International Journal of Radiation Oncology*Biophysics*, 65 (3): 851-858.
- Critchlow, S.E., R.P. Bowater and S.P. Jackson, 1997. Mammalian DNA double-strand break repair protein XRCC4 interacts with DNA ligase IV. *Current Biology*, 7 (8): 588-598.
- D'Amours, D. and S.P. Jackson, 2002. The mre11 complex: at the crossroads of dna repair and checkpoint signalling. *Nature Reviews Molecular Cell Biology*, 3 (5): 317-327.
- Das, A.K., B.P. Chen, M.D. Story, M. Sato, J.D. Minna, D.J. Chen and C.S. Nirodi, 2007. Somatic Mutations in the Tyrosine Kinase Domain of Epidermal Growth Factor Receptor (EGFR) Abrogate EGFR-Mediated Radioprotection in Non-Small Cell Lung Carcinoma. *Cancer Research*, 67 (11): 5267-5274.
- Dean-Colomb, W. and F.J. Esteva, 2008. Her2-positive breast cancer: Herceptin and beyond. *Eur. J. Cancer*, 44 (18): 2806-2812.
- Dedon, P.C., 2008. The Chemical Toxicology of 2-Deoxyribose Oxidation in DNA. *Chem. Res. Toxicol.*, 21 (1): 206-219.
- Derbyshire, D.J., B.P. Basu, L.C. Serpell, W.S. Joo, T. Date, K. Iwabuchi and A.J. Doherty, 2002. Crystal structure of human 53BP1 BRCT domains bound to p53 tumour suppressor. *EMBO J.*, 21 (14): 3863-3872.
- Deweese, J.E. and N. Osheroff, 2008. The DNA cleavage reaction of topoisomerase II: wolf in sheep's clothing. *Nucleic Acids Res.*, 37 (3): 738-748.
- Di, X., R.P. Shiu, I.F. Newsham and D.A. Gewirtz, 2009. Apoptosis, autophagy, accelerated senescence and reactive oxygen in the response of human breast tumor cells to Adriamycin. *Biochem. Pharmacol.*, 77 (7): 1139-1150.

- Dianov, G.L., K.M. Sleeth, I.I. Dianova and S.L. Allinson, 2003. Repair of abasic sites in DNA. *Mutation Research/Fundamental and Molecular Mechanisms of Mutagenesis; Oxidative DNA Damage and its Repair Base Excision Repair*, 531 (1): 157-163.
- Dizdaroglu, M., 2005. Base-excision repair of oxidative DNA damage by DNA glycosylases. *Mutation Research/Fundamental and Molecular Mechanisms of Mutagenesis; Mechanistic Approaches to Chemoprevention of Mutation and Cancer*, 591 (1): 45-59.
- Dizdaroglu, M., C. Bauche, H. Rodriguez and J. Laval, 2000. Novel Substrates of Escherichia coli Nth Protein and Its Kinetics for Excision of Modified Bases from DNA Damaged by Free Radicals. *Biochemistry (N. Y.)*, 39 (18): 5586-5592.
- Doherty, A.J., S.R. Ashford, H.S. Subramanya and D.B. Wigley, 1996. Bacteriophage T7 DNA Ligase: OVEREXPRESSION, PURIFICATION, CRYSTALLIZATION, AND CHARACTERIZATION. *J. Biol. Chem.*, 271 (19): 11083-11089.
- Downs, J.A. and S.P. Jackson, 2004. A means to a DNA end: the many roles of Ku. *Nat. Rev. Mol. Cell Biol.*, 5 (5): 367-378.
- Dragoi, A., X. Fu, S. Ivanov, P. Zhang, L. Sheng, D. Wu, G.C. Li and W. Chu, 2005. DNA-PKcs, but not TLR9, is required for activation of Akt by CpG-DNA. *EMBO J.*, 24 (4): 779-789.
- Eide, L., M. Bjørås, M. Pirovano, I. Alseth, K.G. Berdal and E. Seeberg, 1996. Base excision of oxidative purine and pyrimidine DNA damage in *Saccharomyces cerevisiae* by a DNA glycosylase with sequence similarity to endonuclease III from *Escherichia coli*. *Proceedings of the National Academy of Sciences*, 93 (20): 10735-10740.
- Evans, M.D., M. Dizdaroglu and M.S. Cooke, 2004. Oxidative DNA damage and disease: induction, repair and significance. *Mutation Research/Reviews in Mutation Research*, 567 (1): 1-61.
- Falck, J., J. Coates and S.P. Jackson, 2005. Conserved modes of recruitment of ATM, ATR and DNA-PKcs to sites of DNA damage. *Nature*, 434 (7033): 605-611.
- Freedman, G.M., 2008. Radiation therapy for operable breast cancer. *Cancer*, 113 (S7): 1779-1800.
- Frenkel, K., M.S. Goldstein and G.W. Teebor, 1981. Identification of the cis-thymine glycol moiety in chemically oxidized and γ -irradiated DNA by HPLC analysis. *Biochemistry (N. Y.)*, 20 (26): 7566-7571.
- Frosina, G., P. Fortini, O. Rossi, F. Carrozzino, G. Raspaglio, L.S. Cox, D.P. Lane, A. Abbondandolo and E. Dogliotti, 1996. Two Pathways for Base Excision Repair in Mammalian Cells. *J. Biol. Chem.*, 271 (16): 9573-9578.
- Futreal, P.A., Q. Liu, D. Shattuck-Eidens, C. Cochran, K. Harshman, S. Tavtigian, L.M. Bennett, A. Haugen-Strano, J. Swensen, Y. Miki, K. Eddington, M. McClure, C. Frye, J. Weaver-Feldhaus, W. Ding, Z. Gholami, P. Söderkvist, L. Terry, S. Jhanwar, A. Berchuck, J.D. Iglehart, J. Marks, D.G. Ballinger, J.C.

- Barrett, M.H. Skolnick, A. Kamb and R. Wiseman, 1994. BRCA1 Mutations in Primary Breast and Ovarian Carcinomas. *Science*, 266 (5182): pp. 120-122.
- Gómez-Herreros, F., R. Romero-Granados, Z. Zeng, A. Álvarez-Quiló, C. Quintero, L. Ju, L. Umans, L. Vermeire, D. Huylebroeck, K.W. Caldecott and F. Cortés-Ledesma, 2012. TDP2 Dependent Non-Homologous End-Joining Protects against Topoisomerase II Induced DNA Breaks and Genome Instability in Cells and In Vivo. *PLoS Genetics*, 9 (3): e1003226.
- Getmanova, E.V., Y. Chen, L. Bloom, J. Gokemeijer, S. Shamah, V. Warikoo, J. Wang, V. Ling and L. Sun, 2006. Antagonists to Human and Mouse Vascular Endothelial Growth Factor Receptor 2 Generated by Directed Protein Evolution *In Vitro*. *Chem. Biol.*, 13 (5): 549-556.
- Giaccia, A.J., N. Denko, R. MacLaren, D. Mirman, C. Waldren, I. Hart and T.D. Stamato, 1990. Human chromosome 5 complements the DNA double-strand break-repair deficiency and gamma-ray sensitivity of the XR-1 hamster variant. *Am. J. Hum. Genet.*, 47 (3): 459-469.
- Gilley, D., H. Tanaka, M.P. Hande, A. Kurimasa, G.C. Li, M. Oshimura and D.J. Chen, 2001. DNA-PKcs is critical for telomere capping. *Proceedings of the National Academy of Sciences*, 98 (26): 15084-15088.
- Gonzalez-Angulo, A.M., F. Morales-Vasquez and G.N. Hortobagyi, 2007. Overview of Resistance to Systemic Therapy in Patients with Breast Cancer. In: *Breast Cancer Chemosensitivity* (eds D. Yu and M. Hung) pp. 1-22. Springer New York.
- Goun, E.A., R. Shinde, K.W. Dehnert, A. Adams-Bond, P.A. Wender, C.H. Contag and B.L. Franc, 2006. Intracellular Cargo Delivery by an Octaarginine Transporter Adapted to Target Prostate Cancer Cells through Cell Surface Protease Activation. *Bioconjugate Chem.*, 17 (3): 787-796.
- Goytisolo, F.A., E. Samper, S. Edmonson, G.E. Taccioli and M.A. Blasco, 2001. The Absence of the DNA-Dependent Protein Kinase Catalytic Subunit in Mice Results in Anaphase Bridges and in Increased Telomeric Fusions with Normal Telomere Length and G-Strand Overhang. *Molecular and Cellular Biology*, 21 (11): 3642-3651.
- Gudmundsdottir, K. and A. Ashworth, 2006. The roles of BRCA1 and BRCA2 and associated proteins in the maintenance of genomic stability. *Oncogene*, 25 (43): 5864-5874.
- Guillen Schlippe, Y.V., M.C.T. Hartman, K. Josephson and J.W. Szostak, 2012. In Vitro Selection of Highly Modified Cyclic Peptides That Act as Tight Binding Inhibitors. *J. Am. Chem. Soc.*, 134 (25): 10469-10477.
- Gupta, S. and K. Meek, 2005. The leucine rich region of DNA-PKcs contributes to its innate DNA affinity. *Nucleic Acids Res.*, 33 (22): 6972-6981.
- HABRAKEN, Y. and W.G. VERLY, 1988. Further purification and characterization of the DNA 3'-phosphatase from rat-liver chromatin which is also a polynucleotide 5'-hydroxyl kinase. *European Journal of Biochemistry*, 171 (1-2): 59-66.

- Hacker, D., M. Almohaini, A. Anbazhagan, Z. Ma and M.T. Hartman, 2015. Peptide and Peptide Library Cyclization via Bromomethylbenzene Derivatives, (ed R. Derda) pp. 105-117. Springer New York.
- Hammel, M., M. Rey, Y. Yu, R.S. Mani, S. Classen, M. Liu, M.E. Pique, S. Fang, B.L. Mahaney, M. Weinfeld, D.C. Schriemer, S. Lees-Miller and J.A. Tainer, 2011. XRCC4 Protein Interactions with XRCC4-like Factor (XLF) Create an Extended Grooved Scaffold for DNA Ligation and Double Strand Break Repair. *The Journal of Biological Chemistry*, 286 (37): 32638-32650.
- Hammers, C.M. and J.R. Stanley, 2014. Antibody Phage Display: Technique and Applications. *J. Invest. Dermatol.*, 134 (2): e17-e17.
- Han, W. and K. and Yu, 2009. Response of cells to ionizing radiation,. In: *In Advances in Biomedical Sciences and Engineering* pp. 204-262. Bentham Science Publisher Ltd.
- Hanes, J. and A. Plieth, 1997. In vitro selection and evolution of functional proteins by using ribosome display. *Proc. Natl. Acad. Sci. U. S. A.*, 94 (10): 4937-4942.
- Hartman, M.C.T., K. Josephson, C. Lin and J.W. Szostak, 2007. An Expanded Set of Amino Acid Analogs for the Ribosomal Translation of Unnatural Peptides. *PLoS ONE*, 2 (10): e972.
- Hayes, R.C., L.A. Petrullo, H. Huang, S.S. Wallace and J.E. LeClerc, 1988. Oxidative damage in DNA: Lack of mutagenicity by thymine glycol lesions. *J. Mol. Biol.*, 201 (2): 239-246.
- Hegde, M.L., T.K. Hazra and S. Mitra, 2008. Early Steps in the DNA Base Excision/Single-Strand Interruption Repair Pathway in Mammalian Cells. *Cell Res.*, 18 (1): 27-47.
- Heimann, R., 2010. The Role of Radiotherapy in Breast Cancer Management: 277-295.
- Helleday, T., J. Lo, D.C. van Gent and B.P. Engelward, 2007. DNA double-strand break repair: From mechanistic understanding to cancer treatment. *DNA Repair*, 6 (7): 923-935.
- Higueruelo, A.P., H. Jubb and T.L. Blundell, 2013. Protein-protein interactions as druggable targets: recent technological advances. *Current Opinion in Pharmacology; Anti-infectives. New technologies*, 13 (5): 791-796.
- Huang, H., B.M. Jedynak and J.S. Bader, 2007. Where Have All the Interactions Gone? Estimating the Coverage of Two-Hybrid Protein Interaction Maps. *PLoS Computational Biology*, 3 (11): e214.
- Inamdar, K.V., J.J. Pouliot, T. Zhou, S. Lees-Miller, A. Rasouli-Nia and L.F. Povirk, 2002. Conversion of Phosphoglycolate to Phosphate Termini on 3' Overhangs of DNA Double Strand Breaks by the Human Tyrosyl-DNA Phosphodiesterase hTdp1. *J. Biol. Chem.*, 277 (30): 27162-27168.
- Inamdar, K.V., J.J. Pouliot, T. Zhou, S. Lees-Miller, A. Rasouli-Nia and L.F. Povirk, 2002. Conversion of Phosphoglycolate to Phosphate Termini on 3' Overhangs of DNA Double Strand Breaks by the Human Tyrosyl-DNA Phosphodiesterase hTdp1. *J. Biol. Chem.*, 277 (30): 27162-27168.

- Isildar, M., M.N. Schuchmann, D. Schulte-Frohlinde and C. von Sonntag, 1981. ^3H -Radiolysis of DNA in Oxygenated Aqueous Solutions: Alterations at the Sugar Moiety. *Int. J. Radiat. Biol.*, 40 (4): 347-354.
- Jameel, J.K.A., V.S.R. Rao, L. Cawkwell and P.J. Drew, 2004. Radioresistance in carcinoma of the breast. *The Breast*, 13 (6): 452-460.
- Jankovic, M., A. Nussenzweig and M.C. Nussenzweig, 2007. Antigen receptor diversification and chromosome translocations. *Nat. Immunol.*, 8 (8): 801-808.
- Jemal, A., F. Bray, M.M. Center, J. Ferlay, E. Ward and D. Forman, 2011. Global cancer statistics. *CA: A Cancer Journal for Clinicians*, 61 (2): 69-90.
- Jemal, A., R. Siegel, J. Xu and E. Ward, 2010. Cancer Statistics, 2010. *CA: A Cancer Journal for Clinicians*, 60 (5): 277-300.
- Jin, S., S. Kharbanda, B. Mayer, D. Kufe and D.T. Weaver, 1997. Binding of Ku and c-Abl at the Kinase Homology Region of DNA-dependent Protein Kinase Catalytic Subunit. *J. Biol. Chem.*, 272 (40): 24763-24766.
- Johnson, S.M., J.A. Shaw and R.A. Walker, 2002. Sporadic breast cancer in young women: Prevalence of loss of heterozygosity at p53, BRCA1 and BRCA2. *International Journal of Cancer*, 98 (2): 205-209.
- Johnson, S.M., J.A. Shaw and R.A. Walker, 2002. Sporadic breast cancer in young women: Prevalence of loss of heterozygosity at p53, BRCA1 and BRCA2. *International Journal of Cancer*, 98 (2): 205-209.
- Jones, K.R., D.A. Gewirtz, S.M. Yannone, S. Zhou, D.G. Schatz, K. Valerie and L.F. Povirk, 2005. Radiosensitization of MDA-MB-231 breast tumor cells by adenovirus-mediated overexpression of a fragment of the XRCC4 protein. *Molecular Cancer Therapeutics*, 4 (10): 1541-1547.
- Joo, W.S., P.D. Jeffrey, S.B. Cantor, M.S. Finnin, D.M. Livingston and N.P. Pavletich, 2002. Structure of the 53BP1 BRCT region bound to p53 and its comparison to the Brca1 BRCT structure. *Genes Dev.*, 16 (5): 583-593.
- Junop, M.S., M. Modesti, A. Guarne, R. Ghirlando, M. Gellert and W. Yang, 2000. Crystal structure of the Xrcc4 DNA repair protein and implications for end joining. *EMBO J.*, 19 (22): 5962-5970.
- Kastan, M.B. and J. Bartek, 2004. Cell-cycle checkpoints and cancer. *Nature*, 432 (7015): 316-323.
- Kesari, S., S.J. Advani, J.D. Lawson, K.T. Kahle, K. Ng, B. Carter and C.C. Chen, 2011. DNA damage response and repair: insights into strategies for radiation sensitization of gliomas. *Future Oncology*, 7 (11): 1335-1346.
- Klionsky, D.J., Z. Elazar, P.O. Seglen and D.C. Rubinsztein, 2008. Does bafilomycin A₁ block the fusion of autophagosomes with lysosomes?. *Autophagy*, 4 (7): 849-850.

- Lancaster, J.M., R. Wooster, J. Mangion, C.M. Phelan, C. Cochran, C. Gumbs, S. Seal, R. Barfoot, N. Collins, G. Bignell, S. Patel, R. Hamoudi, C. Larsson, R.W. Wiseman, A. Berchuck, J.D. Iglehart, J.R. Marks, A. Ashworth, M.R. Stratton and P.A. Futreal, 1996. BRCA2 mutations in primary breast and ovarian cancers. *Nat. Genet.*, 13 (2): 238-240.
- Laura M. Williamson, Chris T. Williamson, and Susan P. Lees-Miller, 2009. DNA Double Strand Break Repair: Mechanisms and Therapeutic Potential,. In: *The DNA Damage Response: Implications on Cancer Formation and Treatment* (ed Kum Kum Khanna, Yosef Shiloh) pp. 157-178. Springer, New York.
- Lee, J.W., L. Blanco, T. Zhou, M. Garcia-Diaz, K. Bebenek, T.A. Kunkel, Z. Wang and L.F. Povirk, 2004. Implication of DNA Polymerase β in Alignment-based Gap Filling for Nonhomologous DNA End Joining in Human Nuclear Extracts. *J. Biol. Chem.*, 279 (1): 805-811.
- Lees-Miller, S. and K. Meek, 2003. Repair of DNA double strand breaks by non-homologous end joining. *Biochimie*, 85 (11): 1161-1173.
- Lehmann, B.D., J.A. McCubrey, H.S. Jefferson, M.S. Paine, W.H. Chappell and D.M. Terrian, 2007. A Dominant Role for p53-Dependent Cellular Senescence in Radiosensitization of Human Prostate Cancer Cells. *Cell Cycle*, 6 (5): 595-605.
- Li, S., N.S.Y. Ting, L. Zheng, Phang-Lang Chen, Y. Ziv, E.Y.-P. Lee and Wen-Hwa Lee, 2000. Functional link of BRCA1 and ataxia telangiectasia gene product in DNA damage response. *Nature*, 406 (6792): 210.
- Li, X. and W. Heyer, 2008. Homologous recombination in DNA repair and DNA damage tolerance. *Cell Res.*, 18 (1): 99-113.
- Li, Z., T. Otevrel, Y. Gao, H. Cheng, B. Seed, T.D. Stamato, G.E. Taccioli and F.W. Alt, 1995. The XRCC4 gene encodes a novel protein involved in DNA double-strand break repair and V(D)J recombination. *Cell*, 83 (7): 1079-1089.
- Liang, K., Y. Lu, W. Jin, K.K. Ang, L. Milas and Z. Fan, 2003. Sensitization of breast cancer cells to radiation by trastuzumab. *Molecular Cancer Therapeutics*, 2 (11): 1113-1120.
- Lieber, M.R., 2010. The Mechanism of Double-Strand DNA Break Repair by the Nonhomologous DNA End-Joining Pathway. *Annu. Rev. Biochem.*, 79 (1): 181-211.
- Lindahl, T., 1993. Instability and decay of the primary structure of DNA. *Nature*, 362 (6422): 709-715.
- Lliakis, G., 1991. The role of DNA double strand breaks in Ionizing radiation-induced killing of eukaryotic cells. *Bioessays*, 13 (12): 641-648.
- Ma, Y., K. Schwarz and M.R. Lieber, 2005. The Artemis:DNA-PKcs endonuclease cleaves DNA loops, flaps, and gaps. *DNA Repair*, 4 (7): 845-851.

- Ma, Y., U. Pannicke, K. Schwarz and M.R. Lieber. Hairpin Opening and Overhang Processing by an Artemis/DNA-Dependent Protein Kinase Complex in Nonhomologous End Joining and V(D)J Recombination. *Cell*, 108 (6): 781-794.
- Ma, Z. and M.C. Hartman, 2012. In Vitro Selection of Unnatural Cyclic Peptide Libraries via mRNA Display. *Methods Mol. Biol.*, 805: 367-390.
- Mahaney, B.L., K. Meek and S. Lees-Miller, 2009. Repair of ionizing radiation-induced DNA double-strand breaks by non-homologous end-joining. *Biochem. J.*, 417 (3): 639-650.
- Malivert, L., V. Ropars, M. Nunez, P. Drevet, S. Miron, G. Faure, R. Guerois, J. Mornon, P. Revy, J. Charbonnier, I. Callebaut and J. de Villartay, 2010. Delineation of the Xrcc4-interacting Region in the Globular Head Domain of Cernunnos/XLF. *Journal of Biological Chemistry*, 285 (34): 26475-26483.
- Matsumura, N., T. Tsuji, T. Sumida, M. Kokubo, M. Onimaru, N. Doi, H. Takashima, E. Miyamoto-Sato and H. Yanagawa, 2010. mRNA display selection of a high-affinity, Bcl-XL-specific binding peptide. *The FASEB Journal*, 24 (7): 2201-2210.
- McCullough, A.K., M.L. Dodson and R.S. Lloyd, 1999. Initiation of Base Excision Repair: Glycosylase Mechanisms and Structures. *Annu. Rev. Biochem.*, 68 (1): 255-285.
- Meek, K., S. Gupta, D.A. Ramsden and S.P. Lees-Miller, 2004. The DNA-dependent protein kinase: the director at the end. *Immunol. Rev.*, 200 (1): 132-141.
- Meek, K., V. Dang and S. Lees-Miller, 2008. Chapter 2 DNA-PK: The Means to Justify the Ends?. In: *Advances in Immunology* (ed Frederick W. Alt) pp. 33-58. Academic Press.
- Miki, Y., J. Swensen, D. Shattuck-Eidens, P.A. Futreal, K. Harshman, S. Tavtigian, Q. Liu, C. Cochran, L.M. Bennett, W. Ding, R. Bell, J. Rosenthal, C. Hussey, T. Tran, M. McClure, C. Frye, T. Hattier, R. Phelps, A. Haugen-Strano, H. Katcher, K. Yakumo, Z. Gholami, D. Shaffer, S. Stone, S. Bayer, C. Wray, R. Bogden, P. Dayananth, J. Ward, P. Tonin, S. Narod, P.K. Bristow, F.H. Norris, L. Helvering, P. Morrison, P. Rosteck, M. Lai, J.C. Barrett, C. Lewis, S. Neuhausen, L. Cannon-Albright, D. Goldgar, R. Wiseman, A. Kamb and M.H. Skolnick, 1994. A Strong Candidate for the Breast and Ovarian Cancer Susceptibility Gene BRCA1. *Science*, 266 (5182): 66-71.
- Millar, E.K., P.H. Graham, S.A. O'Toole, C.M. McNeil, L. Browne, A.L. Morey, S. Eggleton, J. Beretov, C. Theocharous, A. Capp, E. Nasser, J.H. Kearsley, G. Delaney, G. Papadatos, C. Fox and R.L. Sutherland, 2009. Prediction of local recurrence, distant metastases, and death after breast-conserving therapy in early-stage invasive breast cancer using a five-biomarker panel . *J. Clin. Oncol.*, 27 (28): 4701-4708.
- Mordes, D.A., G.G. Glick, R. Zhao and D. Cortez, 2008. TopBP1 activates ATR through ATRIP and a PIKK regulatory domain. *Genes Dev.*, 22 (11): 1478-1489.
- Moshous, D., I. Callebaut, R. de Chasseval, B. Corneo, M. Cavazzana-Calvo, F. Le Deist, I. Tezcan, O. Sanal, Y. Bertrand, N. Philippe, A. Fischer and J. de Villartay. Artemis, a Novel DNA Double-Strand Break

- Repair/V(D)J Recombination Protein, Is Mutated in Human Severe Combined Immune Deficiency. *Cell*, 105 (2): 177-186.
- Nagaraju, G. and R. Scully, 2007. Minding the gap: The underground functions of BRCA1 and BRCA2 at stalled replication forks. *DNA Repair*, 6 (7): 1018-1031.
- Nick McElhinny, S.A. and D.A. Ramsden, 2004. Sibling rivalry: competition between Pol X family members in V(D)J recombination and general double strand break repair. *Immunol. Rev.*, 200 (1): 156-164.
- Nikjoo, H., P. O'Neill, M. Terrissol and D.T. Goodhead, 1999. Quantitative modelling of DNA damage using Monte Carlo track structure method. *Radiat. Environ. Biophys.*, 38 (1): 31-38.
- Olson, C.A., H. Liao, R. Sun and R.W. Roberts, 2008. mRNA Display Selection of a High-Affinity, Modification-Specific Phospho- β -Binding Fibronectin. *ACS Chem. Biol.*, 3 (8): 480-485.
- Olson, C.A., J.D. Adams, T.T. Takahashi, H. Qi, S.M. Howell, T. Wu, R.W. Roberts, R. Sun and H.T. Soh, 2011. Rapid mRNA-Display Selection of an IL-6 Inhibitor Using Continuous-Flow Magnetic Separation. *Angewandte Chemie (International ed.in English)*, 50 (36): 8295-8298.
- Pheiffer, B.H. and S.B. Zimmerman, 1982. γ -Phosphatase activity of the DNA kinase from rat liver. *Biochem. Biophys. Res. Commun.*, 109 (4): 1297-1302.
- Poinsignon, C., R. de Chasseval, S. Soubeyrand, D. Moshous, A. Fischer, R. Haché and J. de Villartay, 2004. Phosphorylation of Artemis following irradiation-induced DNA damage. *Eur. J. Immunol.*, 34 (11): 3146-3155.
- Povirk, L.F., 2006. Biochemical mechanisms of chromosomal translocations resulting from DNA double-strand breaks. *DNA Repair; Mechanisms of chromosomal translocation*, 5 (9): 1199-1212.
- Povirk, L.F., 2012. Processing of damaged DNA ends for double-strand break repair in mammalian cells. *ISRN molecular biology*, 2012: 10.5402/2012/345805.
- Povirk, L.F., T. Zhou, R. Zhou, M.J. Cowan and S.M. Yannone, 2007. Processing of γ -Phosphoglycolate-terminated DNA Double Strand Breaks by Artemis Nuclease. *J. Biol. Chem.*, 282 (6): 3547-3558.
- Rahmanian, S., R. Taleei and H. Nikjoo, 2014. Radiation induced base excision repair (BER): A mechanistic mathematical approach. *DNA Repair*, 22 (0): 89-103.
- Ramsden, D.A., 2010. Polymerases in Nonhomologous End Joining: Building a Bridge over Broken Chromosomes. *Antioxidants & Redox Signaling*, 14 (12): 2509-2519.
- Rappold, I., K. Iwabuchi, T. Date and J. Chen, 2001. Tumor Suppressor P53 Binding Protein 1 (53bp1) Is Involved in DNA Damage-Signaling Pathways. *J. Cell Biol.*, 153 (3): 613-620.
- Roberts, R.W. and J.W. Szostak, 1997. RNA-peptide fusions for the in vitro selection of peptides and proteins. *Proceedings of the National Academy of Sciences*, 94 (23): 12297-12302.

- Ropars, V., P. Drevet, P. Legrand, S. Baconnais, J. Amram, G. Faure, J.A. Márquez, O. Piétrement, R. Guerois, I. Callebaut, E. Le Cam, P. Revy, J. de Villartay and J. Charbonnier, 2011. Structural characterization of filaments formed by human Xrcc4–Cernunnos/XLF complex involved in nonhomologous DNA end-joining. *Proceedings of the National Academy of Sciences*, 108 (31): 12663-12668.
- Rosen, E.M., S. Fan, R.G. Pestell and I.D. Goldberg, 2003. BRCA1 gene in breast cancer. *J. Cell. Physiol.*, 196 (1): 19-41.
- Rothkamm, K., I. Kruger, L.H. Thompson and M. Lobrich, 2003. Pathways of DNA Double-Strand Break Repair during the Mammalian Cell Cycle. *Mol. Cell. Biol.*, 23 (16): 5706-5715.
- San Filippo, J., P. Sung and H. Klein, 2008. Mechanism of Eukaryotic Homologous Recombination. *Annu. Rev. Biochem.*, 77 (1): 229-257.
- Saul, R.L. and B.N. Ames, 1986. Background levels of DNA damage in the population. In: *Mechanisms of DNA Damage* (eds M.G. Simic, L. Grossman and A. C. Upton) pp. 529-535. Repair Plenum Press, New York.
- Schaue, D. and W.H. McBride, 2005. Counteracting tumor radioresistance by targeting DNA repair. *Molecular Cancer Therapeutics*, 4 (10): 1548-1550.
- Shenkier, T., L. Weir, M. Levine, I. Olivotto, T. Whelan, L. Reyno and for The Steering Committee on Clinical Practice Guidelines for the Care and Treatment of Breast Cancer, 2004. Clinical practice guidelines for the care and treatment of breast cancer: 15. Treatment for women with stage III or locally advanced breast cancer. *Canadian Medical Association Journal*, 170 (6): 983-994.
- Shibata, A., S. Conrad, J. Birraux, V. Geuting, O. Barton, A. Ismail, A. Kakaroukas, K. Meek, G. Taucher-Scholz, M. Löbrich and P.A. Jeggo, 2011. Factors determining DNA double-strand break repair pathway choice in G2 phase. *EMBO J.*, 30 (6): 1079-1092.
- Shiloh, Y., 2003. ATM and related protein kinases: safeguarding genome integrity. *Nature Reviews Cancer*, 3 (3): 155.
- Studier, F.W., 2005. Protein production by auto-induction in high-density shaking cultures. *Protein Expr. Purif.*, 41 (1): 207-234.
- Sung, P. and H. Klein, 2006. Mechanism of homologous recombination: mediators and helicases take on regulatory functions. *Nature Reviews Molecular Cell Biology*, 7 (10): 739-750.
- Svilar, D., E.M. Goellner, K.H. Almeida and R.W. Sobol, 2010. Base Excision Repair and Lesion-Dependent Subpathways for Repair of Oxidative DNA Damage. *Antioxidants & Redox Signaling*, 14 (12): 2491-2507.
- Tahernia, A., D. Erdmann and M.R. Zenn, 2010. Breast Reconstructive Surgery,. In: *Management of Breast Diseases* (eds I. Jatoi and M. Kaufmann) pp. 261. Springer, New York.

- Takashima, H., C.F. Boerkoel, J. John, G.M. Saifi, M.A.M. Salih, D. Armstrong, Y. Mao, F.A. Quiocho, B.B. Roa, M. Nakagawa, D.W. Stockton and J.R. Lupski, 2002. Mutation of TDP1, encoding a topoisomerase I-dependent DNA damage repair enzyme, in spinocerebellar ataxia with axonal neuropathy. *Nat. Genet.*, 32 (2): 267-272.
- Ullrich, E., M. Bonmort, G. Mignot, G. Kroemer and L. Zitvogel, 2008. Tumor stress, cell death and the ensuing immune response. *Cell Death & Differentiation*, 15 (1): 21-28.
- Valerie, K. and L.F. Povirk, 2003. Regulation and mechanisms of mammalian double-strand break repair. *Oncogene*, 22 (37): 5792-5812.
- Walker, J.R., R.A. Corpina and J. Goldberg, 2001. Structure of the Ku heterodimer bound to DNA and its implications for double-strand break repair. *Nature*, 412 (6847): 607-614.
- Wang, H. and R. Liu, 2011. Advantages of mRNA display selections over other selection techniques for investigation of protein-protein interactions. *Expert Review of Proteomics*, 8 (3): 335-346.
- Wang, H., Z. Zeng, T. Bui, S.J. DiBiase, W. Qin, F. Xia, S.N. Powell and G. Iliakis, 2001. Nonhomologous End-Joining of Ionizing Radiation-induced DNA Double-Stranded Breaks in Human Tumor Cells Deficient in BRCA1 or BRCA2. *Cancer Res.*, 61 (1): 270-277.
- Wang, J., J.M. Pluth, P.K. Cooper, M.J. Cowan, D.J. Chen and S.M. Yannone, 2005. Artemis deficiency confers a DNA double-strand break repair defect and Artemis phosphorylation status is altered by DNA damage and cell cycle progression. *DNA Repair*, 4 (5): 556-570.
- Ward, J., 1998. Nature of Lesions Formed by Ionizing Radiation, (eds J. Nickoloff and M. Hoekstra) pp. 65-84. Humana Press.
- West, R.B., M. Yaneva and M.R. Lieber, 1998. Productive and Nonproductive Complexes of Ku and DNA-Dependent Protein Kinase at DNA Termini. *Mol. Cell. Biol.*, 18 (10): 5908-5920.
- Weterings, E. and D.J. Chen, 2007. DNA-dependent protein kinase in nonhomologous end joining: a lock with multiple keys?. *J. Cell Biol.*, 179 (2): 183-186.
- Weterings, E. and D.J. Chen, 2008. The endless tale of non-homologous end-joining. *Cell Res.*, 18 (1): 114-124.
- White, E.R., L. Sun, Z. Ma, J.M. Beckta, B.A. Danzig, D.E. Hacker, M. Huie, D.C. Williams, R.A. Edwards, K. Valerie, J.N.M. Glover and M.C.T. Hartman, 2015. Peptide Library Approach to Uncover Phosphomimetic Inhibitors of the BRCA1 C-Terminal Domain. *ACS Chem. Biol.*, 10 (5): 1198-1208.
- Whitehouse, C.J., R.M. Taylor, A. Thistlethwaite, H. Zhang, F. Karimi-Busheri, D.D. Lasko, M. Weinfeld and K.W. Caldecott. XRCC1 Stimulates Human Polynucleotide Kinase Activity at Damaged DNA Termini and Accelerates DNA Single-Strand Break Repair. *Cell*, 104 (1): 107-117.
- Wiesmann, C., G. Fuh, H.W. Christinger, C. Eigenbrot, J.A. Wells and A.M. de Vos, 1997. Crystal Structure at 1.7 Å Resolution of VEGF in Complex with Domain 2 of the Flt-1 Receptor. *Cell*, 91 (5): 695-704.

- Wilson, C.A., L. Ramos, M.R. Villasenor, K.H. Anders, M.F. Press, K. Clarke, B. Karlan, J. Chen, R. Scully, D. Livingston, R.H. Zuch, M.H. Kanter, S. Cohen, F.J. Calzone and D.J. Slamon, 1999. Localization of human BRCA1 and its loss in high-grade, non-inherited breast carcinomas. *Nat. Genet.*, 21 (2): 236-240.
- Wiseman, H. and B. Halliwell, 1996. Damage to DNA by reactive oxygen and nitrogen species: role in inflammatory disease and progression to cancer. *Biochem. J.*, 313: 17-29.
- Wooster, R., G. Bignell, J. Lancaster, S. Swift, S. Seal, J. Mangion, N. Collins, S. Gregory, C. Gumbs, G. Micklem, R. Barfoot, R. Hamoudi, S. Patel, C. Rices, P. Biggs, Y. Hashim, A. Smith, F. Connor, A. Arason, J. Gudmundsson, D. Ficene, D. Kelsell, T. Ford DeborahPatricia, D. Timothy Bishop, N.K. Spurr, B.A.J. Ponder, R. Eeles, J. Peto, P. Devilee, C. Cornelisse, H. Lynch, S. Narod, G. Lenoir, V. Egilsson, R. Bjork Barkadottir, D.F. Easton, D.R. Bentley, P.A. Futreal, A. Ashworth and M.R. Stratton, 1995. Identification of the breast cancer susceptibility gene BRCA2. *Nature*, 378 (6559): 789-792.
- Xu, L., P. Aha, K. Gu, R.G. Kuimelis, M. Kurz, T. Lam, A.C. Lim, H. Liu, P.A. Lohse, L. Sun, S. Weng, R.W. Wagner and D. Lipovsek, 2002. Directed Evolution of High-Affinity Antibody Mimics Using mRNA Display. *Chem. Biol.*, 9 (8): 933-942.
- Yang, S.W., A.B. Burgin, B.N. Huizenga, C.A. Robertson, K.C. Yao and H.A. Nash, 1996. A eukaryotic enzyme that can disjoin dead-end covalent complexes between DNA and type I topoisomerases. *Proc. Natl. Acad. Sci. U. S. A.*, 93 (21): 11534-11539.
- Yoneda, T., P.J. Williams, T. Hiraga, M. Niewolna and R. Nishimura, 2001. A Bone-Seeking Clone Exhibits Different Biological Properties from the MDA-MB-231 Parental Human Breast Cancer Cells and a Brain-Seeking Clone In Vivo and In Vitro. *Journal of Bone and Mineral Research*, 16 (8): 1486-1495.
- Yoo, S. and W.S. Dynan, 1999. Geometry of a complex formed by double strand break repair proteins at a single DNA end: recruitment of DNA-PKcs induces inward translocation of Ku protein. *Nucleic Acids Res.*, 27 (24): 4679-4686.
- Zha, S., F.W. Alt, H. Cheng, J.W. Brush and G. Li, 2007. Defective DNA repair and increased genomic instability in Cernunnos-XLF-deficient murine ES cells. *Proceedings of the National Academy of Sciences*, 104 (11): 4518-4523.
- Zhao, Y., H.D. Thomas, M.A. Batey, I.G. Cowell, C.J. Richardson, R.J. Griffin, A.H. Calvert, D.R. Newell, G.C.M. Smith and N.J. Curtin, 2006. Preclinical Evaluation of a Potent Novel DNA-Dependent Protein Kinase Inhibitor NU7441. *Cancer Research*, 66 (10): 5354-5362.
- Zhuang, J., J. Zhang, H. Willers, H. Wang, J.H. Chung, D.C. van Gent, D.E. Hallahan, S.N. Powell and F. Xia, 2006. Checkpoint Kinase 2-Mediated Phosphorylation of BRCA1 Regulates the Fidelity of Nonhomologous End-Joining. *Cancer Research*, 66 (3): 1401-1408.
- Zimmermann, M. and T. de Lange, 2013. 53BP1: Pro Choice in DNA Repair. *Trends Cell Biol.*, 24 (2): 108-117.

VITA

Mohammed Al Mohaini was born on June 06, 1982 in Alahsa, Saudi Arabia. He graduated with a degree of Bachelor in Pharmaceutical Sciences from King Saud University, Riyadh, Saudi Arabia in 2006. He worked in King Abdulaziz Hospital, Alahsa, Saudi Arabia as a pharmacist in the Pharmaceutical Care department from 2006 to 2008. He worked at King Saud bin Abdulziz University for Health Sciences (KSAU-HS) from 2008-2009 as a teaching assistant of pharmacology. He was awarded a scholarship from KSAU-HS to study Master and PhD abroad. He joined Virginia Commonwealth University in 2010 and finished his Master of Sciences in Pharmacology and Toxicology in 2012.